

**SUGAR ALCOHOLS: A NOVEL PLATFORM FOR FUNCTIONAL  
MOLECULAR GELS**

**by**

**SWAPNIL ROHIDAS JADHAV**

**A dissertation submitted to the Graduate Faculty in Chemistry in partial fulfillment  
of the requirements for the degree of Doctor of Philosophy,  
The City University of New York**

**2012**

© 2012

Swapnil Rohidas Jadhav

All Rights Reserved

This Manuscript has been read and accepted for the Graduate  
Faculty in Chemistry in satisfaction of the dissertation  
requirement for the degree of Doctor of Philosophy

Professor George John

12/21/2011

Date

Chair of Examining Committee

Professor Maria Tamargo

12/21/2011

Date

Executive Officer

Professor Alexander Couzis

Professor Shi Jin

Professor Ruth E. Stark

Supervising Committee

THE CITY UNIVERSITY OF NEW YORK

*Dedicated to My Dad and Loved One(s)*

## **Abstract**

### **SUGAR ALCOHOLS: A NOVEL PLATFORM FOR FUNCTIONAL MOLECULAR GELS**

by

Swapnil Rohidas Jadhav

Advisor: Professor George John

The rise in interest in molecular gels is evident from the ample variety of molecular gelators (MGrS) being developed for diverse applications, ranging from medicinal to electronic devices. MGrS, typically amphiphiles, exhibit high biocompatibility and biodegradability, accounting for their emergence as potential successors to polymeric gelators. However, most of these gelators have been discovered serendipitously. Therefore there is a strong impetus to probe: (i) the process of gelation; and (ii) structural requirements for a molecule to be a successful gelator. Such systematic investigation rationalizes the relationship between the gelator structure and properties of gels. In this research work, this challenge is addressed for a new class of gelators: sugar alcohol-fatty acid conjugates.

The natural abundance and vast structural diversity of sugar alcohols and fatty acids make them ideal candidates for use in the synthesis of new MGrS. Mannitol, sorbitol and xylitol were chosen as representative entities to study the effect of subtle structural variation in sugar alcohols on the gelation mechanism. Lipase-mediated regioselective transesterification was employed to quantitatively conjugate sugar alcohols with fatty acids. The hydrophobicity of the amphiphiles was fine tuned by varying fatty

acid chain length from C4 to C14. The gelation tendency (or self-assembly) of sugar alcohol-based amphiphiles was investigated in water and organic liquids. Several techniques such as XRD, microscopy (optical, SEM and TEM) and spectroscopy (FT-IR) were used to characterize the gels and to decipher the self-assembly mechanism responsible for gelation. The characterization techniques collectively helped in elucidating the relationship between the gelation efficiency and amphiphilic structure (stereochemistry of sugars or chain length of fatty acid).

These non-toxic and readily biodegradable amphiphiles exhibited unprecedented gelation in crude oil fractions, edible oil and liquid pheromones. Their utility was successfully demonstrated by developing: (i) oil spill recovery materials (Chapter 3); (ii) controlled release devices for pheromones and biopesticides (Chapter 4); and (iii) healthy vegetable oil structuring agents (Chapter 5). This entire study successfully demonstrates the prudent utilization of biobased resources and biocatalysis for developing multifunctional amphiphiles. Such value-added chemicals developed through the biorefinery concept may have an impact on industrial applications and new products.

## Acknowledgements

It is with great pleasure that I extend my deep sense of gratitude to Prof. George John, my thesis supervisor and mentor, for suggesting the research problem, for his constant guidance, support and encouragement, leading to the successful completion of this work.

I would also like to extend my special sincere gratitude to three of Prof. John's post doctoral fellows; namely, Dr. Praveen Kumar Vemula, Dr. Jyothish Kuthanapillil and Dr. Vijai Shankar Balachandran. They were extremely helpful and instrumental in making my PhD research a successful stint.

My Sincere thanks are also due to:

1. Prof. S. Raghavan (University of Maryland), Dr. G. Glenn (USDA, Ca.) and Prof. Q. Huang (Rutgers University) for their valuable suggestions and collaborating with us in different successful projects.
2. All my committee members (in alphabetical order), Prof. Alexander Couzis, Prof. Shin Jin and Prof. Ruth E. Stark for evaluating my progress annually and providing valuable suggestions throughout my thesis research.
3. Dr. Padmanava Pradhan for introducing me to NMR instrumentation and experimental protocols.
4. Dr. Jorge Morales for introducing me to SEM and TEM instruments and continued support.
5. Prof. S. Raghavan and Mr. Karanjkar Prasad for introducing me to the science and instrumentation of rheology.

6. All my past and present group members for making the last 5 and a half year memorable.
7. All my friends at CCNY, which is in fact a big family, for their love and support.
8. My family, back in India, for their love and support.
9. CENSES (NSF) for financial assistance in last 2 years of my PhD program.

## Table of Contents

<b>Abstract</b>		<b>v</b>
<b>Acknowledgements</b>		<b>vii</b>
<b>Abbreviations</b>		<b>xiii</b>
<b>List of Tables</b>		<b>xv</b>
<b>List of Figures</b>		<b>xvi</b>
<b>List of Appendices</b>		<b>xxi</b>
<b>Chapter 1</b>	<b>Introduction to Molecular Gels</b>	<b>01-34</b>
1.1.	Gels	01
1.2.	Molecular Gels	02
1.3.	Status Quo and Advantages of Molecular Gels	09
1.4.	Challenges in Molecular Gels	22
1.5.	Alternative Approach	22
1.6.	Biorefinery Concept for the Discovery of Molecular Gels	24
1.7.	Origin, Objectives and Approach to the Thesis	31
<b>Chapter 2</b>	<b>Sugar Alcohols-based Gelators: Structure-property Correlation Studies</b>	<b>35-68</b>
2.1.	Abstract	35

2.2.	Introduction	35
2.3.	Results and Discussion	42
2.3.1.	Synthesis of Ester-based Sugar Alcohol Gelators	42
2.3.2.	Gelation Studies	43
2.3.3.	Morphology of Organogels	46
2.3.4.	Effect of Solvents on Gelation Efficiency	48
2.3.5.	Effect of Acyl Chain Length on Gelation Efficiency	52
2.3.6.	Effect of Sugar Head Group on Gelation	54
2.4.	Conclusion	62
2.5.	Experimental Section	62
<b>Chapter 3</b>	<b>Sugar-derived Phase-selective Molecular Gelators as Model Solidifiers for Oil Spills</b>	<b>69-88</b>
3.1.	Abstract	69
3.2.	Introduction	69
3.3.	Results and Discussion	73
3.3.1.	Evaluation of Gelation Efficiency in Crude Oil Fractions (oils)	74
3.3.2.	Phase-selective Gelation of Oils	76
3.3.3.	Mechanism of Phase-selective Gelation	79
3.3.4.	Gelation and Removal of Diesel from Diesel-Water Mixture	82
3.4.	Conclusion	85

3.5.	Experimental Section	86
<b>Chapter 4</b>	<b>Molecular Gels-based Controlled Release Devices for Pheromones</b>	<b>89-109</b>
4.1.	Abstract	89
4.2.	Introduction	89
4.3.	Results and Discussion	92
4.3.1.	Gelation of Pheromones	92
4.3.2.	Thermal and Mechanical Properties of 2-Heptanone Gels	93
4.3.3.	Morphology of 2-Heptanone Gels	95
4.3.4.	Self-assembly Mechanism of M8 in Pheromones	98
4.3.5.	Biodegradability of M8	100
4.3.6.	Evaporation rate of 2-Heptanone from M8-gel	101
4.3.7.	M8 Gel-based CRD	103
4.4.	Conclusion	104
4.5.	Experimental Section	105
<b>Chapter 5</b>	<b>Medium Chain Sugar Amphiphiles: Healthy &amp; Alternative Vegetable Oil Structuring Agents</b>	<b>110-133</b>
5.1.	Abstract	110
5.2.	Introduction	110
5.3.	Results and Discussion	114

5.3.1.	Cytotoxicity of M8 and S8	114
5.3.2.	Vegetable Oil Gelation: Efficiency and Self-assembly Mechanism	116
5.3.3.	Structuring Efficiency of Gelators	119
5.3.4.	Effect of Concentration of Gelators	120
5.3.5.	Effect of Ageing on Properties of Structured Oil	124
5.3.6.	Effect of Small Deformation for Long Time	127
5.3.7.	Effect of the Type of Oil	128
5.4.	Conclusion	129
5.5.	Experimental Section	130
<b>Appendices</b>		<b>134</b>
<b>List of Publications</b>		<b>142</b>
<b>Cover Pages</b>		<b>143</b>
<b>Bibliography</b>		<b>144-160</b>

## List of Abbreviations

<b>MG</b>	Molecular Gel
<b>MGr</b>	Molecular Gelator
<b>SAFIN</b>	Self-assembled Fibrillar Network
<b>SWNT</b>	Single-walled Carbon Nanotubes
<b>NAA</b>	N-alkylaldonamides
<b>M8</b>	Mannitol dioctanoate
<b>S8</b>	Sorbitol dioctanoate
<b>SGH</b>	1,3-syn hydroxyl groups
<b>CALB</b>	Candida Antartica Lipase B
<b>MGC</b>	Minimum Gelation Concentration
<b>T<sub>gel</sub></b>	Gel-to-sol Transition Temperature
<b>UV-vis</b>	Ultraviolet–visible spectroscopy
<b>SEM</b>	Scanning Electron Microscopy
<b>TEM</b>	Transmission Electron Microscopy
<b>XRD</b>	X-ray Diffraction
<b>FT-IR</b>	Fourier Transform Infrared Spectroscopy
<b><sup>1</sup>H NMR</b>	Proton Nuclear Magnetic Spectroscopy
<b><sup>13</sup>C NMR</b>	Carbon-13 Nuclear Magnetic Spectroscopy
<b>EI-MS</b>	Electron Ionization Mass Spectroscopy
<b>PSG</b>	Phase-selective Gelation
<b>PSGr</b>	Phase-selective Gelator

<b>G'</b>	Elastic Modulus
<b>G''</b>	Viscosity Modulus
<b><math>\sigma_0</math></b>	Yield Stress
<b>CRD</b>	Controlled Release Device
<b>TFA</b>	Trans Fatty Acids
<b>SFA</b>	Saturated Fatty Acids
<b>FDA</b>	The Food and Drug Administration
<b>HepG2</b>	Human Hepatocellular Carcinoma Cells
<b>MTT</b>	3-(4,5-dimethyl-2-thiazolyl)-2,5-diphenyl-2H-tetrazolium bromide
<b>GRAS</b>	Generally Recognized as Safe
<b>CO</b>	Canola Oil
<b>OO</b>	Olive Oil
<b>GO</b>	Grapeseed Oil
<b>SO</b>	Soybean Oil
<b><math>\sigma_y</math></b>	Yield Strain

## List of Tables

<b>Table 1.1.</b>	Different non-covalent interactions and their respective strength.	<b>04</b>
<b>Table 2.1.</b>	Molecular gelation efficiency of sugar alcohol dialkanoates.	<b>45</b>
<b>Table 2.2.</b>	Observed wavenumbers ( $\text{cm}^{-1}$ ) of the vital vibrational groups of M8 and S8.	<b>56</b>
<b>Table 3.1.</b>	Gelation abilities of M8 and S8 in various crude oil fractions and oils.	<b>75</b>
<b>Table 3.2.</b>	Comparison of properties of gels obtained from phase-selective gelation (PSG) by aliquot method or pure solvent gelation by heating method.	<b>80</b>
<b>Table 4.1.</b>	Thermal and mechanical properties of 2-heptanone gels of M8.	<b>95</b>
<b>Table 5.1.</b>	Vegetable oil gelation efficiency and versatility of M8 and S8.	<b>116</b>
<b>Table 5.2.</b>	Mechanical, thermal and structural data obtained for CO gels with varying concentration of M8 and S8.	<b>122</b>
<b>Table 5.3.</b>	Mechanical, thermal and structural data obtained for CO gels (5% wt/v) aged for different time scale.	<b>126</b>
<b>Table 5.4.</b>	Structuring data obtained for M8 and S8 gels (5% wt/v) in different vegetable oils.	<b>129</b>

## List of Figures

<b>Figure 1.1.</b>	A representative gel and its network.	<b>01</b>
<b>Figure 1.2.</b>	Schematic representation of non-covalent interactions arising from different functional groups.	<b>03</b>
<b>Figure 1.3.</b>	Progressive stages involved in the mechanism of molecular gelation.	<b>05</b>
<b>Figure 1.4.</b>	Multiple non-covalent interactions existing in self-assembly process of molecular gelators.	<b>07</b>
<b>Figure 1.5.</b>	An enzyme induced gelation.	<b>11</b>
<b>Figure 1.6.</b>	An example of metal ion induced gelation.	<b>12</b>
<b>Figure 1.7.</b>	Biocompatible peptide for biomedical applications.	<b>13</b>
<b>Figure 1.8.</b>	Drug-based molecular gels as drug-delivery vehicle.	<b>15</b>
<b>Figure 1.9.</b>	Self-assembly induced enhancement of charge transfer.	<b>16</b>
<b>Figure 1.10.</b>	Amplification of catalytic activity in MG.	<b>17</b>
<b>Figure 1.11.</b>	Helical structures of silica transcription on self-assembled amphiphiles.	<b>19</b>
<b>Figure 1.12.</b>	Hybridization of MG with carbon nanotubes.	<b>21</b>
<b>Figure 1.13.</b>	Schematic representation of biorefinery concept.	<b>23</b>
<b>Figure 1.14.</b>	Enzyme-catalyzed regioselective synthesis of sugar amphiphiles.	<b>25</b>
<b>Figure 1.15.</b>	Amygdalin-based hydrogels as drug-delivery vehicles.	<b>26</b>
<b>Figure 1.16.</b>	Trehalose-based gelators with very high gelation efficiency.	<b>28</b>

<b>Figure 1.17.</b>	Alignment of metal nanoparticles via sugar-based MG.	<b>30</b>
<b>Figure 1.18.</b>	Fisher projections of molecular structures of sugars.	<b>32</b>
<b>Figure 2.1.</b>	N-alkylaldonamides and electron micrographs of their aggregates in water.	<b>37</b>
<b>Figure 2.2.</b>	Organo and liquid crystalline gels from functionalized N-alkyl-D-aldonamide.	<b>38</b>
<b>Figure 2.3.</b>	Organometallic isolable of gluconamide, an organogelator.	<b>39</b>
<b>Figure 2.4.</b>	Benzylidene derivative of sorbitol, an ether-based gelator.	<b>40</b>
<b>Figure 2.5.</b>	Strong gels made from sugar alcohol organogelators.	<b>40</b>
<b>Figure 2.6.</b>	Schematic representation of enzymatic catalysis of sugar alcohols.	<b>42</b>
<b>Figure 2.7.</b>	Photographs of gels made by using sugar alcohol dialkanoates.	<b>44</b>
<b>Figure 2.8.</b>	Optical micrographs of gels of 1,8-dibromooctane.	<b>46</b>
<b>Figure 2.9.</b>	SEM images self-assembled structures of sugar alcohol-based amphiphiles.	<b>47</b>
<b>Figure 2.10.</b>	Effect of solvent's functional groups on the gelation efficiency of mannitol-based gelators.	<b>50</b>
<b>Figure 2.11.</b>	Effect of length of solvent's hydrocarbon chain on the gelation efficiency of mannitol-based gelators.	<b>51</b>
<b>Figure 2.12.</b>	Effect of acyl chain length (4-14) of gelator on the gelation efficiency of mannitol-based gelators.	<b>52</b>
<b>Figure 2.13.</b>	FT-IR spectrum of different samples of gelators.	<b>55</b>

<b>Figure 2.14.</b>	XRD patterns of powder and toluene gel samples of M8 and S8.	<b>58</b>
<b>Figure 2.15.</b>	Influence of chirality induced 1,3-hydroxyl interaction on the conformation of sugar alcohol gelators.	<b>59</b>
<b>Figure 2.16.</b>	Schematic representation of molecular assembly of M8 and S8 in organic solvents.	<b>61</b>
<b>Figure 3.1.</b>	Molecular structures of representative phase-selective gelators.	<b>73</b>
<b>Figure 3.2.</b>	Generic structure of sugar alcohol dialkanoate and specific molecular structures of mannitol dioctanoate and sorbitol dioctanoate.	<b>74</b>
<b>Figure 3.3.</b>	Schematic representations of phase-selective gelation via conventional heating and cooling method.	<b>76</b>
<b>Figure 3.4.</b>	Schematic representations of room temperature phase-selective gelation method (aliquot method).	<b>77</b>
<b>Figure 3.5.</b>	M8 aided phase-selective gelation of toluene.	<b>79</b>
<b>Figure 3.6.</b>	Characterization of M8 gels obtained from pure or phase-selective gelation of solvents.	<b>81</b>
<b>Figure 3.7.</b>	Schematic representation of self-assembly mechanism of M8 during phase-selective gelation of different oils from oil-water mixture.	<b>81</b>
<b>Figure 3.8.</b>	Phase-selective gelation and diesel recovery from two phase system.	<b>83</b>

<b>Figure 3.9.</b>	Dynamic rheology of M8-diesel gel (5 % wt/v).	<b>84</b>
<b>Figure 3.10.</b>	Scooping out a thin-layer of diesel gel from the top of water	<b>85</b>
<b>Figure 4.1.</b>	Molecular structures of representative volatile pheromones.	<b>90</b>
<b>Figure 4.2.</b>	Chemical structures of polymeric materials used for developing controlled release devices.	<b>91</b>
<b>Figure 4.3.</b>	Photographs of liquid 2-heptanone and its corresponding gel state (the inverted cuvette) obtained after addition of mannitol dioctanoate (M8 at 5% wt/v).	<b>92</b>
<b>Figure 4.4.</b>	Oscillatory frequency sweep measurements of 2-heptanone gels containing different concentrations (% wt/v) of M8.	<b>94</b>
<b>Figure 4.5.</b>	Optical micrographs of sequential views during the gelling process of M8 in 2-heptanone (3 %wt/v).	<b>96</b>
<b>Figure 4.6.</b>	Scanning electron micrograph of critical point dried 2-heptanone gel of M8 (5% wt/v) at different magnification level.	<b>97</b>
<b>Figure 4.7.</b>	XRD patterns of different M8 samples. ‘ <i>d</i> ’ indicates the long d-spacing values of corresponding samples.	<b>98</b>
<b>Figure 4.8.</b>	FT-IR spectra of M8 powder (Blue) and 2-heptanone gel of M8 (Red).	<b>99</b>
<b>Figure 4.9.</b>	Biodegradability of M8 (red) and starch control (black) in terms of percent mineralization over time (days).	<b>101</b>
<b>Figure 4.10.</b>	Weight loss from evaporation of 2-heptanone from a liquid (O)	<b>102</b>

or 2-heptanone gel (▲).

- Figure 4.11.** Percent weight loss over time of two controls and two activated control-release devices. **103**
- Figure 5.1.** Pictorial depiction of liquid and structured oil. An optical micrograph of structured oil showing the crystalline fat network present in it. **111**
- Figure 5.2.** Molecular structures of different classes of gelators that have been investigated for structuring applications. **113**
- Figure 5.3.** Molecular and 3-D space filling model of M8 and S8 along with their cytotoxicity data. **115**
- Figure 5.4.** Photograph, optical microscope image and XRD pattern of grapeseed oil gels (5% wt/v). **118**
- Figure 5.5.** Rheological and optical analyses of M8-CO gels at various concentrations of M8 (1, 3 and 5% wt/v). **120**
- Figure 5.6.** Rheological and optical analyses of CO gels developed by using various concentrations of S8 (3 and 5% wt/v). **123**
- Figure 5.7.** Effect of ageing on the mechanical and structural properties of CO gels (5 % wt/v). **125**
- Figure 5.8.** Oscillatory time sweep measurements of CO gel (5% wt/v). **127**
- Figure 5.9.** Frequency sweep measurements of different oil gels (5% wt/v). **128**

## List of Appendices

- Appendix 1.** Gel-to-sol transition temperature for the sugar alcohol-based organogels ( $T_{\text{gel}}$  °C). **134**
- Appendix 2.** Effect of different classes of solvents (bromo, esters and alcohols) and the length of their hydrophobic chain on the gelation efficiency of M8 and S8. **135**
- Appendix 3.** Spectroscopic characterization of mannitol dioctanoate (M8). **136**
- Appendix 4.** Spectroscopic characterization of sorbitol dioctanoate (S8). **138**
- Appendix 5.** Spectroscopic characterization of xylitol dioctanoate (X8). **140**

---

## Chapter 1

---

### Introduction to Molecular Gels

---

#### 1.1. Gels

*Gels* are an integral entity of nature. The ubiquity and vitality of gels are best exemplified in natural materials, common examples being the gelatinous pith of the Aloe Vera plant and the whole body of a jellyfish. Even the protoplasm, which constitutes a basic unit of life (cell) is essentially a gel. Via an intricate yet proficient bottom-up strategy, the production of gels in natural systems occurs for numerous biological functions.<sup>1-3</sup> In the quest to develop man-made multifunctional gels, the materials research community has been involved in mimicking such biological jelly materials and extending the logistics towards non-biological applications.<sup>4,5</sup>

Gels, a class of functional soft materials, are essentially an immobilized state of liquids. Consistent with the iconic definition coined by Flory in 1974, a gel state can be described as: “a semi-rigid colloidal state of matter that consists of a 3-D network of solute (dispersed solid phase) uniformly distributed in a pool of solvent (continuous liquid phase)” (Figure 1.1).<sup>6</sup> The solid network entraps the solvent molecules within its interstices with the aid of capillary forces, preventing the solvent from flowing at the macroscopic level. The liquid phase in turn prevents the collapse of the network. Due to such synergistic co-existence of these two phases, gels

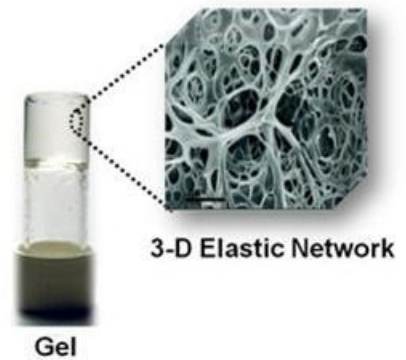


**Figure 1.1.** A representative gel and its network

are principally viscoelastic. Under equilibrium conditions, gels are able to store the work employed in their deformation, and recover their original shape after the release of the work.<sup>7</sup> However, on deformation of a gel beyond critical value (yield stress,  $\sigma_y$ ) it fails to regain its original shape and begins to flow like a viscous fluid.

Given that a solute component of a gel is responsible for solvent immobilization, solute is called a *gelator*. Depending on the chemical constitution of gelators, polymers or monomers, gels are broadly classified as polymeric or non-polymeric systems. Traditionally, the gel science evolved around developing polymer gels and understanding their physico-chemical properties. In *polymer gels*, long strands of polymer chains are either physically or chemically cross-linked to form a 3-D solid-matrix.<sup>8</sup> They have been extensively used in food and pharmaceutical industry, for exhibition of functions such as controlled release, viscosity modifiers, and coatings etc.<sup>9,10</sup> However, since polymers are (a) inaccessible for systematic functionalization, and (b) inefficient in gelling wide range of solvents (especially organic solvents), their utility has been limited to narrow range of industrial sector. The recent trend has been shifting towards the development of low mass molecular gelators; the resulting gels are termed as molecular gels. *Molecular gels (MGs)* circumvent several limitations of polymer gels and enable usage of gels in diverse applications.<sup>5</sup> Consequently, they have emerged as a potential alternative to polymer gels.

## 1.2. Molecular Gels

Macroscopically, molecular gels are similar to polymer gels; i.e., they exhibit viscoelasticity and are comprised of pool of solvent and solvent holding solid-matrix. However, unlike polymeric gelators (molecular wt. 5-10,000 Da.), the molecular gelators are low molecular weight monomeric building blocks (average molecular wt. <1000

Da.).<sup>11,12</sup> The propensity of such small molecules to give rise to 3-D networks stems from their tendency to hierarchically self-assemble in quasi one dimensional manner by using weak intermolecular interactions to form well-defined, high-aspect-ratio aggregates. Based on the nature of solvent, water or organic liquids, MGs are categorized as hydrogels or organogels. Accordingly, the gelators are termed as hydro-/organogelators.

### 1.2.1. Hierarchical Self-assembly of Molecular Gelators

The self-organization of molecular gelators is governed by several directional non-covalent interactions such as hydrogen bonds, van der Waals forces,  $\pi$ - $\pi$  stacking, organometallic co-ordination bonds, electrostatic interactions (ionic bonds) and hydrophobic forces (Figure 1.2).<sup>11</sup> For hydrogels, the self-assembly is primarily directed by hydrophobic forces and all other non-covalent interactions are either secondary or completely absent.<sup>13</sup> In contrast, for organogels hydrophobic forces are secondary.

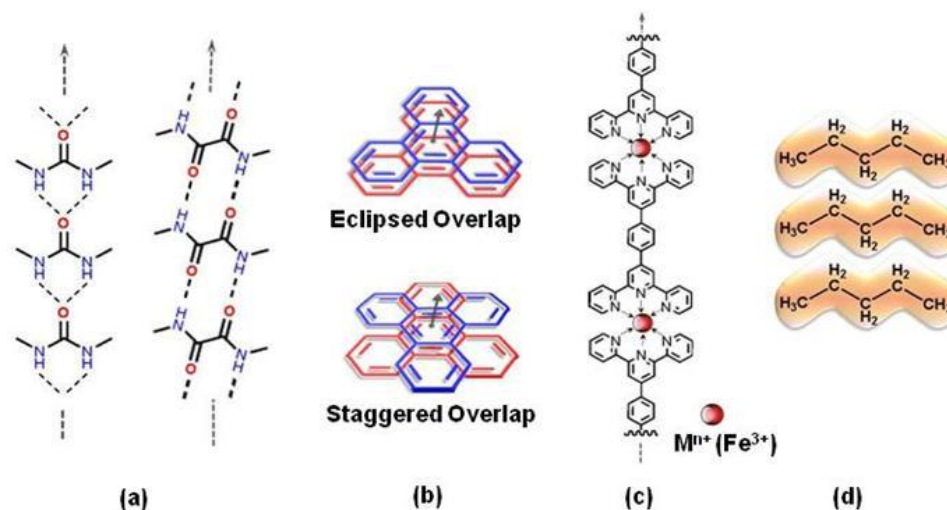


**Figure 1.2.** Schematic representation of non-covalent interactions arising from different functional groups. (a) Hydrogen bonding, (b)  $\pi$ - $\pi$  stacking, (c) organometallic co-ordination, (d) van der Waals forces. The axes indicate the directionality of the interactions in self-assembly.

Compared to covalent bonds (100-400 kJ/mol), non-covalent interactions are considerably weak, typically their interaction energies vary from less than 5 kJ/mol (van der Waals forces) to approximately 40 kJ/mol (hydrogen bonds, Table 1.1). When these weak non-covalent forces are collectively present in a self-assembly process, they produce a synergistic effect, which provides a self-supporting strength to the aggregates. Thus, the strength of the network, and hence of MGs, stems from type and degree of interactions involved during self-assembly.

**Table 1.1.** Different non-covalent interactions and their respective strength.

Type	Strength (kJ/mol)	Range	Character
Hydrogen bond	10-65	Short	Directional
Ionic	50-200	Long	Non-directional
Dipole-dipole	5-50	Short	-
$\pi$ - $\pi$	0-50	Short	Directional
van der Waals forces	0-5	Short	Non-directional
Metal-ligand coordination	0-400	Short	Directional
Hydrophobic Interaction	Difficult to quantify	Short	Non-directional

### 1.2.2. Mechanism of Molecular Gelation

Molecular gelation phenomenon is often accounted as a balance between crystallization and solubilization (i.e. self-assembly mediated incomplete

crystallization).<sup>14</sup> Generally, the molecular gelators hierarchically self-assemble from nanoscale aggregates to the macroscale networks. Progressive gelation process consists of three stages of increasing length scale: nano, micro and meso (Figure 1.3).<sup>14,15</sup>

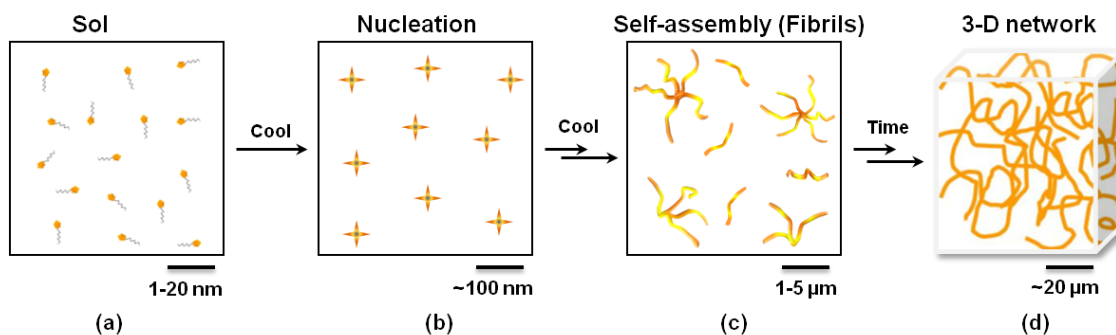


**Figure 1.3.** Progressive stages involved in the mechanism of molecular gelation. (a) Individual gelator molecules in solvent at high temperature i.e. Sol. (b) Nano-size nuclei of gelator molecules. (c) Hierarchically self-assembled micron-size aggregates. (d) Cross-linking of fibers to produce meso- to macro-scale network.

The preliminary phase involves molecular dispersion of the gelator molecules in the liquid medium. This is an energy intensive step and is achieved via heating. The resulting gelator-liquid mixture is a clear and homogeneous solution (sol) (Figure 1.3a). On cooling the sol, the dissolved gelator molecules start condensing and supersaturating the solution, resulting in the formation of numerous nuclei of nanoscale dimension (Figure 1.3b). The gelator molecules anisotropically aggregate around the nuclei through highly directional non-covalent interactions. Several 1-D or 2-D fibrous assemblies of micron dimension emanate from single nuclei and penetrate into liquid medium (Figure 1.3c). Finally, the individual fibers mechanically interlock with each other to form a continuous network extending throughout the liquid (Figure 1.3d). The fibrillar interactions in the network are either transient (simple entanglement of fibers) or

permanent (branched fibers). The type of cross-links prevailing in the network determines the overall property of gels. For instance, networks containing long, flexible and thin fibers are better than those with shorter fibers to entrap solvent and form mechanically stronger gels. Owing to the fibrous morphology of MGs, the network is commonly referred to as ‘Self-Assembled Fibrillar Network (SAFIN)’.

### **1.2.3. Designing of Molecular Gelators**

Although the first account on the development of molecular gelator was documented in late 19<sup>th</sup> century (1891)<sup>16</sup>, it was not until the late 20<sup>th</sup> century<sup>17,18</sup> that serious attempts were made to comprehensively design them. Over the past two decades the field of MGs has emerged tremendously from making serendipitous discovery of molecular gelators to designing of gelators for targeted applications.<sup>19</sup> The initial stage of development is marked by discovery of new molecular gelator systems followed by understanding the influence of molecular structure on self-assembly and gelation mechanism.<sup>20</sup>

From the principles of self-assembly and gelation phenomenon, the basic structural features required in a molecule to be an efficient gelator can be stated as follows:<sup>21,22</sup>

1. The molecule should possess both solvophilic and solvophobic moieties to achieve a proper balance between dissolution and crystallization. Accordingly, most of the reported molecular gelators are amphiphilic in nature; i.e., they have both polar and non-polar functional groups.

- The molecule should exhibit greater affinity for gelator-gelator (intermolecular) interactions than for gelator-solvent interaction – it is essential for formation of 3-D network.
- The functional groups present in the molecule must have potential to exhibit multiple non-covalent interactions.
- The non-covalent interactions must promote self-assembly to favor formation of 1-D aggregates.

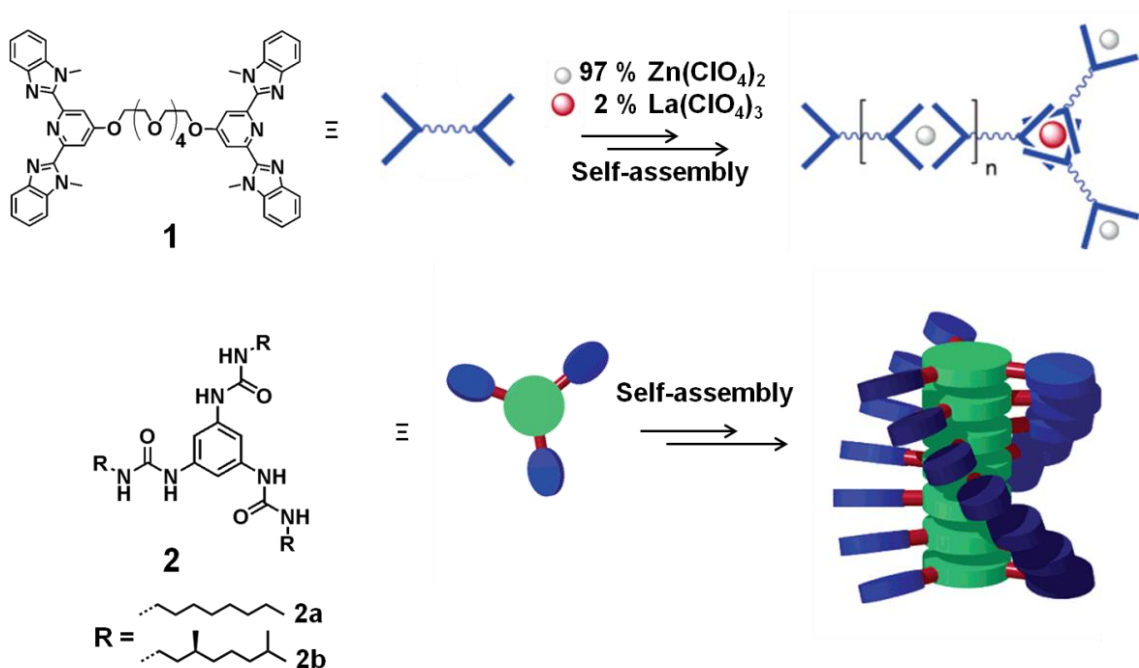


**Figure 1.4.** Multiple non-covalent interactions existing in self-assembly process of molecular gelators. **1**: Organometallic coordination and  $\pi$ - $\pi$  stacking.<sup>23</sup> **2**:  $\pi$ - $\pi$  stacking, hydrogen bonding and van der Waals forces.<sup>24</sup>

Figure 1.4 depicts the vital role of multiple interactions in generating 1-D aggregates and hence, continuous 3-D network. A ditopic ligand **1** possesses multiple aromatic moieties conducive for  $\pi$ - $\pi$  stacking.<sup>23</sup> However, **1** is unable to hierarchically

self-assemble with the aid of only  $\pi$  interaction, due to its unfavorable molecular conformation. Incorporation of metal ions capable of coordination with **1** introduces an additional mode of interaction, which in turn propels unidirectional aggregation. Such metal-ligand binding tendency of **1** was judiciously utilized by Rowan and co-workers to produce organogels.  $\text{Zn}^{2+}$  complexes with **1** in 1:2 proportion to chronologically promote chain extension, formation of long fibrils and development of gels. The second example of figure 1.4 illustrates that in addition to exhibiting multiple non-covalent interactions, keeping a proper balance between them is equally critical for molecular gelation phenomenon.<sup>24</sup> The derivative of **2** containing linear aliphatic chain (**2a**) hierarchically self-assemble via multiple interactions such as  $\pi$ - $\pi$  stacking (aromatic groups), hydrogen bonding (amide groups) and van der Waals forces (linear aliphatic chain). They synergistically act to form a strong network and gels in polar solvents. However, the derivative with branched aliphatic chain (**2b**) does not form any gels. Substitution of linear aliphatic chain by a branched chain was found to destabilize the self-assembly and completely disrupt the gelation tendency of **2**. Thus, ‘supramolecular chemistry’ involving an understanding of the non-covalent interactions between molecules forms the foundation for designing molecular gelators.

Varieties of molecular gelators have been developed from structurally diverse building blocks such as saccharides<sup>25</sup>, amino acids<sup>26</sup>, peptides<sup>27</sup> and complex organic structures (e.g. dendrimers<sup>28</sup> and poly aromatic compounds<sup>29</sup>). Several seminal works of dedicated research groups (namely; Shinkai, Weiss, John, Feringa & van Esch and Maitra) has contributed tremendously towards establishing structure-property (gelator-gelation) correlation.<sup>29,30</sup> Such a vast knowledge has been assisting in rationally designing

new and effective molecular gelators with desired functionalities, marking the next stage of development in the field of MGs.

### **1.3. Status Quo and Advantages of Molecular Gels**

In contrast to polymeric gels, the gelation mechanism of MGs is underpinned solely by supramolecular chemistry and non-covalent interactions during self-assembly. The most interesting aspect of supramolecular chemistry (hence, hierarchical self-assembly) is that a small molecular-scale modification alters the nature of self-assembled micro-structures, thereby changing the macroscopic properties of the resulting material.<sup>31</sup> In other words, self-assembly process enables the transcription of molecular functions onto the micro- or even macro-scale materials. Nature has demonstrated the prowess of hierarchical self-assembly by employing it in development and functioning of almost everything existing in the nature, e.g. DNA, viral capsids, cell-membranes, quaternary structures of proteins etc.<sup>32</sup> All these attributes of supramolecular chemistry can be exploited for developing MGs.

Moreover, with molecular gelators being simple organic molecules, it is quite accessible to either synthesize novel gelators by using natural/synthetic building blocks or introduce functional motif in the existing gelator framework. Therefore, by harnessing the principles of supramolecular chemistry and organic chemistry, it is possible to design molecular gelators with unique functionalities and develop gel-based material that exhibit desired properties. Applications of well-designed MGs have been successfully exemplified in various areas such as biomedicine<sup>5</sup>, art restoration<sup>33</sup>, crystal engineering<sup>34</sup>, gel-electrophoresis<sup>35</sup>, catalysis<sup>36</sup>, electronics and photonics<sup>5</sup>. In addition to this fundamental advantage, they also exhibit other unique qualities resulting from their

supramolecular nature. These qualities and diversity in gelator structures are illustrated below with appropriate examples:

### 1.3.1. Stimuli Responsiveness

MGs are intrinsically thermo-responsive; in essence they are thermoreversible. An increase in temperature disrupts self-assembly and triggers gel-to-sol transition; conversely, on cooling, gelator molecules re-assemble and undergo sol-to-gel transition. In addition to temperature, non-covalent interactions are also influenced by other chemical or physical perturbations. Hence, by incorporation of appropriate receptive unit in the gelator molecule, MGs can be programmed to undergo reversible sol-to-gel phase transition in response to external stimuli. MGs sensitive to variety of external stimuli (e.g. pH, ionic strength, metal ions, UV radiation, magnetic field, enzymatic reactions etc.) have been developed.<sup>37</sup> The expression of stimuli-responsive reversible phase transition renders MGs exploitable for developing new functional materials, such as sensors, actuators, molecular devices, etc.

Xu and co-workers have demonstrated that an amino acid-based hydrogel can be developed from enzyme-labile peptide precursor, Fmoc-tyrosine phosphate (**3**).<sup>38</sup> Peptide derivative **3** is inherently hydrophilic and readily dissolves in water. When the dilute aqueous solution of **3** was treated with alkaline solution of phosphatase enzyme, the phosphate group of **3** was cleaved by the enzyme, converting **3** to a relatively hydrophobic molecule **4** (Figure 1.5). The hydrolysis product, **4**, exhibited adequate hydrophilic-hydrophobic balance to induce its hierarchical self-assembly and gelation of water. Like-wise enzyme-mediated *in situ* formation of gelators from its precursors can

also be designed. Enzyme-stimulated gelation has important implications in developing screening systems for enzyme inhibitors and other biomaterials.

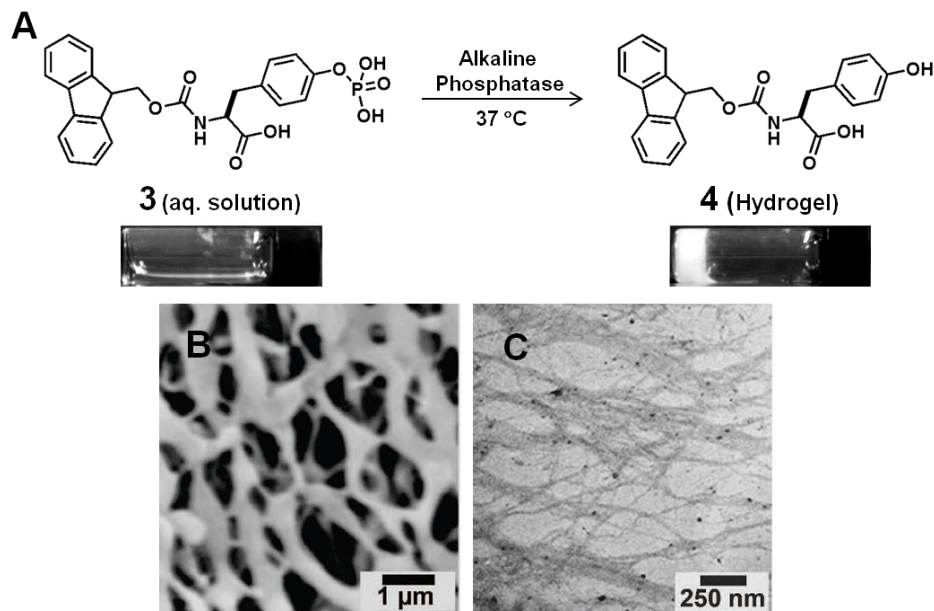


**Figure 1.5.** An enzyme induced gelation. A) Schematic representation of enzymatic conversion of precursor, **3**, to a hydrogelator, **4**, and their corresponding optical images. B) SEM and C) TEM images of hydrogel of **4**.<sup>38</sup>

Versatility of molecular gelators in exhibiting stimuli sensitivity has been substantiated by Liu et al.<sup>39</sup> Gallic acid-based gelator (**5**) was synthesized, which readily dissolves in organic solvents. On addition of silver ions ( $\text{Ag}^+$ ) the metal-ligand coordination bonding between  $\text{Ag}^+$  and pyridyl group of gelator induced aggregation, causing gelation of organic solvents. Owing to the number of receptive units present on the gelator's framework, the gelator exhibited reversible gel-to-sol transition in response to number of stimuli; namely halogen anions, pH and external binding agent (Figure 1.6). Additions of ethanolic solution of halogen anions ( $\text{X}^-$ ) to the gel, caused precipitation of  $\text{Ag}^+$  in the form of  $\text{AgX}$  and disrupted the aggregation, thereby transforming a gel to a sol

(Figure 1.6C). However, on addition of excess  $\text{Ag}^+$  to the sol, the gel was reformed (Figure 1.6D). Similarly, gel-to-sol transformation by dissociating the  $\text{Ag}^+$ -pyridyl coordination bond was triggered by variation in pH. Decrease in the pH of the organogels leads to protonation of pyridyl group, rendering it incapable of binding with  $\text{Ag}^+$ . On the other hand, increase in the pH triggers the reaction between  $\text{Ag}^+$  and hydroxide ion to form silver oxide, which lacks pyridyl-binding capability. Interestingly, these gels also exhibited similar reversible responses on diffusion of gases through the gel, such as  $\text{H}_2\text{S}$  and  $\text{NH}_3$  (Figure 1.6D and E).

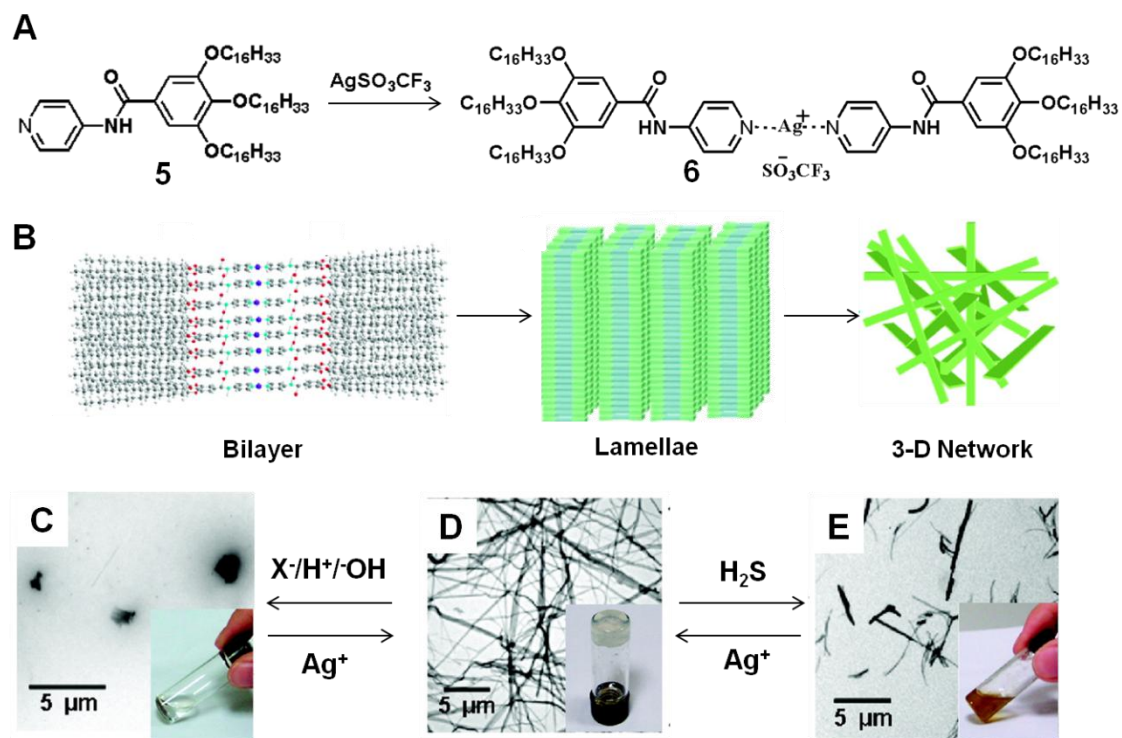


**Figure 1.6.** An example of metal ion induced gelation. A)  $\text{Ag}^+$  co-ordination scheme of **5**. B) Hierarchical self-assembly of **6** to yield gels. 1-D molecular stacking with the aid of H-bonding and  $\pi$ - $\pi$  stacking form a bilayer. Aggregation of bilayers to form lamellae, which in turn entangle to form a gel forming network. C-E) TEM image and corresponding photographs of reversible responsive behavior of **6** with respect to various stimuli.<sup>39</sup>

### 1.3.2. Biodegradable and Biocompatible

Cytotoxicity of gels is primarily a function of nature of the gelators, which in turn is related to the nature of its building blocks. Thus by selecting molecules that are harmless and for which metabolism pathway has been accurately documented (e.g. sugars, amino acids, peptides and lipids) biocompatible molecular gelators can be successfully designed. The resulting MGs (hydro-/ organogels) have been applied for making regenerative medicines, enzyme inhibitors, scaffolds, biomimetic materials, drug delivery systems etc. Molecular gels are rapidly emerging as promising materials for biomedical applications.<sup>40,41</sup>

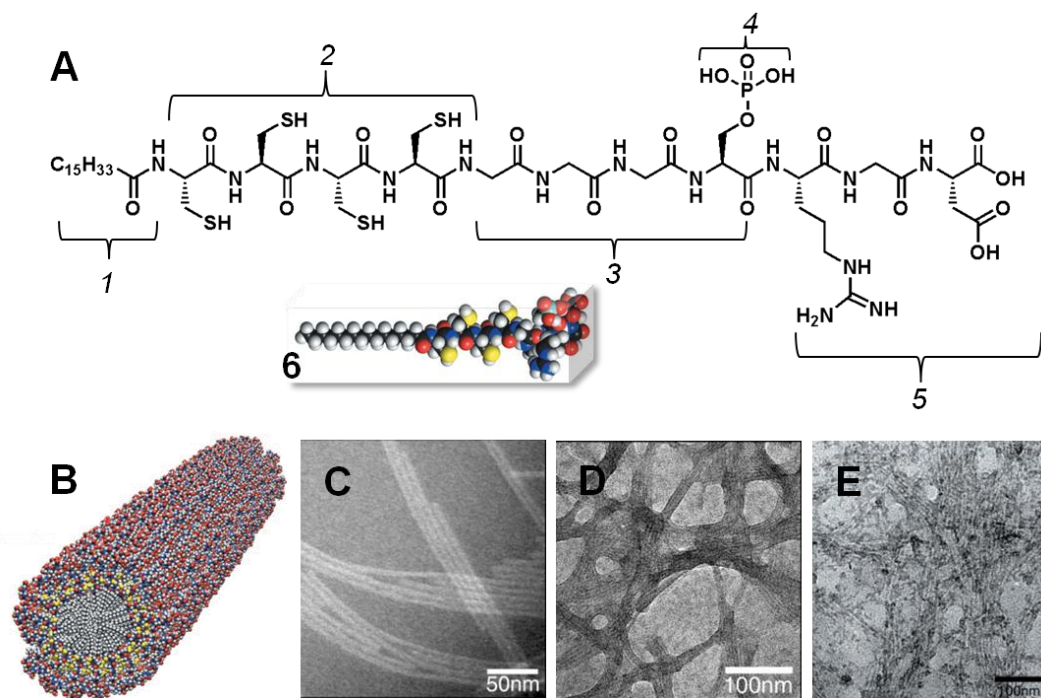


**Figure 1.7.** Biocompatible peptide for biomedical applications. A) Chemical structure of the peptide amphiphile, **6**, highlighting five key structural features. Molecular model of **6** in an inset. B) Self-assembled cylindrical micelle of **6**. C) TEM image of nanofibers of **6**, before oxidation. D) TEM image of nanofibers after oxidative cross-linking. E) TEM image of biomineralized and cross-linked nanofibers.<sup>42</sup>

Stupp and co-workers designed and fine tuned a biocompatible peptide-based gelator (**6**) for targeted biomineralization and tissue repair (Figure 1.7).<sup>42</sup> The amphiphiles consisted of 5 key structural features essential for hydrogelation and expression of desired function: (1) long hydrocarbon chain that provide hydrophobic character, endowing overall amphiphilicity to molecule; (2) four cysteine residues that can form disulfide bonds upon oxidation; (3) three glycine residues as flexible linker; (4) a phosphorylated serine residue to interact with  $\text{Ca}^{2+}$  ions and direct hydroxyapatite crystallization; and (5) the cell adhesion ligand RGD.

Peptide-amphiphile **6** formed hydrogel in acidic condition ( $\text{pH} < 4$ ). Later, the cysteine groups present in the self-assemblies were cross-linked, *in situ*, via Iodine mediated oxidation. Cross-linking imparts additional strength and stability to fibers. These reinforced fibers were able to direct mineralization of hydroxyapatite along the long axes of the fibers. The resulting biocomposite was found to be analogous to the alignment observed between collagen fibers and hydroxyapatite crystals in bone. By using similar design approach, a series of well-programmed peptide-based hydrogelators have been synthesized for specific biomedical applications like regenerative medicines and tissue engineering.<sup>43</sup>

Vemula et al. illustrated a novel method to develop efficient drug delivery systems: drug-fatty acid conjugated gelators (Figure 1.8).<sup>44</sup> Amphiphiles from the common drug acetaminophen (or N-(4-hydroxyphenyl) acetamide) was developed by conjugating it with fatty acids via ester linkage. These amphiphiles, especially **7**, were able to gel water at very low concentration ( $< 3$  %wt). **7**-based hydrogels exhibited excellent biocompatibility towards mesenchymal stem cells. The ester linkage renders

these gelators prone to lipase-mediated degradation. Thus, on treatment with lipase the gel was broken and the drug, acetaminophen, was released. Furthermore, the hydrogel matrix was also able to encapsulate model hydrophobic drug curcumin, effecting release of multiple drugs on enzyme-mediated degradation of gels. The rate of release of single/multiple drug can be controlled by regulating the temperature or enzyme concentration.

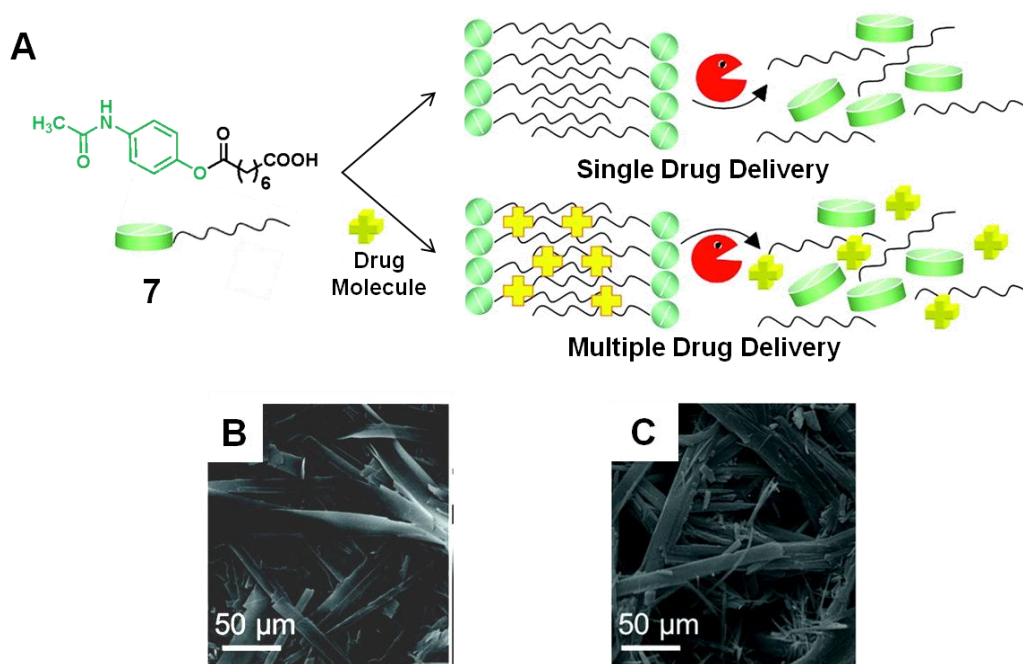


**Figure 1.8.** Drug-based molecular gels as drug-delivery vehicle. A) Molecular structure of **7** and schematic representation of single and multiple drug delivery. B) SEM micrographs of hydrogels of **7**. C) SEM micrographs of curcumin encapsulated **7** hydrogel.<sup>44</sup>

### 1.3.3. Amplification of Properties

The self-assembly process of molecular gelation induce unidirectional hierarchical arrangement of both molecular gelators and functional constituents attached

to it. Such high degree of precise molecular ordering enables expression of functionality in concerted manner causing amplification of the functional output, which otherwise is insignificant in the corresponding isotropic state.<sup>30i,45</sup>

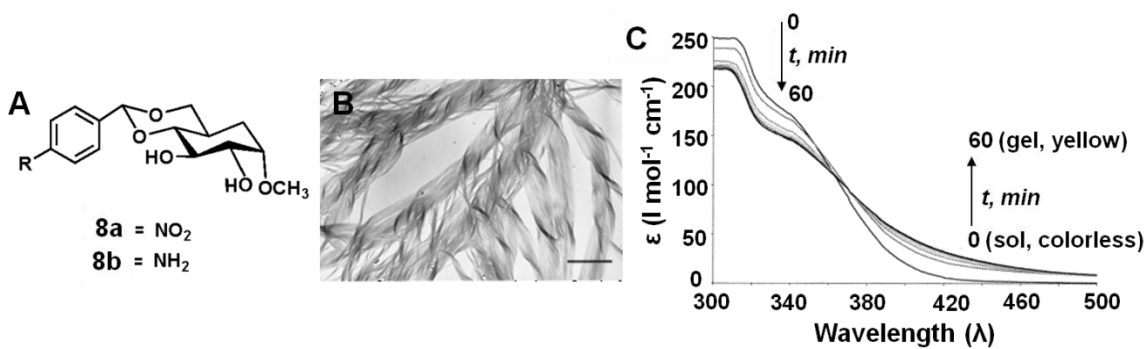


**Figure 1.9. Hierarchical** self-assembly induced enhancement of charge transfer. A) Molecular structures of **8a** and **8b**. B) SEM image of diphenyl ether gel (3 wt %) containing 1:1 molar ratio of **8a** and **8b**. Scale bar = 1  $\mu\text{m}$ . C) UV-Vis spectra of a 2 wt % sample of 1 and 2, in a 1:1 molar ratio, in octanol. At  $t = 0$  min the sample is completely dissolved, at  $t = 10$  min gelation occurs, and between  $t = 10$  and  $t = 60$  min the yellow color of the gel intensifies considerably.<sup>46</sup>

Shinkai's group reported a gelation enhanced charge transfer phenomenon in sugar-based organogelators (**8a-b**).<sup>46</sup> Sugar derivative **8a** contains a charge acceptor group, while **8b** contains a charge donor group. The 1:1 molar mixture of **8a** and **8b** were able to synergistically self-assemble and gel non-polar organic solvents like 1-octanol. TEM images of the gels revealed very large, helical bundles of intertwined fibers (250-500 nm in diameter). An interesting phenomenon was observed during gelation process, the sol of 1-octanol and 1:1 gelators was colorless (UV-vis  $\lambda_{\text{max}} = 335$  nm), whereas the gel itself was intense yellow (UV-vis  $\lambda_{\text{max}} = 420$  nm). The colorization during gelation process was attributed to the self-assembly induced increased donor acceptor interactions

(or charge transfer) between **8a** and **8b** (Figure 1.9). Such interactions are absent in the solution phase, hence, the sol appears colorless. Like charge transfer, energy and electron transfer between acceptor-donor systems is also enhanced in the gel state. Such phenomenon makes MGs conducive to developing light harvesting materials, light emitting diodes, transistors etc.

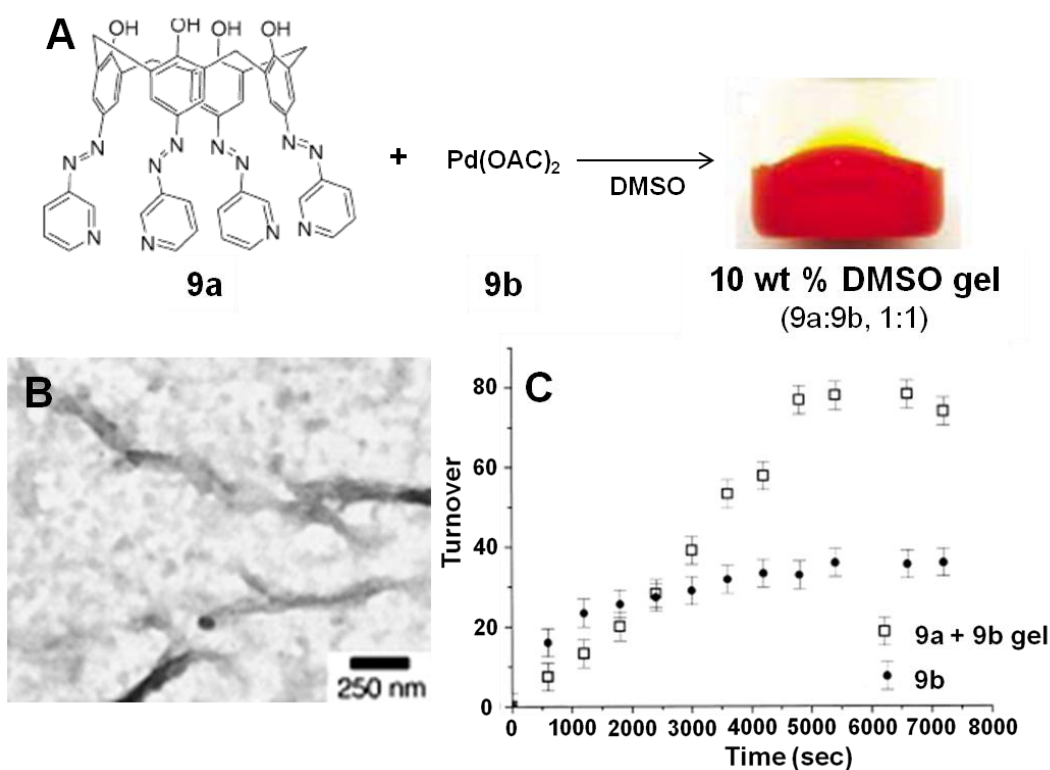


**Figure 1.10.** Amplification of catalytic activity in MG. A) Molecular structures of **9a**, **9b** and gelation scheme. B) SEM image of DMSO gel containing 1:1 molar ratio of **9a** and **9b**. C) The catalytic turnover of model reaction. Comparison of efficiency of gel over the catalyst **9b**.<sup>47</sup>

Property amplification attributes of MGs is also noticed in other systems like gels with catalytic activity. In one such study, Xu et al. utilized a DMSO gel system formed by metal-ligand co-ordination between pyridine based ligand (**9a**) and Pd(OAc)<sub>2</sub> (**9b**,

metal ion donor and catalyst) (Figure 1.10).<sup>47</sup> The resulting DMSO gels were stable in common organic solvents/water and at elevated temperature (>100 °C). Due to its robustness, the gels were analyzed for their catalytic activity. A model oxidation reaction, benzyl alcohol to benzaldehyde, was carried out by suspending the gel in the benzyl alcohol and bubbling air into the reaction mixture. The molar ratio of catalyst present in gel and benzyl alcohol was approximately 1:10<sup>4</sup>. After two hours, the catalytic turnover of the gel was found to be twice than that obtained by using **9b** as the catalyst. The higher activity of can be attributed to: i) the superior stability of catalyst in the gel; and ii) amphiphilicity of the nanofibers which enhances diffusion of the substrates from surrounding media to the catalytic sites in the gel and the vice-versa for the product.

#### 1.3.4. Well-defined Nano-architectures

Perturbations in molecular structure are known to significantly influence self-assembled structures. Similarly, in MGs the morphology of the aggregates present in the 3-D network can be optimized to desired form by varying the structure of molecular gelators. MGs containing vivid aggregates such as fibers, tubes, thin sheets, helical (chiral) and lamellar structures have been developed. These morphologies can be used as templates to produce microscopic 2-/3-D porous inorganic materials.<sup>48</sup> The resulting inorganic materials exhibit great potential in many fields. Controlled release of substance from hollow inorganic sphere, chiral inorganic materials for chiral catalysis, nanowires/nanobelts for nano-devices are few of the envisioned applications.

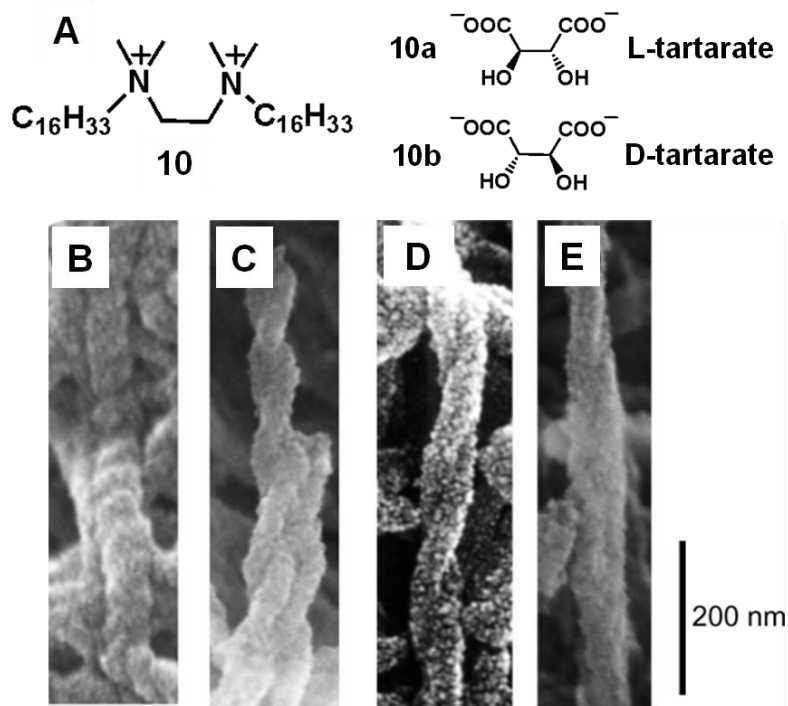


**Figure 1.11.** Helical structures of silica transcription on self-assembled amphiphiles. A) Cetyl trimethylammonium tartrate salts. **10a**: L-tartrate salts, **10b**: D-tartrate salts. B-E) TEM images of Silica transcription. Influence of the ee (L-1 in excess) on the helical pitch of transcribed double stranded silica: B, 100% ee; C, 50% ee; D, 33% ee; E, 20% ee.<sup>49</sup>

Oda et al. demonstrated the formation of helical silica structures by transcription of silica on the gel fibers made from cationic gemini amphiphiles and their chiral tartrate counter ions (**10a-b**).<sup>49</sup> The amphiphiles in presence of counter ions formed gels in both, organic solvents and water, by assembling to twisted fibers. Interestingly, the handedness of the ribbons and their helical pitch could be tuned systematically upon varying the ratio between L and D tartrate. The fine tuning capability of this system allowed well-defined transcription of chirality into the silica fibers (Figure 1.11). A typical sol-gel polycondensation process was employed for transcription. For instance, by using a gel made from either pure **10a** or **10b**, during polycondensation, silica fibers with respective

right or left handedness were obtained. In addition, the gel containing 1:1 ratio of **10a** and **10b** resulted in formation of double stranded helical structures. Similarly, diverse MGs have been explored as template to enable transcription of not only silica but also of other metals (Ag, Zn, Cu, Cd, Ti, W, Zr and Ba) and its derivatives (oxides, sulfides and sulfates).<sup>50</sup>

### 1.3.5. Hybridization with other Materials

Hybridization or composite formation typically involves homogeneous incorporation of one component in to the matrix of second component.<sup>51</sup> Usually the incorporated systems are in the form of particles, whiskers, fibers, lamellae or a mesh. The advantage of hybridization is that it enables combination of components with dissimilar properties in one material, possibly creating materials with superior or even novel properties compared to the original components. The well-defined 3-D network of molecular gels provides an ideal matrix for hybridization and has been utilized to develop novel functional materials with unique applications.<sup>52</sup>

Rao and co-workers have developed a novel nanocomposite consisting of a MG and single-walled carbon nanotubes (SWNTs), which displays interesting mechanical, thermal and electrical properties (Figure 1.12).<sup>53</sup> A triphenylenevinylene-based gelator (**11**) capable of gelling toluene and pristine-SWNT (pr-SWNT) or hexadecyl functionalized SWNT (C<sub>16</sub>-SWNT) was utilized for the study. SWNT-binding functionality of **11** (core aromatic rings) and relatively high solubility of SWNT in toluene was the rationale behind using toluene gel of **11** for developing the nanocomposite. Irrespective of type of SWNT used for hybridization, the properties of the composite were superior to those of bare **11**-toluene gel. The strong interaction

between SWNTs and gelator molecules reinforces the network of **11**-toluene gel and improve its viscoelastic and thermal properties. The doping of **11**-toluene gel with mere 0.25% of SWNT improved the mechanical strength by 20-fold.

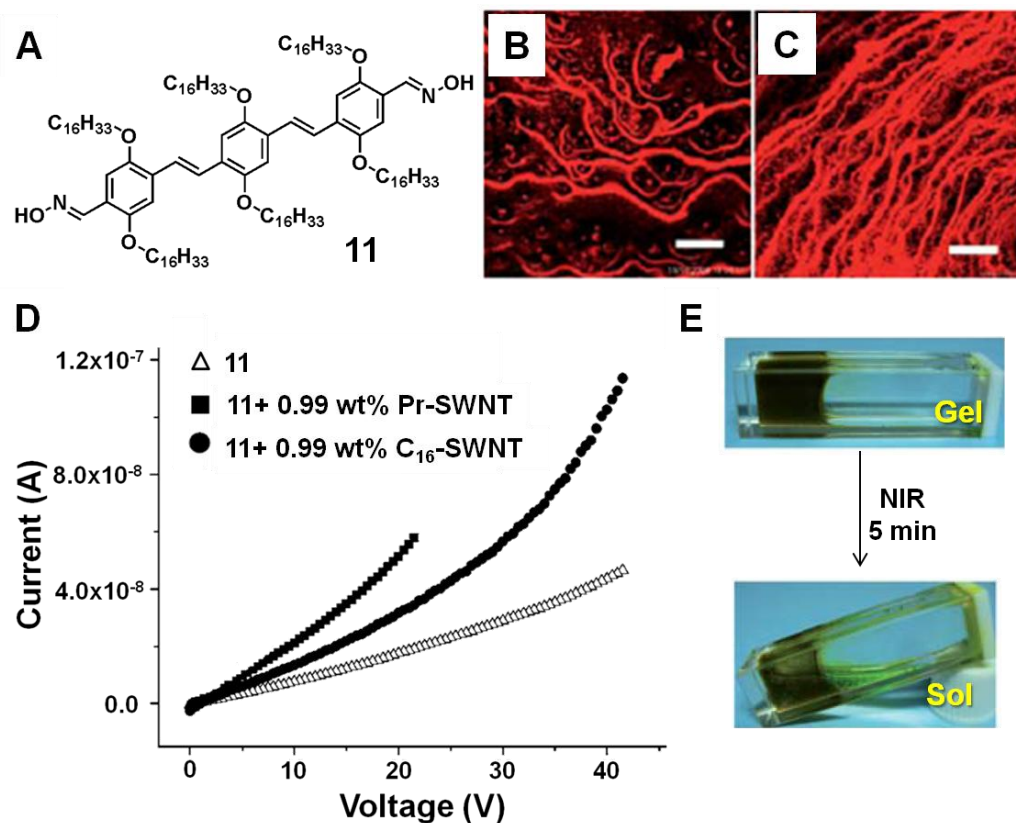


**Figure 1.12.** Hybridization of MG with carbon nanotubes. A) Molecular structure of **11**. B, C) Confocal microscope images (excitation at 488 nm) of dried fibers of **11** and **11**+Pr-SWNT gel. D) Current-Voltage measurement of **11**, **11**+Pr-SWNT gel and **11**+C<sub>16</sub>-SWNT gel. E) Irreversible gel-to-sol transition of **11**+Pr-SWNT gel on exposure to Near Infrared Radiation.<sup>53</sup>

The composite also displayed enhanced electrical conductivity by several folds compare to native gel. More astonishingly, the nanocomposite was found to be responsive to NIR (near infrared radiation). SWNTs are known to absorb in the NIR region and show NIR laser driven exothermicity, which disrupts the self-assembly and

trigger the irreversible gel-to-sol transition. NIR radiation is unreactive to biological systems. Thus, NIR responsive SWNT-MG composite could be used as a stimulus for controlled release drug-delivery.

#### **1.4. Challenges in Molecular Gels**

The ever increasing diversity in MGs applications is paralleled by its rising commercial popularity, which in turn pose a future prerequisite of (i) manufacturing feasibility of molecular gelators and (ii) adoption of type of synthetic technique. At present, like other commercial materials (e.g. polymers, fuels, synthetic chemicals), the development of molecular gelators is relies on depleting petroleum resources. Wide variety of molecular gelators (including sugar/amino acid based gelators) contains structural/functional motifs that are derived from non-renewable resources. Even though the designing of functional molecular gelators is accessible, their syntheses are frequently multi-step, involve energy intensive purification steps and require complex expensive catalysts. These aspects of molecular gels will impede its commercial operations. Hence, challenges still exist to identify biobased starting materials and develop efficient synthetic route for ensuring sustainable and environmentally benign advancement of molecular gels.

#### **1.5. Alternative Approach**

With paradigm shift from non-renewable to renewable resources being observed in chemical industry for economic and environmental concerns, integration of sustainable technology in scientific research has become of great significance.<sup>54</sup> The major oil crisis of 1970s and fast depletion of petroleum resources has emphasized the need to increase

reliance on biomass feedstock. In addition to utilizing biomass, the processes that transform them into valuable products are required to be selective, energetically efficient, high yielding, and environmentally benign. In this context, methodologies employing principles of biotechnology and green chemistry have been developed to yield pure products and consume less energy. Utilization of nature's catalyst, micro-organisms and enzymes, has dominated in new methodologies.<sup>55</sup> Such a concept of integrating biomass feedstocks with green processes to sustainably produce commodities analogous to petroleum refinery is termed as 'biorefinery' (Figure 1.13).<sup>56</sup> 'Technology Vision 2020: The US Chemical Industry' envisages 25% of the production of organic chemical products from renewable feedstocks by 2020. These collective efforts have resulted in manufacturing of valuable products such as resins, chemicals, solvents, and fuels from feedstocks such as starch, sucrose and cellulose.<sup>57</sup>

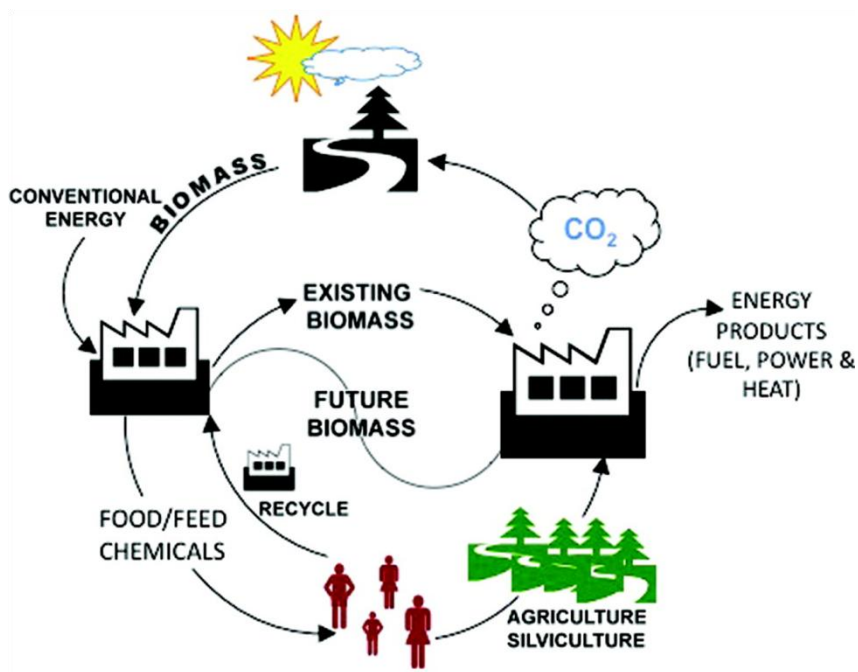


**Figure 1.13.** Schematic representation of a biorefinery concept.<sup>56</sup>

Nature offers a myriad of hydrophilic (sugars, proteins, nucleotides) and hydrophobic molecules (e.g. lipids, phytosterols, waxes, polyphenols) that can be exploited to tailor the amphiphilic structure for desired application. Hence from MGs perspective, natural building blocks can be utilized to exquisitely control the gelator's structure and consequently develop MGs for various uses. Adoption of biorefinery concept in development of molecular gelators will have a significant impact on the qualitative evolution of the field of MGs. The potential of biorefinery in developing functional molecular gelators has been demonstrated by John and co-workers (discussed in succeeding section).<sup>58</sup> Taking an inspiration from previous work, the current thesis embodies the same approach and demonstrates the efficiency of natural building blocks for generating biobased, multifunctional molecular gelators.

## **1.6. Biorefinery Concept for the Discovery of Molecular Gels**

Carbohydrates (cellulose, starch, lignocellulose) represent a major portion of biomass processed in biorefineries.<sup>57</sup> Different types of sugars with structural, stereochemical and functional differences are manufactured from natural resources. The resulting sugars can further be readily transformed to various products by chemical/microbial/enzymatic synthetic routes. Hence, they have emerged as a major class of platform chemicals to produce value-added chemicals such as phenols, hydrocarbons and fuel. Furthermore, sugars being poly-hydroxy entities, they are hydrophilic and provide structural motifs for H-bonding, one of the critical physical interactions required in molecular gelators. All of these attributes, such as high diversity, natural abundance and favorable reactivity, make sugars a prospective platform chemical for developing biobased molecular gelators.

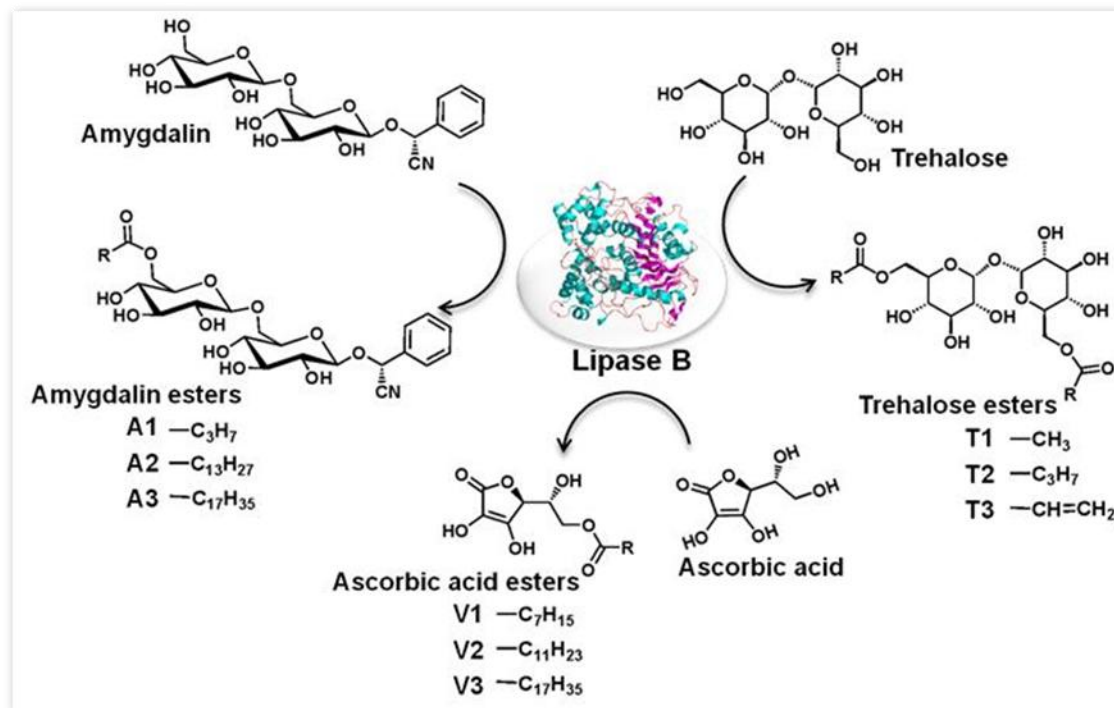


**Figure 1.14.** Enzyme-catalyzed regioselective synthesis of sugar amphiphiles. Sugars such as amygdalin, trehalose and ascorbic acid are shown in the figure.

John's group has demonstrated the feasibility of converting biomass-derived sugars and sugar-like compounds into molecular gelators, thereby highlighting them as an ideal platform for developing functional MGs.<sup>59</sup> Three compounds, namely amygdalin, trehalose, and ascorbic acid, were transformed into amphiphiles by appending a biobased hydrophobic group, fatty acids. Amygdalin and trehalose are natural sugars, whereas ascorbic acid is a sugar-like compound. Ascorbic acid is derived from a sugar, glucose, and has structural resemblance to ribose. Importantly, it demonstrates the prowess of biorefinery concept in developing functional molecular gelators. Highly regioselective lipase-mediated route (enzyme catalysis) was adopted for synthesis, which was optimized to produce amphiphiles in quantitative yield (Figure 1.14). It offers excellent control towards the introduction of acyl moiety on the primary hydroxyl group of sugars. The

amphiphiles showed exceptional hydro-/organogelation capabilities within a range of solvents (water or organic solvent). The resulting MGs exhibited their potential utility as drug-delivery systems and excellent templates for hybrid-nanomaterials synthesis. The sugar-gelator systems are detailed in the following sections.

### 1.6.1. Amygdalin-based Molecular Gels

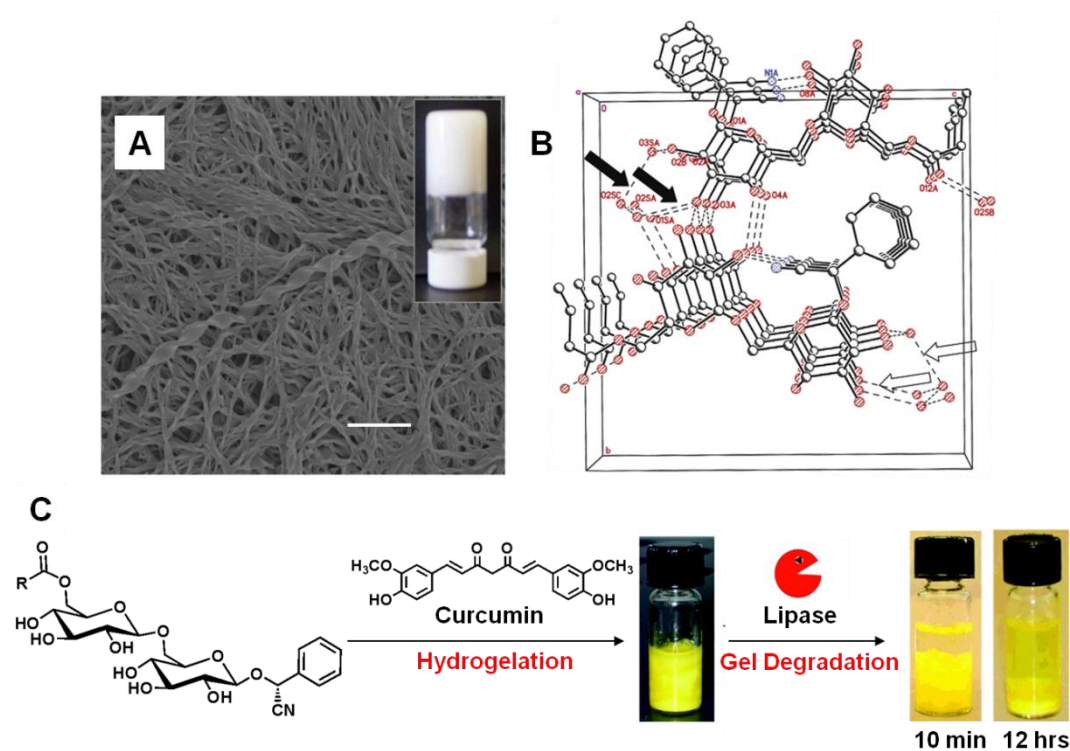


**Figure 1.15.** Amygdalin-based hydrogels as drug-delivery vehicles. A) SEM image of hydrogel of **A3**. Scale bar = 1 μm. B) Molecular stacking of amygdalin amphiphiles, proposed on the basis of single crystal analysis of **A1**. It exhibits  $\pi$ - $\pi$  stacking of phenyl rings and hydrogen bonding as key non-covalent interactions involved between two amygdalin molecules. (Red) Oxygen. (Blue) Nitrogen. (O) Carbon. (---) Hydrogen-bonds. C) Curcumin encapsulation in **A3** hydrogel and subsequent lipase-triggered gel degradation to control release curcumin.<sup>61</sup>

Amygdalin, a glycoside, is a bioproduct of fruit industry. It is typically solvent extracted from almond or apricot kernel. Commercially, it is used for production of laetrile.<sup>60</sup> Amygdalin-based amphiphiles were found to gel in a broad range of solvents, including both polar and nonpolar organic solvents in addition to water at extremely low concentrations (in the range of 0.05-0.2% w/v).<sup>61</sup> Non-covalent interactions like hydrogen bonding,  $\pi$ - $\pi$  stacking and van der Waals forces governed the self-assembly of amphiphiles. The microscopic analysis revealed that hydro/organogels display rich morphologies like grass-like nanostructures and helical ribbons (Figure 1.15).

The amphiphiles adjoining the non-toxic blocks, sugar and fatty acids, via an ester linkage, are expected to be both biocompatible and enzyme-labile. Furthermore, the inherent hydrophobic domains of self-assembled structures of hydrogels can be utilized as reservoirs for encapsulation of hydrophobic molecules. These features of amygdalin-based hydrogels were exploited to develop an enzyme-triggered drug-delivery system, as depicted in Figure 1.8. A model hydrophobic and chemotherapeutic drug ‘curcumin’ was encapsulated in the **A3** hydrogels. The 0.5 wt% hydrogel could solubilize very high concentration of curcumin; the solubilization power was ~33000 times greater than the solubility of curcumin in water. Subsequently, the drug was released by hydrolase-triggered breaking of the gel under physiological condition (~ 37 °C) (Figure 1.15). Importantly, the drug release kinetics could be modulated by altering the enzyme concentration and/or the temperature. Such hydrogels have the potential to increase the bioavailability of water-insoluble drugs while exhibiting excellent stability in the absence of a hydrolase enzyme without “leaking” the encapsulated drug.

### 1.6.2. Trehalose-based Molecular Gels

Trehalose is a disaccharide that consists of two glucose units linked by an  $\alpha, \alpha$ -1,1-glycoside bond. In nature, trehalose is found in cactus plants, invertebrates, and microorganisms, where it is used for preservation of membrane under anhydrobiotic conditions and for antioxidant capabilities.<sup>62</sup> Commercially, it is manufactured by enzymatic treatment of starch. The use of trehalose extends from food to pharmaceutical and cosmetic applications.<sup>63</sup>

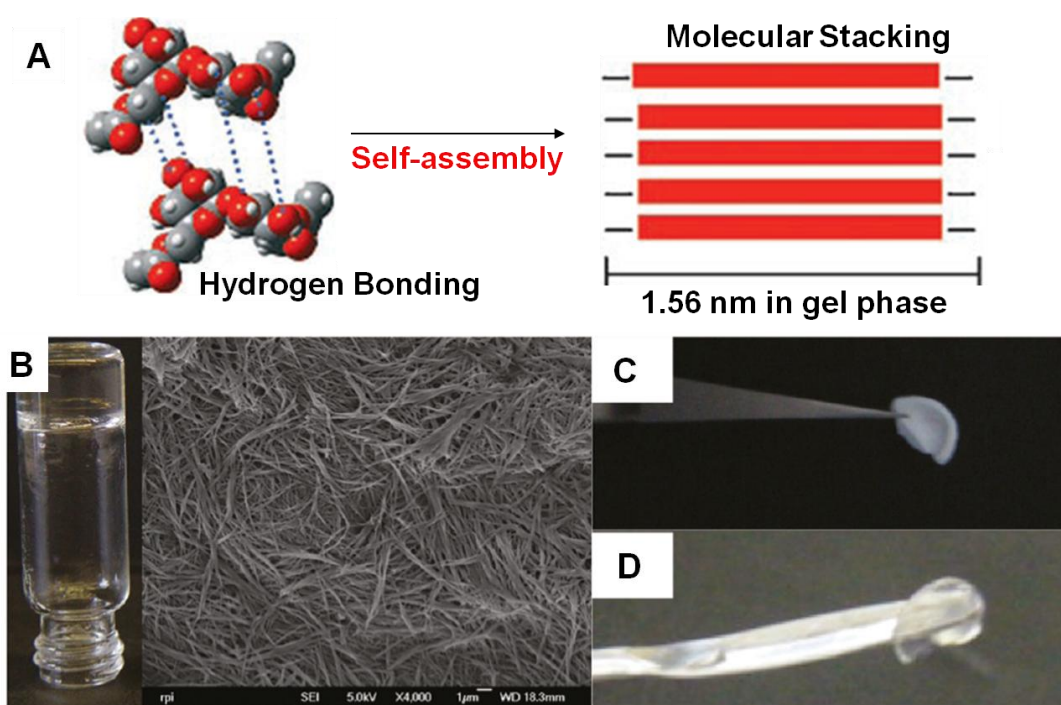


**Figure 1.16.** Trehalose-based gelators with very high gelation efficiency. A) Hydrogen bonding promoted interaction of **T1** (trehalose diacetate) leading to formation of a bilayer, which in turn results in gelation of organic solvents. B) SEM micrograph of an ethyl acetate gel of **T3** (trehalose diacrylate). Scale bar = 1 μm. The inset is a real image of the gel. C) Cross-linked **T3** xerogel in ethyl acetate. (D) Self-standing film of cross-linked **T3** xerogel upon soaking in water.<sup>64</sup>

A series of symmetrical diester amphiphiles was synthesized from trehalose by employing regioselective enzyme catalysis.<sup>64</sup> The symmetrical 6,6'-diesters, especially **T1**, exhibited gelation capability in organic solvents such as ethylacetate, isopropanol, acetone, and xylene at a concentration as low as 0.04 wt %/v, which is the lowest value reported for sugar ester gelators. As evidenced by SEM, the morphology of the gels was fibrous in nature, of several micrometers in length and with diameters in the range of 10-500 nm (Figure 1.16). The extensive hydrogen bonding of the sugar moieties of trehalose was the dominant intermolecular interaction that formed a rigid 3-D network. The presence of 6,6'-symmetrical alkyl chains was necessary for gelation, which could be specifically produced only by using enzymatic catalysis.

Gels containing polymerizable functional groups such as acrylate have been further modified by cross-linking the network. MGs of the diacrylate derivatives of trehalose upon exposure to UV-light in the presence of a photoinitiator formed excellent self-supporting transparent films. Typically, the gelation process was carried out with trehalose diacrylate (**T3**) in ethylacetate in the presence of a photoinitiator. The resultant gel was subsequently irradiated with UV light to initiate polymerization and lyophilized to obtain the free-standing scaffold. When immersed in water, scaffold produced a self-supporting transparent hydrogel. The water gelation tendency of the scaffold was similar to the phenomenon occurring in the cell walls of organisms and plants where trehalose forms a gel phase under the extreme desiccant conditions of nature and preserves the water content, thereby preventing cell disruption. Such a phenomenon observed in synthetic trehalose systems could be an initial step toward generating excellent scaffolds for tissue engineering applications.

### 1.6.3. Ascorbic Acid-based Molecular Gels

Ascorbic acid (or vitamin C) is abundant in citrus fruits and plants. Commercially, it is produced by fermentation of glucose. It is known to be capable of inhibiting lipid peroxidation and reducing metal ions to their lower oxidation state. It is commonly used as food-grade antioxidant and nutritional additive.

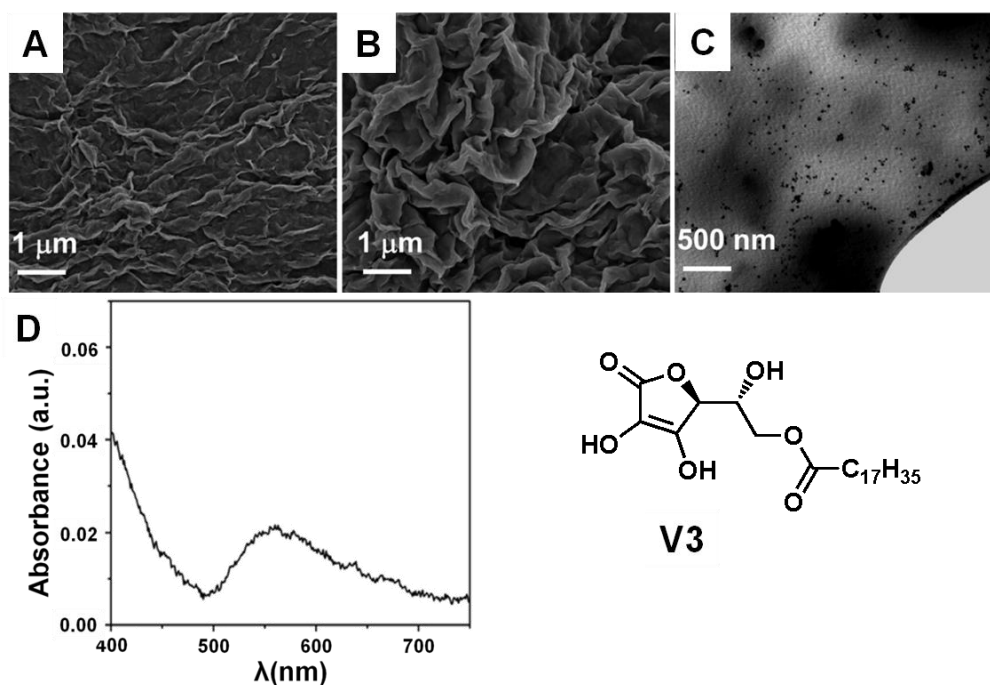


**Figure 1.17.** Alignment of metal nanoparticles via sugar-based MG. SEM images of **V3** hydrogel A) without and B) with AuNPs. C) TEM image of Au-NP embedded in **V3** hydrogel. D) Absorption spectra of AuNPs prepared in **V3** hydrogel. E) Schematic representation of entrapping site of AuNPs in the bilayer arrangement of **V3**.<sup>65</sup>

Ascorbic acid-based amphiphiles **V1**, **V2** and **V3** exhibited excellent self-assembly properties to generate hydro/organogels.<sup>65</sup> Hydrogen bonding and van der Waals interaction contributed towards hierarchical self-assembly of amphiphiles. Interestingly, ascorbic acid-based amphiphiles retained the metal reduction property,

which was exploited to generate metal nanoparticles (Figure 1.17). Gel formation, metal reduction and metal nanoparticle stabilization steps were performed simultaneously to yield vitamin C-based organic-inorganic hybrid materials. **A3**-based hydrogels reduced Au (III) ions, *in situ*, to generate Au-nanoparticles (AuNPs). This process was confirmed by performing a UV-visible spectroscopic analysis on hydrogel containing Au (III) ions; the appearance of a surface plasmon band at longer wavelength (555 nm) suggested the conversion of Au (III) of AuNPs. *In situ* preparation of Au-NPs in hydrogels was demonstrated for the first time. The scanning electron microscopy (SEM) and transmission electron microscopy (TEM) investigation of Au-NPs embedded hydrogels showed Au-NPs (18 nm) confined to sheet-like morphologies (Figure 1.17). The hybrid materials were found to be stable for months; the stability of material was attributed to the network of the hydrogel. The fibrous morphology of the network was believed to entrap Au-NPs and prevent their aggregation.

The advantages of *in situ* NPs preparation strategy are that (i) it eliminates usage of external reducing agent and (ii) it does not affect the inherent morphology of the gel. Previous attempts focused on externally doping Au-NPs in the hydrogel network, which resulted in drastic changes in the basic morphology of gel architecture. The current approach of the *in situ* synthesis of organic-inorganic hybrid materials was found to be a versatile method because the matrix itself acts as both a reducing agent and a stabilizing agent.

## 1.7. Origin, Objectives and Approach to the Thesis

The above three studies exemplify the bright prospect of incorporating biorefinery concept in the field of MGs. Even though the significance of the approach has been

adequately demonstrated, more varieties of sugars are still available that can be readily converted to amphiphiles, which would further establish the notion of developing biobased functional molecular gelators. One such class of unexplored sugars is sugar alcohols.

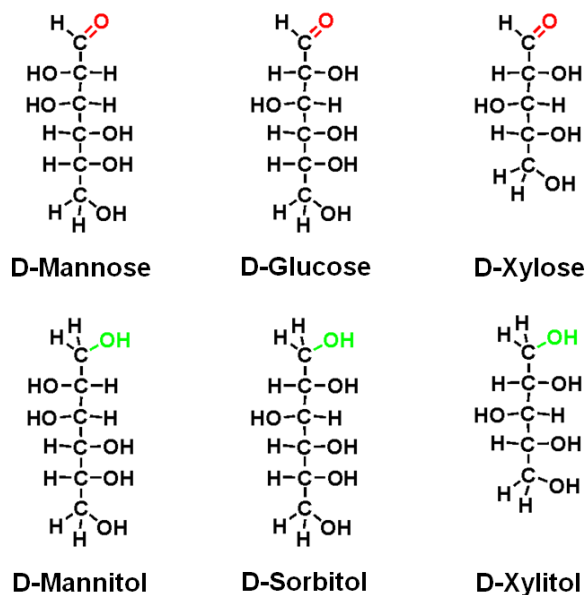


**Figure 1.18.** Fisher projections of molecular structures of sugars. The carbonyl group (red) is converted to alcohol group (green) during conversion of closed chain sugars to open chain sugars.

Sugar alcohols (also called open chain sugar or polyols) are chemically defined as carbohydrate derivatives in which a ketone or an aldehyde group has been replaced by a hydroxyl group (Figure 1.18). Commercially, they are produced by hydrogenation of sugars over Ni catalyst at high temperature and pressure.<sup>66,67</sup> Mannitol is obtained from fructose, sorbitol from glucose and xylitol from xylose. Because of the inherent problems associated with the hydrogenation process, safer and greener biosynthetic routes are gaining importance. Recently, microbes have been engineered to efficiently produce

sugar alcohols.<sup>67,68</sup> Specifically, versatile homofermentative lactic acid bacteria can be engineered to enable production of sugar alcohols from different sugars. Due to their positive health effects, sugar alcohols are primarily used as functional ingredients in various foods, cosmetics and pharmaceutical formulations.<sup>69</sup> For instance, sorbitol is commonly used in chewing gums as a low calorie sweetener and as an effective tooth decay preventive agent. Their properties are listed in the following paragraphs.

Similar to sugars, sugars alcohols too exhibit: (i) structural/stereochemical variations in their framework; (ii) hydrophilicity; (iii) presence of enzyme-reactive primary hydroxyl groups; and (iv) multiple hydroxyl groups required for hydrogen bonding. Thus, sugar alcohols possess all the elements to convert them to amphiphiles by adopting biorefinery concept. They should self-assemble and induce gelation of number of solvents. Interestingly, the absence of reducing groups (aldehydes and ketones) in sugar alcohols renders them chemically, physically and structurally different from typical sugars.<sup>70</sup> Some of the contrasting and intriguing properties of sugar alcohols are as follows:

1. The metabolism of sugar alcohols is not dependent on insulin.
2. Sugar alcohols are highly noncariogenic; i.e., they do not promote plaque of acid formation in the oral cavity. Rather, they stimulate salivation and consequently, promote remineralization of enamel.
3. They exhibit reduced physiological calorific value (~2.4 kcal/g), whereas those for glucose and sucrose are 3.75 and 3.94 kcal/g respectively.
4. Chemically they are more resistant towards acids, alkalis, and temperature.
5. They are non-reducing sugars.

6. Thermal stability is high; they are very stable up to 180 °C and do not readily caramelize.

Due to the different physico-chemical properties of sugar alcohols, the molecular gelators developed from them are expected to be functionally different compared to those derived from typical sugars. Therefore the aim of this thesis is to explore them as novel building blocks for generating unique molecular gelators and demonstrate possible applications of resulting molecular gels. Specifically, three representative molecules sorbitol, mannitol and xylitol were chosen for study. A series of amphiphiles was developed by appending fatty acid of different chain length to sugar alcohols. The amphiphiles were systematically investigated for their solvent gelation tendency and self-assembly mechanism to obtain structure-property (gelator-gelation) correlation. Finally, gelation capability of these novel gelators was utilized in developing materials for petroleum, agricultural and food applications.

---

## Chapter 2

---

### Sugar Alcohols-based Gelators: Structure-property Correlation Studies

---

#### 2.1. Abstract

*In this chapter, a novel class of gelators has been developed by conjugating sugar alcohols with fatty acids via an ester linkage. Enzyme-mediated regioselective transesterification reaction was employed as a synthetic scheme. The gelation efficiency of this class of gelators was systematically investigated by changing the chirality of sugar alcohols (mannitol, sorbitol and xylitol) and the acyl chain length of the fatty acids (C4-C14). The subtle structural variations in the gelator framework were found to induce significant morphological changes in the self-assembled structures; accordingly, the gelation efficiency was affected. Mannitol-based gelators produced fine fibrous aggregates, which are conducive for gelation. However, the gelators developed from its stereoisomers, i.e. sorbitol, self-assembled to form microcrystalline aggregates, which were comparatively inefficient in forming a gel from an organic solvent. The influence of gelator structure on the gelation mechanism was thoroughly investigated by utilizing spectroscopy, microscopy and diffraction techniques. In addition, an attempt has also been made to qualitatively understand the role of solvent in controlling the self-assembly, and hence gelation ability of gelators.*

#### 2.2. Introduction

Self-assembly is seen as an attractive bottom-up strategy to develop next generation functional soft matter.<sup>1</sup> Molecular gels (MGs) are one class of such soft

material that has garnered immense attention from diverse research community. They are of particular interest due to their non-polymeric nature, gel-to-sol reversibility, ability to form high-aspect-ratio assemblies, and biocompatibility. Different classes of starting materials such as sugars, amino acids and poly-aromatics have been utilized for the synthesis of molecular gelators.<sup>2</sup> Among these materials, simple sugars and sugar derivatives have emerged as versatile building blocks for developing novel gelators.

Sugars offer rich library of molecules, and isomers, which can be readily accessed to systematically tailor the structure of gelator and create MGs with controlled physical and chemical properties. Shinkai and co-workers developed an array of gelators from methyl-glucopyranosides, which exhibited gelation ability in water and/or organic solvents.<sup>3</sup> Interestingly, by utilizing configurational variety of monosaccharides they were able to manipulate self-assembling properties of gelators. Xu et al. showed that aminosaccharides like glucosamine can be used for making biocompatible hydrogels, which are useful for rapid healing of wounds.<sup>4</sup> Disaccharides like lactose and maltose have also been explored for creating efficient molecular gelators.<sup>5</sup> Moreover, the ease of appending different functional motifs on sugars has permitted designing of gelators for several applications. For instance, sugars integrated with chemical entities such as porphyrins<sup>6</sup>, polyaromatics<sup>7</sup> and nucleobases<sup>8</sup> were able to form molecular gels useful for light harvesting, electronic and biomedical purposes.

It is noteworthy to mention that sugar gelators reported in the literature are primarily derived from closed chain sugars. However, another abundant class of sugars, i.e., open chain sugars has remained practically underexplored. Ironically, one of the first molecular gelators reported in the literature is derived from an open chain sugar, sorbitol.

In 1891, Meunier discovered gels of 1,3:2,4-di-O-benzylidene-D-sorbitol.<sup>9</sup> Despite structural richness only few classes of gelators derived from open chain sugars (commonly known as sugar alcohols) have been reported. Based on a type of bond through which a hydrophobic moiety is linked to sugar alcohols, the gelators can be broadly classified as: i) Amide-based gelators<sup>10-15</sup>, and ii) Ether-based gelators<sup>16-19</sup>.

*i) Amide-based gelators*

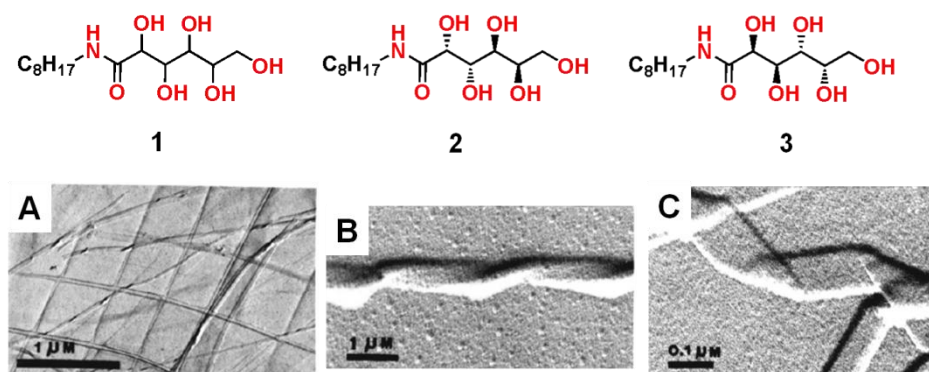


**Figure 2.1.** N-alkylaldonamides and electron micrographs of their aggregates in water. **1:** N-octyl-D-galactonamide. **2:** N-octyl-L-galactonamide. **3:** N-hexyl-D-galactonamide. A) Overview of D-galactonamide gel fibers. B) Left handed twist in ribbons made from **1**. C) Right handed twist in ribbons made from **2**.<sup>10</sup>

Fuhrhop and co-workers were the first to synthesize and investigate the gelation tendency of N-alkylaldonamides (NAA).<sup>10</sup> They were able to methodically demonstrate that the gelation and the aggregate morphology of aldonamides were greatly dependent on the stereochemistry of sugar alcohols. NAA were found to be exclusively hydrogelators. Only enantiomerically pure derivatives self-assembled in water to form fibrous morphology, resulting in gelation of water. For instance, N-octyl-D-galactonamide (**1**) produced hydrogels by forming fibers with left-handed twist, whereas

its L-enantiomer (**2**) produced fibers with right-handed twist (Figure 2.1).<sup>10c</sup> Recently, a hydrogel of N-hexylgalactonamide (**3**) was found to exhibit electroosmosis.<sup>11</sup> The hydrogen bonding induced increased acidity of  $\alpha$ -hydroxyl group was hypothesized to impart relative negative charge to the gel fibers, thereby causing the gel to promote electro-osmotic flow. This property of the hydrogel was utilized for developing: i) gel-based chromatography device; and ii) enzyme immobilized bioreactor.

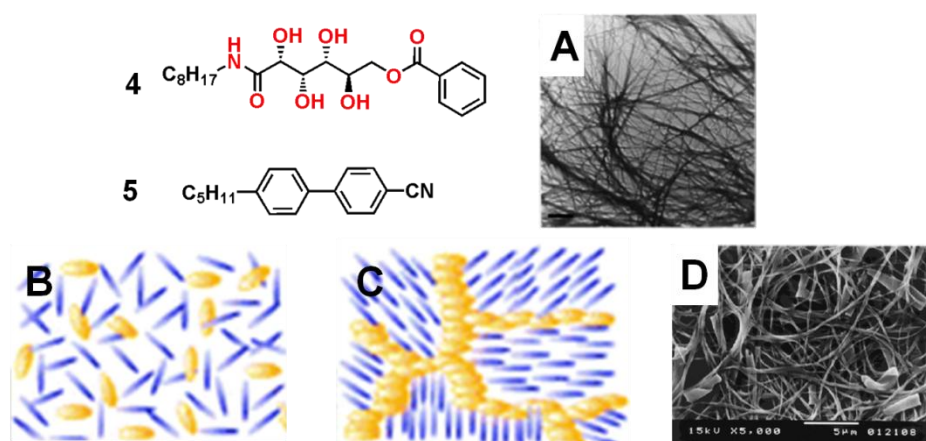


**Figure 2.2.** Organo and liquid crystalline gels from functionalized N-alkyl-D-alDONamide. **4**: N-octyl-D-gluconamide-6-benzoate, an organogelator. **5**: 4-cyano-4-n-pentylbiphenyl, a mesogen. A) A TEM image of a gel of **4** in chloroform. Scale bar 1.6  $\mu\text{m}$ . B,C) Schematic representation of isotropic liquid and fibrous structures of **4** in liquid crystalline material **5**. D) SEM image of aggregates of **4** in **5**.<sup>12,13</sup>

NAA-based organogels were developed by Nolte and co-workers.<sup>12</sup> The free primary hydroxyl group of NAA was functionalized with various hydrophobic moieties to enable them to self-assemble in non-polar solvents. N-octyl-D-gluconamide-6-benzoate (**4**) was able to gel in a range of organic solvents by forming fibrous structures (Figure 2.2A). Intermolecular interactions like hydrogen bonding, van der Waals forces and  $\pi$ - $\pi$  stacking played a collective role in stabilizing aggregates in a hydrophobic

environment. Kato et al. utilized the organogelation ability of **4** to gel mesogenic molecules and consequently produce liquid-crystalline physical gels (a gel-based composite material).<sup>13</sup> The gels primarily consisted of fibrous aggregates of gelators in the liquid-crystalline phase of mesogenic molecules (Figure 2.2D). Owing to the presence of aligned liquid crystalline materials within the network, the gels exhibited unique optical properties and were responsive to electric field.

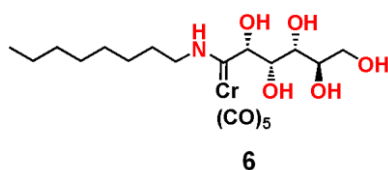


**Figure 2.3.** Organometallic isolable of gluconamide, an organogelator.

Organometallic isolobal analogue N-octyl-D-gluconamide (**6**) exhibited organogelation tendency in chlorinated and aromatic solvents (Figure 2.3).<sup>14</sup> It is the first example of organometallic molecular gelator bearing a direct transition metal-to-carbon

bond. The presence of transition metallic entity directly bonded to gelator enable hierarchical self-assembly of metal atoms, which are potential catalytic sites. Hence, such gels are of relevance to supramolecular catalysis.

### ii) Ether-based gelators

The most studied ether-based sugar alcohol gelators is 1,3:2,4-di-O-benzylidene-D-sorbitol (**7**).<sup>16</sup> It is able to gel both organic liquids and polymer melts through hydrogen-bonding mediated self-assembly process. **7** predominantly form fibrillar aggregates with diameters in the range of 10 nm to 0.8  $\mu\text{m}$ . Organogelation property of **7** is of industrial importance and is used in developing biomedical materials and polymer composites.<sup>17</sup>

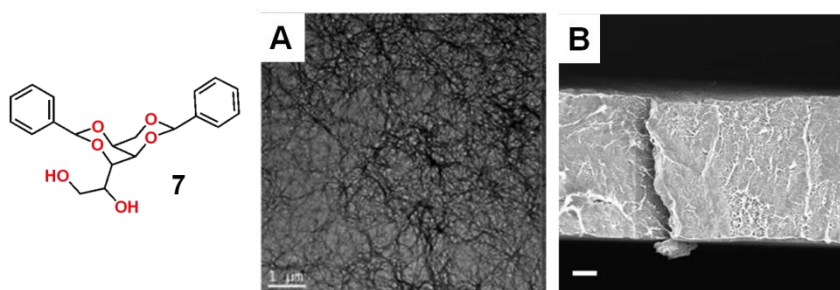


**Figure 2.4.** Benzylidene derivative of sorbitol, an ether-based gelator. A) SEM image of organogel of **7** (2 % wt/v) in styrene melt. B) A cross sectional SEM image of poly(L-lactic acid) crystal made by using fibrous scaffold of **7**.<sup>19</sup>

Wilder et al. produced a **7**-based dental composite.<sup>18</sup> **7** was able to gel the dental monomer, ethoxylated bisphenol A dimethacrylate (EBPADMA), thereby improving its mechanical strength and handling. The self-assembling ability of **7** in polymer melts have been extensively utilized as scaffolds by many research groups to develop polymer nanocomposites and porous materials (Figure 2.4 A,B).<sup>19</sup>

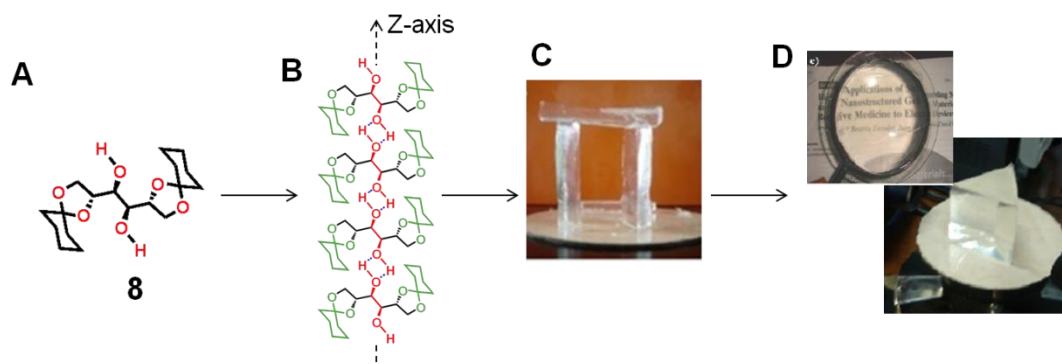


**Figure 2.5.** Strong gels made from sugar alcohol organogelators. A) Molecular structure of cyclohexane ketal derivative of mannitol (**8**). B) Unidirectional self-assembly of **8** in organic solvents. C) Self-standing gel of **8** in pump oil (0.23% wt/v). D) Soft optical devices such as planoconvex lens and prism made from gels of **8** in mineral oil.<sup>20</sup>

Recently, Sureshan et al. described the synthesis of mannitol-based amphiphiles.<sup>20</sup> Specifically, the amphiphiles were diketal derivatives of mannitol, i.e. the polyol part flanked by ketal motifs on both ends (Figure 2.5). The amphiphiles exhibited excellent gelation ability in linear alkanes and aromatic solvents, with an average minimum gelation concentration of <0.5 wt %. The two types of intermolecular forces—hydrophobic and hydrogen bonding, existing between the respective ketal and polyol motifs, synergistically contribute towards an efficient self-assembly. The linear alkane gels of **8** were mechanically strong, highly transparent with low UV transmittance (glass-like refractive index  $n \sim 1.5$ ) and exhibited self-healing ability. Such unique blend of properties enabled development of soft optical devices such as flexible lenses and prism (Figure 2.5).

The aforementioned studies exemplify that sugar alcohols indeed are resourceful starting materials for designing molecular gelators conducive for niche applications. Yet, very few gelators have been developed from sugar alcohols. Moreover, apart from N-aldonamides, the sugar-alcohol based gelators have not been investigated for structure-property correlation studies. In this chapter, a new class of gelators has been developed. The two primary hydroxyl groups present on the sugar alcohols have been functionalized with fatty acids to yield ester-based gelators. Biorefinery concept has been integrated in the study to develop a sustainable method for the synthesis of gelators.<sup>21</sup> In addition, an attempt has been made to initiate the investigation of structural effect of gelator on gelation abilities.

## 2.3. Results and Discussion

### 2.3.1. Synthesis of Ester-based Sugar Alcohol Gelators

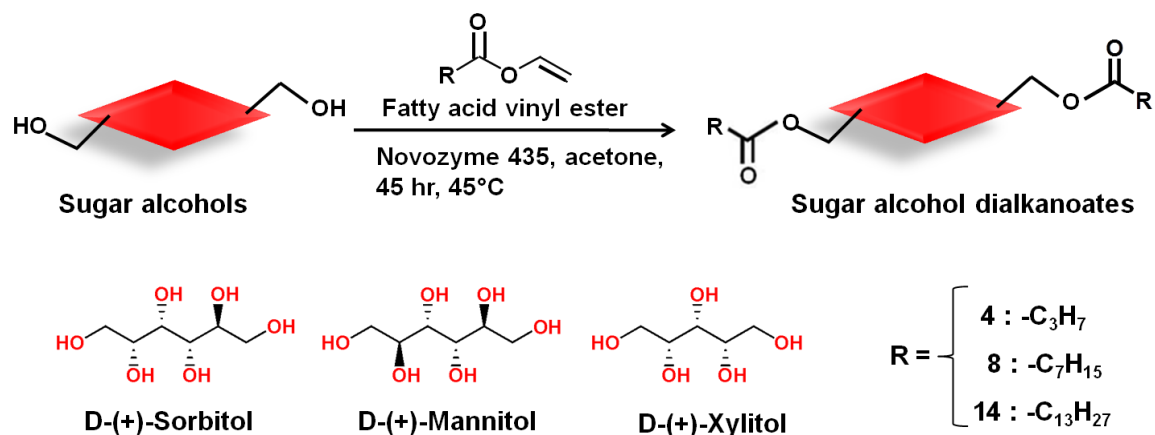


**Figure 2.6.** Schematic representation of enzymatic catalysis of sugar alcohols.

Mannitol, sorbitol and xylitol were chosen as representative candidates to study the effect of subtle structural variation present in them on gelation ability. The amphiphiles were synthesized by enzyme mediated trans-esterification of sugars with fatty acid donors. Novozyme 435 (*Candida Antartica* Lipase B) was used for trans-esterification. The reaction is mild, single step and highly regioselective, i.e., only the two primary hydroxyl groups of sugars are acylated. The typical synthesis scheme for gelators is shown in Figure 2.6. The overall yield is approximately 75% for all derivatives. Tuning of hydrophobicity is achieved by using fatty acids of different alkyl chain lengths; butyric acid ( $\text{C}_4$ ), caprylic acid ( $\text{C}_8$ ) and myristic acid ( $\text{C}_{14}$ ). The ease of synthesis and abundant natural occurrence of sugar alcohols translate into low cost production of sugar-based gelators. The developed amphiphiles are typically denoted by a

letter followed by a number, e.g., M8 is an amphiphile having a mannitol head and two C<sub>8</sub> tails.

### 2.3.2. Gelation Studies

The synthesized sugar alcohol gelators were investigated for their gelation capability in organic solvents (polar and non-polar) as well as in water. For this chapter, the maximum concentration of gelator at which its gelation ability was studied was prefixed at 5 %wt/v, a common notion observed in the field of molecular gelators. In other words, if the concentration of gelator required to immobilize a solvent was greater than 5%, the gelator was considered to be inefficient in gelling that solvent. The gelation efficiency of a gelator was characterized in terms of minimum gelation concentration (MGC) and gel-to-sol transition temperature ( $T_{\text{gel}}$ ).

MGC is defined as minimum amount of gelator (g) required for forming a volume filling and solvent entrapping 3-D network in 100 mL of given solvent. Since, gelation is an incomplete crystallization of gelator molecules; the MGC is analogous to the supersaturation point in the formation of crystals. The degree of phase separation of the self-assembled aggregates from the solvent differentiates crystallization from gelation; the former being on a macroscopic scale, while the later on a micro/ nanoscopic scale.  $T_{\text{gel}}$  represents a temperature range beyond which the solvent immobilization tendency of a gelator network is lost, i.e., the gel starts flowing like a viscous liquid. The loss of gelation is triggered by heat induced dissolution of fibers in the solvent. It indicates the thermal stability of gel; higher the  $T_{\text{gel}}$  value greater is the thermal stability. The gelling efficiency of a gelator is inversely proportional to MGC values, where as it is directly proportional to  $T_{\text{gel}}$  values.

The gelation capability of sugar alcohol gelators is summarized in Table 2.1. The mannitol and sorbitol-based gelators were found to be exclusive organogelators, capable of gelling a wide range of organic liquids – acyclic and cyclic hydrocarbons, aromatic solvents and vegetable oils. Xylitol-based amphiphiles were unable to gel any of the studied organic liquids, rather precipitated from its isotropic solution. Minimum gelation concentration (MGC) for all the organogels was found to be in the range of ~1.5-5 % wt/v. Gels made from sorbitol-based gelators were more translucent compared to those made from mannitol-based gelators (Figure 2.7). All the organogels exhibited thermal reversibility with excellent thermal and temporal stability. The gel-to-sol transition temperature ( $T_{\text{gel}}$ ) for all the gels was determined at the concentration of 5 % wt/v using tube inversion method. Depending on the organic liquid, the  $T_{\text{gel}}$  was found to be in the range of 82-125 °C for mannitol gelators and 38-69 °C for sorbitol gelators (Appendix 1).

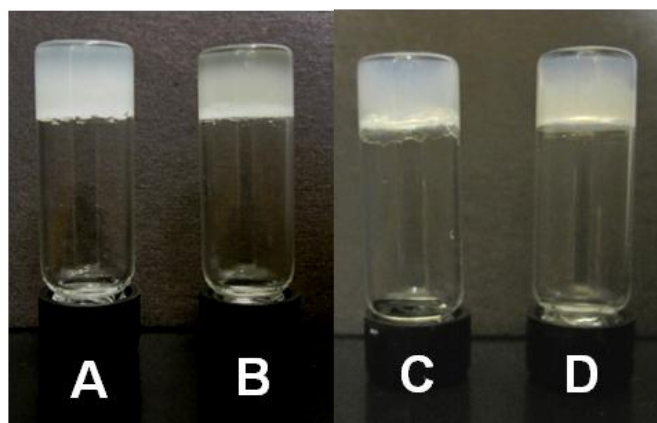


**Figure 2.7.** Photographs of gels made by using sugar alcohol dialkanoates. A, B) M8 gel of toluene and 1,8-dibromooctane (5% wt/v) respectively. C, D) S8 gel of toluene and 1,8-dibromooctane (5% wt/v) respectively.

**Table 2.1.** Molecular gelation efficiency of sugar alcohol dialkanoates.<sup>a,b</sup>

<b>Solvents</b>	<b>M4</b>	<b>M8</b>	<b>M14</b>	<b>S4</b>	<b>S8</b>	<b>S14</b>
HCs (n<10) <sup>c</sup>	<b>P</b>	<b>P</b>	<b>P</b>	<b>P</b>	<b>P</b>	<b>P</b>
Dodecane	<b>P</b>	<b>G</b> 2.50	<b>G</b> 2.50	<b>P</b>	<b>G</b> 5.00	<b>G</b> 4.50
1-bromododecane	<b>G</b> 4.00	<b>G</b> 3.33	<b>G</b> 1.67	<b>P</b>	<b>G</b> 3.33	<b>G</b> 3.33
Methylaurate	<b>G</b> 4.28	<b>G</b> 1.00	<b>G</b> 1.40	<b>P</b>	<b>P</b>	<b>G</b> 3.33
1-bromooctane	<b>G</b> 4.00	<b>G</b> 3.00	<b>G</b> 2.50	<b>G</b> 5.00	<b>G</b> 3.33	<b>G</b> 3.33
Methyloctanoate	<b>G</b> 4.28	<b>G</b> 1.67	<b>G</b> 3.00	<b>P</b>	<b>PG</b>	<b>C</b>
2-octanone	<b>G</b> 3.75	<b>G</b> 1.00	<b>G</b> 4.00	<b>P</b>	<b>C</b>	<b>P</b>
Octanamine	<b>S</b>	<b>S</b>	<b>S</b>	<b>S</b>	<b>S</b>	<b>S</b>
Octanol	<b>G</b> 4.28	<b>G</b> 1.67	<b>G</b> 3.33	<b>P</b>	<b>S</b>	<b>PG</b>
Octanoic acid	<b>G</b> 4.28	<b>G</b> 2.00	<b>G</b> 3.33	<b>S</b>	<b>C</b>	<b>G</b> 5.00
1,8-dibromooctane	<b>G</b> 3.00	<b>G</b> 1.67	<b>G</b> 2.50	<b>G</b> 3.75	<b>G</b> 2.50	<b>G</b> 2.00
Cyclohexane	<b>G</b> 3.00	<b>G</b> 2.50	<b>G</b> 3.33	<b>G</b> 3.00	<b>G</b> 2.50	<b>G</b> 3.33
Benzene	<b>G</b> 2.50	<b>G</b> 1.50	<b>G</b> 1.67	<b>G</b> 3.25	<b>G</b> 3.00	<b>P</b>
Toluene	<b>G</b> 2.50	<b>G</b> 1.50	<b>G</b> 1.4	<b>G</b> 3.00	<b>G</b> 2.50	<b>P</b>
Squalene	<b>P</b>	<b>G</b> 2.00	<b>G</b> 1.00	<b>P</b>	<b>G</b> 2.50	<b>G</b> 1.670
Mineral Oil	<b>PG</b>	<b>G</b> 1.20	<b>G</b> 0.91	<b>PG</b>	<b>G</b> 1.50	<b>G</b> 1.40
Canola Oil	<b>G</b> 4.00	<b>G</b> 1.00	<b>G</b> 1.4	<b>G</b> 5.00	<b>G</b> 3.00	<b>G</b> 2.00

<sup>[a]</sup> X8 is not shown in the table, as it precipitated in all of the tested organic solvents. G = gel; PG = partial gel; P = Precipitate; C = crystalline needle-like precipitate. <sup>[b]</sup> Values next to 'G' are MGC values of corresponding gelator (% wt/v, mg/100 mL). <sup>[c]</sup> HC (n<10) represents hydrocarbons such as hexane, heptane, octane and iso-octane.

### 2.3.3. Morphology of Organogels

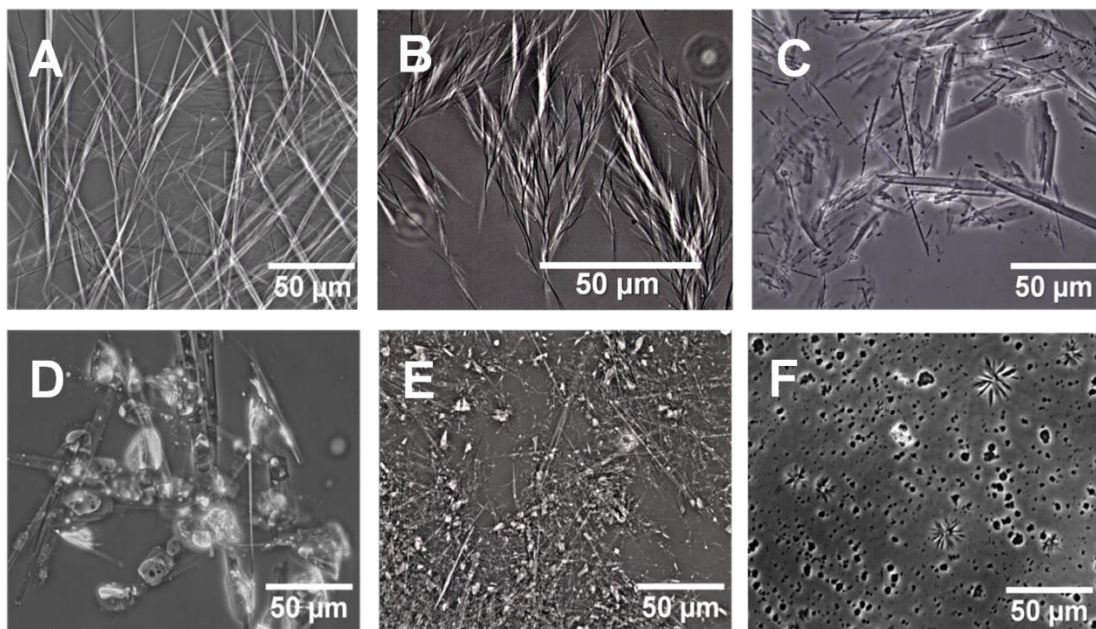


**Figure 2.8.** Optical micrographs of gels of 1,8-dibromooctane. A) M4, B) M8, C) M14, D) S4, E) S8 and F) S14.

The morphologies of gels were characterized by using optical (for high boiling solvents, e.g. mineral oil) and electron microscope (for volatile solvents, e.g. toluene). The preliminary analyses of optical micrographs revealed that the two sugar alcohol-based gelators self-assembled in organic liquid in two different modes. Mannitol-based gelators produced uniformly dispersed fiber-like aggregates exhibiting fractal type of growth (Figure 2.8 A-C). In contrast, the sorbitol-based amphiphiles produced needle-like small crystalline aggregates with randomly distributed microcrystalline aggregates (Figure 2.8 D-F). Similar structures were observed for the sugar gelators in all of the tested organic liquids.

SEM images of toluene gels are consistent with the optical microscopy results. The SEM image of the M8 gel of toluene (Figure 2.9A) shows that the fibers are actually

flat ribbons with width in nanometer range and the gel network is presumably an entangled mesh of these ribbons. The needle-like aggregates of S8 gel of toluene consisted of ill-defined microcrystalline platelets ( $\sim 2\text{-}10\ \mu\text{m}$ ) (Figure 2.9C). The micron-size crystals result in small void places to entrap the organic liquid; a probable rationale for sorbitol-based gelators' comparatively higher MGC and lower  $T_{\text{gel}}$  values. The SEM images of cyclohexane gels showed no significant difference in morphology compared to their respective toluene gels. M8 gel was found to consist of sheets-like structure; the morphology can be considered to be resulting from fusion of ribbons during drying process as few ribbons like structure can also be observed in the image (Figure 2.9B). Cyclohexane gel of S8 consisted of similar microcrystalline platelets (Figure 2.9D).

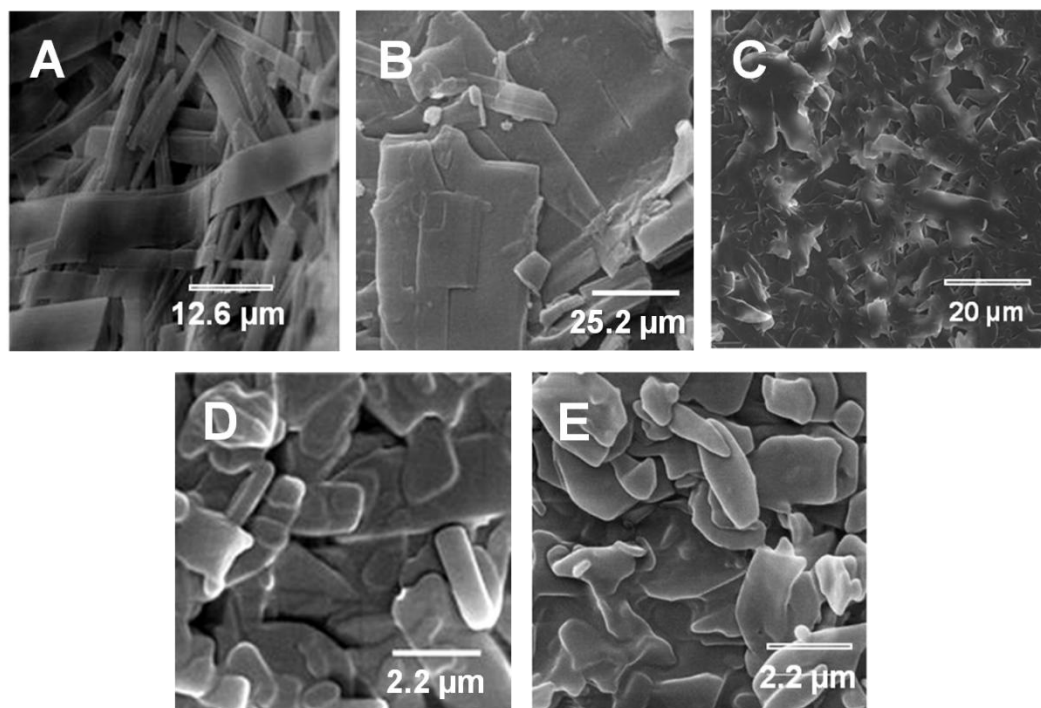


**Figure 2.9.** SEM images self-assembled structures of sugar alcohol-based amphiphiles. A) M8-toluene gel, B) M8-cyclohexane gel, C) S8-toluene gel, D) S8-cyclohexane gel, and E) X8 aggregates in cyclohexane. In above all experiments, gelator concentration was 2.5 % wt/v.

Though the Xylitol derivative (X8) lacked gelling ability, it is believed that it will exhibit self-assembling tendency owing to its amphiphilic nature. Its morphology resulting from the cyclohexane isotropic solution was observed, and it was found to exhibit crystalline platelets similar to that of S8 (Figure 2.9E). Therefore, its incapability to form a gel can be attributed to its inability to form a continuous network from the aggregates.

#### **2.3.4. Effect of Solvents on Gelation Efficiency**

The major driving force for amphiphiles to exhibit self-assembly, and hence gelation, is its ability to interact with other gelator molecules. The self-assembly of gelators reported in this chapter also depend on their propensity to exhibit inter-gelator interactions (as described in the later section of this chapter). However, in addition to such interactions, the solvent-gelator interactions are also critical for a gelator to induce gelation. In the literature, different gelation behavior of a particular gelator has been observed by changing the type of the solvent.<sup>22</sup> Hence, understanding the solvent-gelator interaction is important to correlate the gelation efficiency of a gelator to its molecular structure.

In general, during gelation process several specific (e.g. hydrogen bonding) and non-specific intermolecular forces (e.g. dispersion and van der Waals forces) exist between gelator-gelator and solvent-gelator molecules. The gelator-gelator interactions govern the crystallization process, whereas solvent-gelator interactions dictate the solubility of gelator molecules in solvent. The dominance of one of the interaction over the other will disrupt the gelation ability of a gelator. Hence, maintaining a critical balance between these two interactions is essential for an effective gelation of a solvent.

As observed from the gelation table (Table 2.1), the sugar alcohol gelators precipitated out from octane (a hydrocarbon), but formed gels in longer chain hydrocarbons (mineral oil, silicon oil and pump oil), which indicates that there is an association of the hydrocarbon chain with the alkyl chain of gelators. Due to an inefficient interaction of short chain hydrocarbons with the gelator, the gelator-gelator interaction outweighed the solvent-gelator interaction, resulting in precipitation of gelator assemblies. More interestingly, on introduction of a functional group (bromo) on the C<sub>8</sub> hydrocarbon (1-bromooctane), the gelators were able to form stable gels. The tendency of bromine atom to interact with the hydroxyl groups of gelators via dipole-dipole forces can be attributed to impart gelation ability to sugar amphiphiles.<sup>23</sup> The introduction of functional groups capable of exhibiting intermolecular forces increases solvent polarity and its solvation power towards gelators. Consequently, the precipitation of gelator assembly is inhibited, resulting in gelation of the solvent. Thus, the solvent properties indeed play a vital role in directing the gelation process of sugar alcohol-based gelators. To further understand the influence of degree of association between solvent and gelator on gelation process, solvent polarity was systematically varied by changing its functionality or its chain length.

Figure 2.10A and B depicts the effect of different functionalities attached to C<sub>8</sub> solvent on the gelation ability of mannitol-based gelators (M4, M8, M14). The solvents are arranged in increasing order of polarity (monohalohydrocarbons < dihalohydrocarbons < amines < esters < alcohols < acids).<sup>24</sup> A clear trend is observed in all the three gelators. Initially, the gelation efficiency of the gelator increased with the polarity of the solvent (from mono- to dihalohydrocarbons), indicated by the lowering of

the MGC values. However, further increment in the solvent polarity (ester, alcohol and acid) lowered the gelation efficiency of gelators, indicated by increasing MGC and decreasing  $T_{gel}$  values.

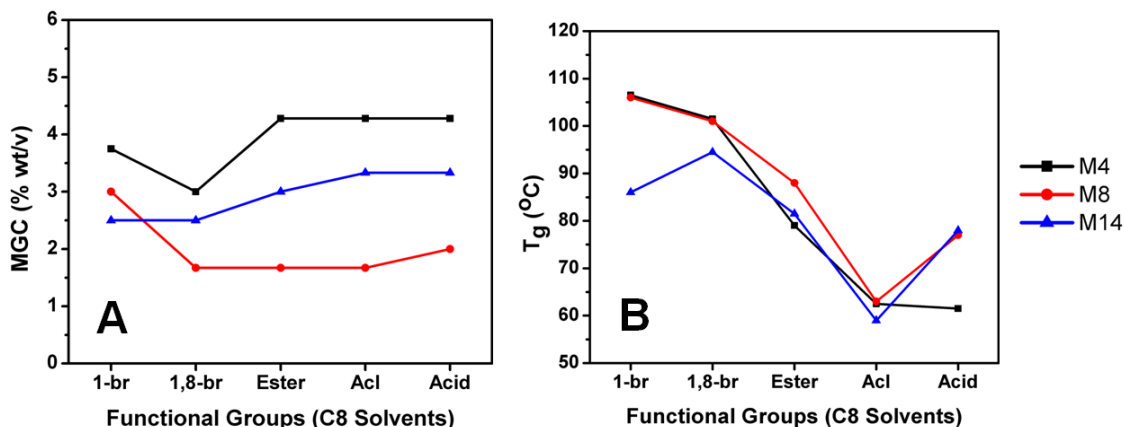


**Figure 2.10.** Effect of solvent's functional groups on the gelation efficiency of mannitol-based gelators. A) Variation in MGC values, and B) Variation in  $T_{gel}$  values. *Legends:* - 1-br: 1-bromooctane; 1,8-br: 1,8-dibromooctane; Ester: methyl octanoate; Acl: octanol; Acid: octanoic acid.

Solvents with high polarity are expected to interact with gelator to a greater extent. This disrupts the inter-gelator interactions, thereby compromising their self-assembly process and gelation efficiency. One notable exception to the observed trend is octanamine. Amines being relatively non-polar than esters, the sugar gelators were expected to gel octanamine. On contrary, the gelators readily dissolved at cutoff gelator concentration (5% wt/v). The cause of this behavior is unclear, but it indicates that more intricate solvent-gelator interactions may exist in addition to solubility and dipole-dipole interaction.

Another parameter that can influence solvents' polarity is the length of its hydrocarbons. Compared to the functional groups, the influence of chain length on

solvent polarity is modest. However, it is sufficient enough to alter the gelation efficiency of gelator molecules. Solvents such as monohalohydrocarbons, alcohols and esters were chosen as model class of solvents, and within each solvent class the hydrocarbon chain length was varied from C4-C12. M8 was used as a representative gelator. The MGC and  $T_{gel}$  graphs (Figure 2.11A and B, Appendix 2) indicate enhancement in gelation efficiency with lengthening of hydrocarbon chains. The increase in solvent chain length favorably decreased its solvation power, in such a way that the solvent-gelator interactions was weakened and gelator-gelator interaction was enhanced to assist the gelation process rather than precipitation of gelators.

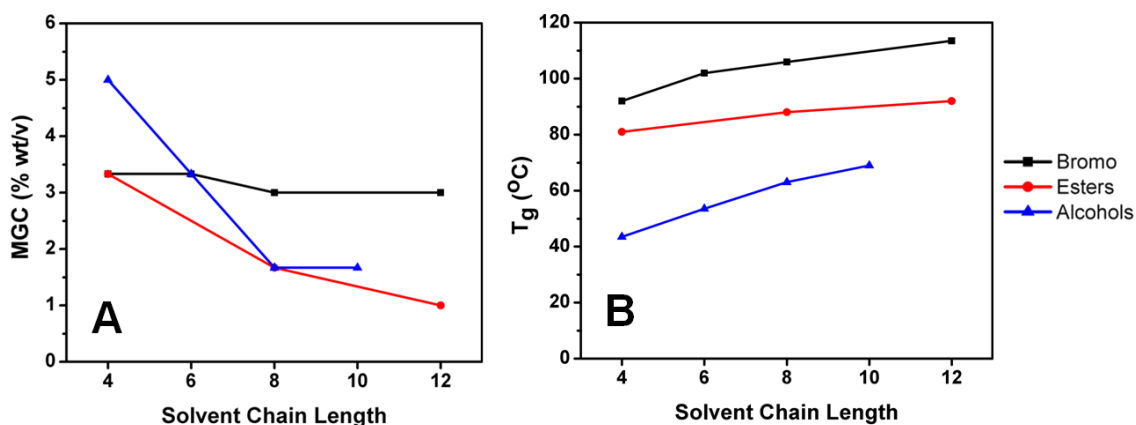


**Figure 2.11.** Effect of length of solvent's hydrocarbon chain on the gelation efficiency of mannitol-based gelators. A) Variation in MGC values, and B) Variation in  $T_{gel}$  values.

These findings indicate that the presence of gelator-interacting functional groups on solvent molecule is essential to induce gelation of a solvent. The degree of solvent polarity and solvent-gelator interaction dictates the gelation efficiency of developed sugar-alcohol based gelators.

### 2.3.5. Effect of Acyl Chain Length on Gelation Efficiency

After understanding the role of solvent, the influence of gelator structure on the gelation efficiency was investigated. At first, the influence of acyl chain length of gelator on its gelation ability was examined; the results for mannitol-based gelators are shown in Figure 2.12A and B. For most of the tested organic solvents, the gelation efficiency of gelators was found to increase on increasing the length of acyl chain of the gelator from C4 to C8. However, further increment from C8 to C14 resulted in decrease in the gelation ability, represented by increase in MGC and decrease in  $T_{gel}$  values.

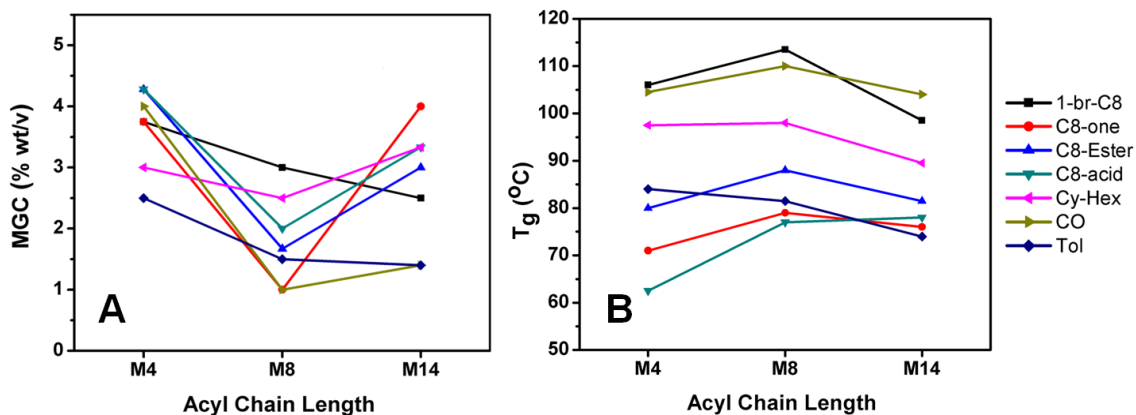


**Figure 2.12.** Effect of acyl chain length (4-14) of gelator on the gelation efficiency of mannitol-based gelators. A) Variation in MGC values, and B) Variation in  $T_{gel}$  values. *Legends:* - 1-br-C8: 1-bromooctane; C8-one: octanone; Ester: methyl octanoate; C8-acid: octanoic acid; Cy-Hex: cyclohexane; CO: canola oil; Tol: toluene.

Increase in acyl chain length of a sugar amphiphile is known to improve its lateral hydrophobic interactions, which in turn enhances the inter-amphiphilic interactions and its melting point.<sup>25</sup> In present case similar melting point trend was observed as well; the melting point order was M4 (114-116 °C) < M8 (123-125 °C) < M14 (132-133 °C). Thus, the propensity of mannitol-based gelators to self-aggregate can be considered to get

better with increase in chain length. Initially, such enhancement favored the self-assembly of gelator molecules in solvents leading to better gelation efficiency. However, beyond C8 derivatives, presumably the greater inter-gelator interactions dominated the solvent-gelator interactions leading to fast aggregation and low gelation efficiency. The above rationalization can be enlightened by referring to the difference in morphology of M4, M8 and M14 gels of 1,8-dibromooctane (Figure 2.8A-C).

The M4 gelator aggregated to form long, rigid and broader fibrous structures, resulting in formation of inefficient less-dense 3-D network. However, in case of M8 the longer length of acyl chain favorably improved the inter-gelator interaction to form fine and flexible fractal fiber. The resulting fine fibrous structures produces dense network conducive for efficient gelation of solvent. Further increase in the acyl length to 14 caused the gelator to form random rod-like crystallites, indication of rapid aggregation of gelator molecule from solvent. Such crystallites results in smaller void spaces in the 3-D network, thereby decreasing the gelation efficiency of the gelator.

By analyzing the data shown in Figure 2.12 and Table 2.1, it can be concluded that the optimum chain length for the mannitol-based gelators is in between 8-10. At these chain length, the gelators possess critical balance between hydrophilic (sugar head group) and hydrophobic (acyl chain length) interactions to exhibit efficient gelation tendency. Thus, mannitol gelators with C8 chain length were chosen as representative gelators for further structural studies. Similar solvent-dependent and alkyl chain dependent studies could not be carried out for the sorbitol-based gelators, as they were unable to gel most of the investigated solvent. Nonetheless, the propensity of sorbitol

gelators to gel a solvent was found to increase with decreasing the solvent polarity and increasing the alkyl chain length.

### 2.3.6. Effect of Sugar Head Group on Gelation

Out of the three types of sugar alcohols utilized for producing gelators only mannitol and sorbitol-based gelators exhibited gelation ability. Xylitol derivative, specifically X8, was unable to gel in any of the studied organic liquids, instead precipitated out from the liquid. The number of hydroxyl groups in xylitol compared to sorbitol and mannitol can be accounted for the precipitation of xylitol derivatives from the organic liquids. Xylitol has one less hydroxyl group compared to other sugars, due to which the hydrophilic group of xylitol derivatives may not be able to effectively interact with each other to form extended self-assembled structures (like fibers, sheets etc.) essential for the gelation.

On comparing the properties of the gels obtained from mannitol and sorbitol-based gelators, a clear distinction between them can be observed. Gels made from mannitol-based gelators were opaque, while gels of sorbitol-based gelators were translucent. Based on MGC and  $T_{gel}$  values (Table 2.1 and Appendix 1), gelators derived from mannitol were found to be more efficient gelators compared to those from sorbitol. Interestingly, mannitol and sorbitol are stereoisomers of each other. The only difference between them is the orientation of the hydroxyl group at C2 position of the sugar moiety. As a result, the dissimilarity in the gelation ability can be attributed to the chirality difference between the sugars. It is believed that the chirality affects the directionality of the intermolecular interactions, which in turn affects the self-assembly pattern of amphiphiles.<sup>26</sup> To further gain an insight on the effect of sugar head group on the gelation

mechanism, Fourier transform infrared radiation (FT-IR) and X-ray diffraction (XRD) experiments were conducted on both the gelator powders as well as the corresponding gels.

During the self-assembly process, the amphiphile molecules self-organize with the aid of intermolecular interactions. Thus, the wavenumbers of vital vibrational groups of amphiphiles (like hydroxyl, amide, carbonyl and alkyl) are found to be strongly influenced in the self-assembled state compared to the isotropic solutions.<sup>27</sup> Accordingly, the influence of self-assembly on frequencies of the functional groups of sugar alcohol gelators was probed by using FT-IR spectroscopy. The extent of interaction of the hydroxyl and aliphatic moieties was observed in an isotropic, gel and solid crystalline states. The results with assignments of vital group frequencies are given in Table 2.2 and Figure 2.13A and B.

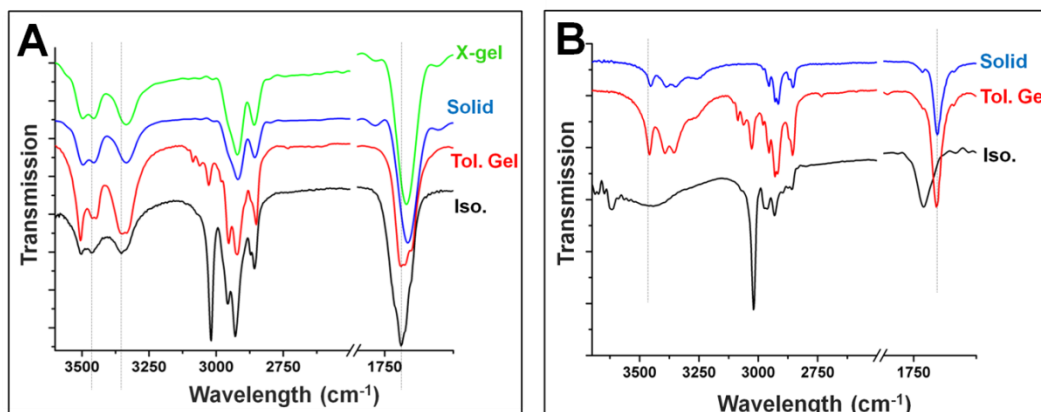


**Figure 2.13.** FT-IR spectrum of different samples of gelators. A) M8 and B) S8. *Legends:* - X-gel: xerogels of toluene gel; Solid: neat crystalline powder of gelator; Tol. Gel: toluene gel; Iso.: isotropic solution of gelator in chloroform.

It is evident that the wavenumbers of characteristic functional groups of powder samples of M8 and S8 are on par with their respective toluene gel samples, indicating that

the sugar amphiphiles in the gel state may exhibit similar aggregation mode as in the crystalline state. A distinct shift observed in the wavenumbers corresponding to hydroxyl groups between the sol and gel states indicates the participation of these groups in hydrogen bonding. Hydrogen bonding is believed to play a vital role in the formation of self-assembled network, and thus in imparting gelling ability to the sugar alcohol gelators. This hypothesis was demonstrated by blocking the hydroxyl groups through benzylidene complex formation. The benzylidene complex of M8 was not able to gel in organic liquids; rather it was easily soluble. Thus, confirming the hypothesis that hydrogen bonding, and hence hydroxyl group, play a constructive role in the formation of a network capable of entrapping solvents.

**Table 2.2.** Observed wavenumbers ( $\text{cm}^{-1}$ ) of the vital vibrational groups of M8 and S8.

		hydroxyl groups	carbonyl stretch	-CH <sub>2</sub> stretching		-CH <sub>2</sub> bending
				symmetric	anti	
<b>M8</b>	Solid	3334, 3455, 3495	1708	2855	2918	1458, 1464 <sup>d</sup>
	Iso. <sup>a</sup>	3352, 3465, 3503	1720	2856	2929	1456
	Gel <sup>b</sup>	3340, 3453, 3503	1709	2850	2920	1458, 1465
	Xerogel <sup>c</sup>	3335, 3455, 3496	1709	2858	2920	1460
<b>S8</b>	Solid	3350, 3388, 3454	1703	2853	2928	1470
	Iso. <sup>b</sup>	3616, 3443	1730	2858	2930	1468
	Gel <sup>c</sup>	3353, 3392, 3457	1704	2855	2929	1471

<sup>[a]</sup> Iso. = Isotropic solution in CHCl<sub>3</sub>. <sup>[b]</sup> Tol. Gel. = Toluene Gel. <sup>[c]</sup> X-Gel = Xerogel. <sup>[d]</sup> Shoulder to 1458 was observed at 1464  $\text{cm}^{-1}$ .

IR spectroscopy also has proved to be a critical tool in comprehensively determining the conformation of an alkyl chain in the self-assembled structures of an amphiphile.<sup>28</sup> Depending on the methylene C-H stretching and C-H bending modes the conformation of an alkyl chain in the gel state of the sugar alcohol gelators was proposed. For M8 samples (powder and gels) the symmetric and anti-symmetric methylene stretching peaks were observed at  $2850\text{ cm}^{-1}$  and  $2920\text{ cm}^{-1}$  respectively, typical for all-trans conformation of alkyl chain. However, for S8 samples the respective peaks appeared at higher wavenumbers chiefly at  $2855\text{ cm}^{-1}$  and  $2929\text{ cm}^{-1}$  suggesting the all-trans conformation of alkyl chain in the assembled S8 but with increased gauche conformation. The alkyl chains interact proficiently when they are in all-trans conformation, and for a strong interaction one should expect splitting of methylene bending peak (at  $\sim 1470\text{ cm}^{-1}$ ) to give two peaks of equal intensities. The splitting of methylene bending peak into two equal intensity peaks at  $1465\text{ cm}^{-1}$  and  $1458\text{ cm}^{-1}$  was observed for M8 samples, whereas for S8 the splitting of corresponding methylene bending peak at  $1471\text{ cm}^{-1}$  was not observed. Thus, it can be concluded that in case of M8 the alkyl chain interaction is more efficient and can be one of the probable reasons for its better gelation tendency than its stereoisomer.

XRD experiments were conducted on both the gelator powders and their corresponding gels. The measurements enable determination of the mode of packing and the length of longest repeating unit in the self-assembled structure.<sup>29</sup> Figure 2.14 shows the XRD patterns of neat powder of M8 and S8. The analysis of these patterns reveals that the Bragg spacing ratio between the subsequent peaks are in the ratio of 1:1/2:1/3 for M8 (2.96, 1.49 and 0.68 nm) and S8 (2.38, 1.11, 0.81 and 0.612 nm). Such spacing ratio

of subsequent peaks is characteristic of lamellar packing, and the mono-layer molecular stacking is its longest repeating unit. Thus, in the crystalline state the gelators stack together to produce lamellar structures with periodicity of 2.99 and 2.38 nm for M8 and S8 respectively. In addition, sharp scattering peaks were observed in the  $d$ -spacing range of 0.35-0.5 nm, indicating the subcell packing of the hydrocarbon chains.<sup>30</sup> Note that the periodic length of M8 is considerably greater than S8, indicating the influence of chirality of sugar group on the self-assembled structure.

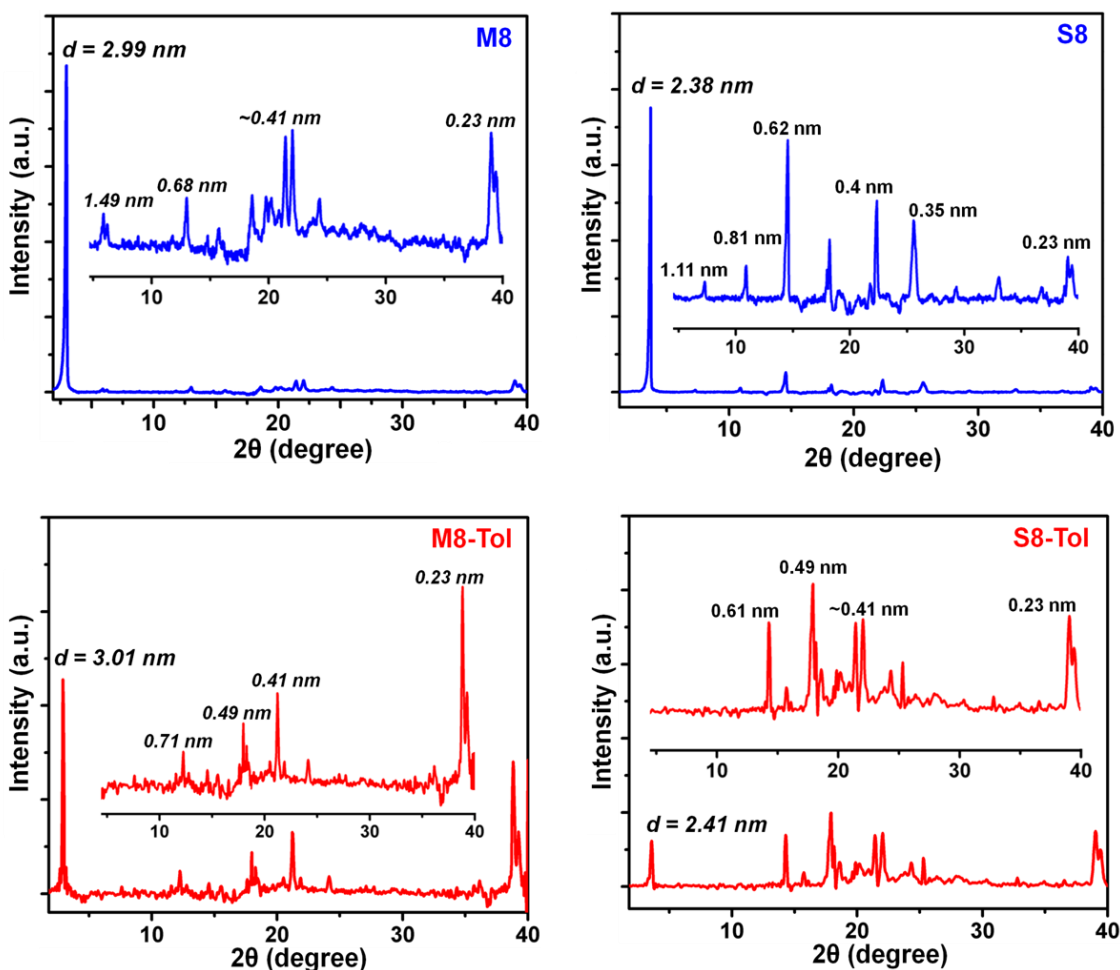


**Figure 2.14.** XRD patterns of powder and toluene gel samples of M8 and S8. In the inset of each figure the magnified region of the pattern from  $2\theta = 5\text{-}40^\circ$  is shown.

XRD patterns of toluene gels of M8 and S8 exhibit primary peaks close to the above  $d$ -spacing values; for M8 gels it was  $\sim 3.01$  nm and S8 gels it was  $\sim 2.41$  nm. In addition, the toluene gels also exhibited strong reflections in the  $d$ -spacing range of 0.35-0.5 nm, similar to the powder state of gelators. Moreover, the long  $d$ -spacings were independent of the nature of the organic liquid. Based on the FT-IR and XRD analyses, it can be concluded that: (i) the gelators exhibit similar lamellar packing in the gel and crystalline (powder) state; (ii) hydrogen bonding and van der Waals forces are primary intermolecular forces governing the self-assembly of gelator molecules; and (iii) the stereochemistry of sugar head group have a marked effect on the degree of packing of sugar gelators.

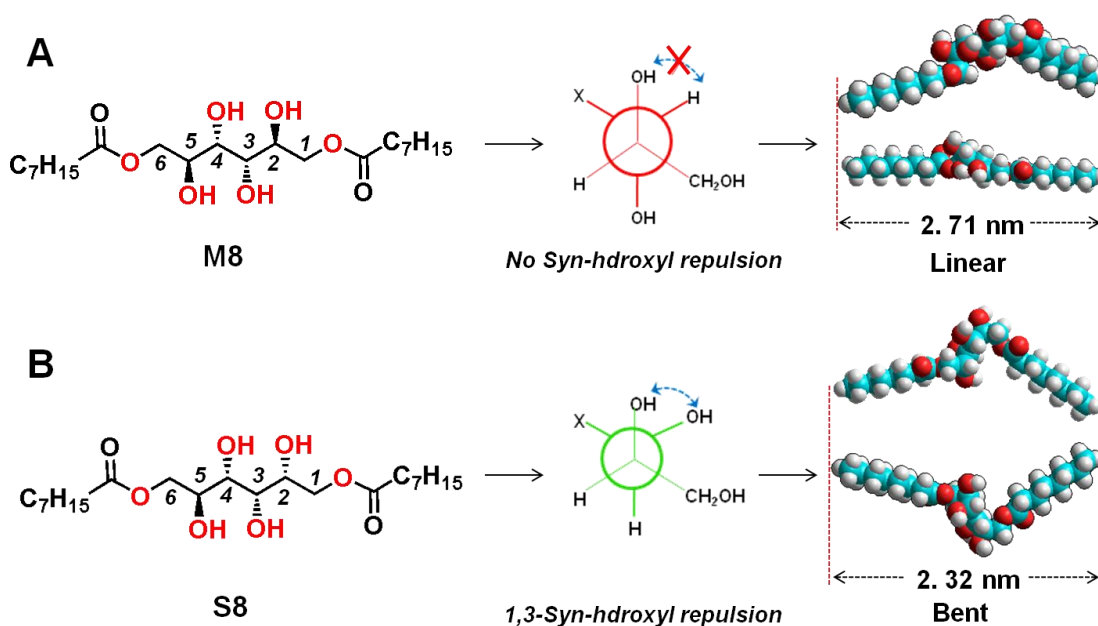


**Figure 2.15.** Influence of chirality induced 1,3-hydroxyl interaction on the conformation of sugar alcohol gelators. A) M8 and B) S8. For each gelator, its molecular structures (with numbering of C-atoms corresponding to sugar part of gelator), a schematic illustration of Newman projection of 1,3-hydroxyl interaction, and energy minimized structure is shown.

In order to pictorially demonstrate the structure of molecular arrangement, the gelator molecules were computationally optimized. The energy minimized structures of M8 (linear conformation) and S8 (bent conformation) are given in Figure 2.15. The differences in molecular conformation stem from the orientation of hydroxyls present on the sugar group of the gelators. Generally, polyols exhibiting *syn*-orientation of alternative hydroxyl groups are reported to experience 1,3-diaxial repulsion; as a result, the molecule attains bent conformation to minimize the repulsive forces.<sup>31</sup> M8 does not contain any *syn*-oriented alternative hydroxyl groups; consequently, it attains linear conformation. However, in case of S8, the *syn*-orientation of the hydroxyl groups at C2 and C4 position of sorbitol causes the bending of the structure, thereby decreasing the effective molecular length, which is also manifested in their d-spacing values. The bending in the head group of sorbitol gelators broadens the head group area and distorts the planar orientation of the alkyl chain thereby lowering their interaction (as observed from FT-IR data). As a result, the S8 molecules fail to stack together compactly and efficiently to form linear extended structures. Hence, such non-efficient stacking may be the reason for the absence of well defined and extended aggregates in its gels thereby resulting in lower gelation efficiency.

In addition to molecular conformation, the presence of 1,3-*syn*-hydroxyl groups (SHG) has been found to alter the solubility of amphiphiles in solvents.<sup>10b,32</sup> Fuhrhop and co-workers reported that the sugar alcohol derivatives with SHG exhibited greater solubility in solvents compared to those with no SGH. The bending-induced increase in the spatial distance of consecutive hydroxyl groups has been reasoned to enhance its solvation tendency, causing it to exhibit greater solubility. Accordingly, the solubility of

S8 was found to be greater than that of M8 by 4-folds. The higher solubility can also be accounted for lower gelation efficiency.

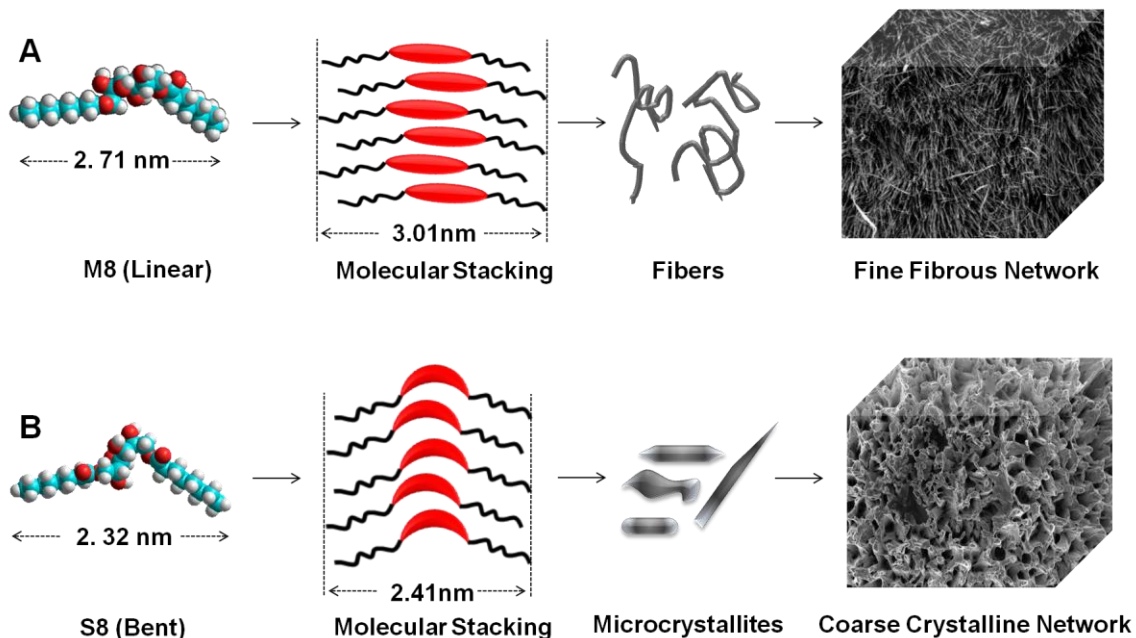


**Figure 2.16.** Schematic representation of molecular assembly of M8 and S8 in organic solvents. The fibrous network of M8 with fine voids is efficient in immobilizing a solvent compared to coarse crystalline network of with large voids.

The probable mode of self-assembly of mannitol and sorbitol-based gelators is illustrated in Figure 2.16. It is worth noting the arrangement of the gelator molecules. The alkyl tails from individual molecules are on the outside, i.e., in contact with the non-polar solvent, while the hydrophilic sugar heads form the interior of the lamellar packing. In other words, the molecular arrangement is reversed compared to that in water. Such multilayer stacking leads to formation of self-assembled structures: fibers (for M8) or crystalline platelets (for S8). These aggregates further interact with each other to form a 3-D volume spanning network, thereby leading to formation of a gel.

## 2.4. Conclusion

In conclusion, a novel class of sugar alcohol-based gelators has been developed by using biocatalysis. These gelators self-assembled in a range of organic solvents and formed gels at concentrations ranging from 1-5 %wt/v. Intermolecular interactions like hydrogen-bonding and van der Waals forces contributed towards self-assembly of gelator molecules in the solvent medium. Mannitol-based amphiphiles were found to be efficient gelators compared to amphiphiles developed from its stereoisomer, sorbitol. The optimum chain length for the developed gelators was in the range of 8-10. At these chain length, the gelators possessed critical balance between hydrophilic (sugar head group) and hydrophobic (acyl chain length) interactions to exhibit efficient gelation tendency. The self-assembly pattern, and hence gelation, was found to be a function of not only the nature of gelator molecule (acyl chain length and chirality) but also of the type of solvent involved in gelation. Solvent possessing functional group capable of interacting with gelator were able to stabilize the gelator assemblies in its matrix, leading to formation of a gel. Increase in the solvent polarity decreased the gelation efficiency of sugar-alcohol based gelators.

## 2.5. Experimental Section

### 2.5.1. Materials

Mannitol, sorbitol and phosphomolybdic acid were purchased from Acros Chemicals (Fisher Scientific Company, Suwanee, GA.). The Novozyme 435 [Lipase B from *Candida Antarctica*, (CALB)] was obtained as a gift from Novozymes through Brenntag North America. Benzaldehyde was purchased from Alfa Aesar (Fisher

Scientific Company, Suwanee, GA.). Vinyl esters of fatty acids were bought from TCI America (Portland, OR). The solvents used in reaction, column chromatography and gelation studies were of ACS grade and were purchased from Acros, TCI or Spectrum Chemicals Ltd.

Flash column chromatography was performed on silica gel (200-300 mesh). Analytical thin layer chromatography (TLC) was performed on glass plates precoated with a 0.25 mm thickness of silica gel. The developed TLC plates were visualized by staining with phosphomolybdic acid solution in ethanol (1% wt/v). Melting points were determined with a Melt-Temp measuring cell of Melt-Temp II Laboratory Devices, USA. <sup>1</sup>H NMR and <sup>13</sup>C NMR analyses conducted on Varion 300/500 MHz spectrometer; the chemical shifts are reported in parts per million ( $\delta$ , in ppm) downfield from tetramethylsilane (TMS). Mass spectroscopic analysis was performed on Applied Biosystems 4000 Q-Trap and the solvent system was methanol with 0.1 % v/v formic acid. The sample was scanned in positive mode by Electron-spray ionization (ESI).

### **2.5.2. Synthesis and Characterization**

#### General enzymatic catalysis method for regioselective esterification of sugar alcohols

Typically, 3 mmol of sugar alcohols (mannitol, sorbitol and xylitol) and 9 mmol of vinyl esters (vinyl butyrate, vinyl caprylate and vinyl myristate) were added to a container containing 40 mL of solvent. Novozyme 435 (1 g) was added in to the mixture. The entire reaction mixture was placed in an incubator shaker at 45 °C for 48 hr, which was shaking at 250 rpm. After the completion of a reaction (monitored by TLC), the reaction mixture was filtered and solvent was removed in rotary evaporator. The obtained

crude product was purified by silica gel flash chromatography using chloroform:methanol (9:1) as an eluent. The afforded pure product was a white solid. The yields were about 75% for all the reactions.

#### Characterization of Sugar alcohol dialkanoates

Mannitol dibutyrate (M4). m.p. 114-116 °C; <sup>1</sup>H NMR (300MHz, DMSO-d<sub>6</sub>): δ 3.36-4.83 (m, 12H), 2.28 (t, 4H), 1.54 (sextet, 4H), 0.88 (t, 6H); <sup>13</sup>C NMR (75MHz, DMSO-d<sub>6</sub>): δ 173.99, 70.01, 69.17, 67.78, 36.43, 18.92, 14.56. EI-MS m/z [M+Na]<sup>+</sup> = 345.2. Anal. Calcd. for C<sub>14</sub>H<sub>26</sub>O<sub>8</sub>: C, 52.16; H, 8.13; O, 39.71. Found: C, 52.00; H, 8.10; O, 39.91.

Mannitol dicaprylate (M8). m.p. 123-125 °C; <sup>1</sup>H NMR (500MHz, DMSO-d<sub>6</sub>): δ 3.33-4.79 (m, 12H), 2.29 (t, 4H), 1.52 (m, 4H), 1.25 (m, 16H), 0.86 (t, 6H); <sup>13</sup>C NMR (75MHz, DMSO-d<sub>6</sub>): δ 173.86, 69.67, 68.81, 67.57, 34.24, 31.84, 29.15, 25.16, 22.77, 14.65. EI-MS m/z [M+Na]<sup>+</sup> = 457.29. Anal. Calcd. for C<sub>22</sub>H<sub>42</sub>O<sub>8</sub>: C, 60.80; H, 9.74; O, 29.45. Found: C, 60.85; H, 9.72; O, 29.49.

Mannitol dimyristate (M14). m.p. 132-134 °C; <sup>1</sup>H NMR (300MHz, DMSO-d<sub>6</sub>): δ 3.33-4.79 (m, 12H), 2.28 (t, 4H), 1.53 (m, 4H), 1.25 (m, 40H), 0.86 (t, 6H); <sup>13</sup>C NMR (75MHz, DMSO-d<sub>6</sub>): δ 173.80, 70.16, 69.43, 67.46, 34.41, 32.01, 29.72, 29.61, 29.44, 29.40, 29.27, 25.22, 22.77, 14.56. EI-MS m/z [M+Na]<sup>+</sup> = 625.6. Anal. Calcd. For C<sub>34</sub>H<sub>66</sub>O<sub>8</sub>: C, 67.74; H, 11.03; O, 21.23. Found: C, 67.91; H, 11.05; O, 21.29.

Sorbitol dibutyrate (S4). m.p. 76-78 °C; <sup>1</sup>H NMR (300MHz, DMSO-d<sub>6</sub>): δ 3.33-4.93 (m, 12H), 2.27 (t, 4H), 1.54 (sextet, 4H), 0.88 (t, 6H); <sup>13</sup>C NMR (75MHz, DMSO-d<sub>6</sub>): δ

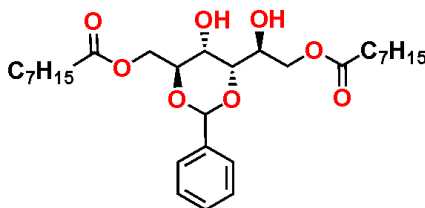
173.98, 173.87, 72.18, 71.62, 70.08, 69.48, 67.32, 66.62, 36.4, 18.92, 14.45. EI-MS  $m/z$   $[M+Na]^+ = 345.2$ . Anal. Calcd. For  $C_{14}H_{26}O_8$ : C, 52.16; H, 8.13; O, 39.71. Found: C, 52.18; H, 8.11; O, 39.74.

Sorbitol dicaprylate (S8). m.p. 80-82 °C;  $^1H$  NMR (500MHz, DMSO- $d_6$ ):  $\delta$  3.33-4.91 (m, 12H), 2.29 (t, 4H), 1.52 (m, 4H), 1.25 (m, 16H), 0.86 (t, 6H);  $^{13}C$  NMR (75MHz,  $CDCl_3$ )  $\delta$  175.12, 174.71, 73.15, 72.74, 70.58, 69.16, 66.03, 65.86, 34.38, 31.85, 29.29, 29.12, 25.08, 22.78, 14.25. EI-MS  $m/z$   $[M+Na]^+ = 457.29$ . Anal. Calcd. for  $C_{22}H_{42}O_8$ : C, 60.80; H, 9.74; O, 29.45. Found: C, 60.73; H, 9.75; O, 29.48.

Sorbitol dimyristate (S14). m.p. 104-105 °C;  $^1H$  NMR (300MHz, DMSO- $d_6$ ):  $\delta$  3.33-4.88 (m, 12H), 2.27 (t, 4H), 1.51 (m, 4H), 1.23 (m, 40H), 0.85 (t, 6H);  $^{13}C$  NMR (75MHz, DMSO- $d_6$ ):  $\delta$  173.70, 72.03, 71.04, 70.03, 69.43, 66.82, 66.18, 34.27, 31.92, 29.63, 29.33, 25.12, 22.68, 14.49. EI-MS  $m/z$   $[M+Na]^+ = 625.6$ . Anal. Calcd. For  $C_{34}H_{66}O_8$ : C, 67.74; H, 11.03; O, 21.23. Found: C, 67.73; H, 11.18; O, 21.48.

Xylitol dicaprylate (X8). m.p. 55-57 °C;  $^1H$  NMR (500MHz, DMSO- $d_6$ ):  $\delta$  3.33-4.83 (m, 10H), 2.27 (t, 4H), 1.52 (m, 4H), 1.26 (m, 16H), 0.86 (t, 6H);  $^{13}C$  NMR (75MHz, DMSO- $d_6$ ):  $\delta$  173.82, 71.66, 69.77, 66.42, 34.46, 32.07, 29.39, 29.32, 25.39, 22.98, 14.83. EI-MS  $m/z$   $[M+Na]^+ = 427.2$ . Anal. Calcd. For  $C_{21}H_{40}O_7$ : C, 62.35; H, 9.97; O, 27.68. Found: C, 62.28; H, 10.00; O, 27.84.

$^1H$  NMR,  $^{13}C$  NMR and EI-MS spectra of representative sugar dioctanoates (M8, S8 and X8) are given in the appendix.

Synthesis of M8-protected (Benzylidene derivative of M8)

A mixture of M8 (0.308 g, 0.7 mmol), benzaldehyde (0.106 g, 0.1 mL, 1mmol) and concentrated sulfuric acid (10  $\mu$ L, catalytic amount) was added to a dry dichloromethane (1.5 mL). The reaction mixture was stirred at room temperature for 15 minutes. The reaction mixture was analyzed by TLC for completion of the reaction, later filtered and concentrated. The obtained crude product was purified by silica gel flash chromatography (prior to usage, silica gel was washed with methanol and dried overnight) using dichloromethane as an eluent. The chromatography afforded 0.339 g of product (92 %) as white solid.

$^1\text{H NMR}$  (500MHz,  $\text{CDCl}_3$ )  $\delta$ : 7.45 (m, 1H), 7.38 (m, 4H), 5.9 (s, 1H), 3.9-4.5 (m, 8H), 3.5 (s, 2H), 2.37 (t, 4H), 1.64 (m, 4H), 1.29 (m, 16H), 0.88 (t, 6H). EI-MS  $m/z$   $[\text{M}]^+ = 522.6$ .

### 2.5.3. Experimental Techniques

#### Gelation Experiments

In a typical gelation experiment, a weighed amount of sugar alcohol dialkanoates (15 mg) and 300  $\mu$ L of solvent were taken in a screw cap bottle. The bottle was heated with continuous agitation until the solid material had dissolved. The solution was allowed to cool to room temperature and gelation was visually observed. Gelation was considered to have occurred if the content in the bottle was stable to inversion of the bottle; i.e., a

solvent was considered to be transformed to gel when it did not exhibit any flow under the gravity.

### **Minimum Gelation Concentration (MGC)**

To a gel sample (15 mg of gelator in 300  $\mu$ L of solvent) obtained from previous experiment, 50  $\mu$ L of additional solvent was added. The mixture was heated, cooled and analyzed for stability on inversion of the container. On formation of a gel, the steps of solvent addition and gelation were repeated. The cycle was repeated until further addition of solvent lead to disruption of gelation, i.e., when the contents in the container started to flow on inversion of the container. The preceding gelator concentration was taken as the MGC value for the gelator in that particular solvent.

### **Gelation Temperature ( $T_{gel}$ )**

Gel temperatures were determined by tube inversion method. In a 2 mL scintillation vial gel (5 %wt/v concentration) was prepared as described above. The vial was immersed in the oil-bath 'upside down' and slowly heated (1  $^{\circ}$ C/min). The temperature at which the gel fell under the influence of gravity from an inverted container was recorded as  $T_{gel}$ .

### **Optical microscopy studies**

A standard glass slide containing a small portion of gel was mounted on Leica DM LB2 microscope stage and the samples were observed with 20x PH1 phase contrast objective.

### **Morphological studies of the gel structure (SEM)**

A Small amount of gel was placed on carbon-tape placed on an aluminum grid and allowed to dry overnight under ambient condition. Later, the sample was coated with

thin-layer of gold (5 nm) by using sputter coating instrument (Denton Desk II Sputter Coater). The specimens were directly imaged under either thermionic electron microscope (Zeiss DSM 940) or field emission microscope (Zeiss Supra 55 VP).

#### **Fourier Transformation Infra-red (FT-IR)**

FT-IR spectroscopic analysis was performed by using Nicolet 380 FT-IR spectrophotometer. For the gel and powder samples ATR attachment was used, while the liquid samples were sandwiched between NaCl plates.

#### **X-ray diffraction studies (XRD)**

A small portion of a gel sample was transferred in a sample holder and immediately the reflectance was measured. The XRD measurement was performed on PANalytical X'Pert PRO equipped with MPD PW 3040/60 generator S/N DY 2974 and monochromatic Cu-Co radiation (45 kV, 40 A).

---

## Chapter 3

# Sugar-derived Phase-selective Molecular Gelators as Model Solidifiers for Oil Spills

---

### 3.1. Abstract

*The frequent occurrence of disastrous oil spills highlights development of materials for its containment and reclamation. Herein, sugar-based gelators have been reported as environmentally benign materials for oil spill remediation. The gelators exhibited unprecedented ability to phase-selectively gel organic liquids (including crude oil fractions) in the presence of water. Additionally, gelation is accomplished at room temperature (RT) without heat. Combined RT and selective gelation abilities enabled application of gelators for oil spill recovery. In a demonstration, bulk oil floating on the salt water was removed using gelator, and the oil was quantitatively recovered by vacuum distillation. The gelators are inexpensive and environmentally benign. Unlike the current clean-up technologies, the developed PSGrs offer: total separation of oil from water bodies, recovery of oil, and most importantly recycling ability of amphiphiles.*

### 3.2. Introduction

The world has witnessed several marine oil spills, including the recent one caused by the blowout of an oil well in the Gulf of Mexico.<sup>1</sup> Every year, over 3 million gallons (10,000 metric tonnes) of oil or refined petroleum product are spilled into the waters of the United States.<sup>2</sup> Such oil spills cause irrecoverable damage to the environment and the ecosystem.<sup>3</sup> The vast scale of such disasters has drawn attention to the need for new

materials to contain oil spills and reclaim the oil. Many types of commercial materials have been formulated for oil spill control and cleanup.<sup>4</sup> However, problems exist with each of these current technologies.

Materials used to contain oil spills are classified under the following categories: dispersants, sorbents, and solidifiers. *Dispersants* break the oil into small droplets that mix into the water and do not re-float: in effect, they emulsify the oil layer.<sup>5</sup> In this case, the emulsified oil-water mixture still needs to be removed and the emulsion will have to be destabilized to recover the oil. *Sorbents* are typically solid powders that absorb the oil – the sorbed material may then be removed more easily and the oil may also be recovered.<sup>6</sup> Finally, *solidifiers* are materials, typically polymers, which transform the liquid oil layer into a coherent, gel-like mass.<sup>7</sup>

One desirable feature of solidifiers (and also sorbents, to some extent) is that they help to contain the spread of the oil and thereby localize the problem area. Additionally, by tweaking the chemistry of polymeric solidifiers, one can ensure that the polymer exclusively partitions into the oil phase, i.e., it has no effect on the water. Typically, this involves making the polymer structure sufficiently hydrophobic. Solidifiers must also have environmentally acceptable features, i.e. it should not have any effect on the aquatic ecosystem or on the environment in general. Disadvantages with current solidifiers include the fact that large amounts need to be used for a large oil spill, which may not be economical. Moreover, polymeric solidifiers cannot be readily blended with viscous oils and the recovery of oil from polymer gels is cumbersome. To summarize, an effective and ideal solidifier for oil spills must be able to: (a) selectively and efficiently gel the oil phase in presence of water at ambient temperature; (b) be synthesized easily and at low

cost; (c) readily apply/mix with the oil; (d) be environmentally benign; (e) facilitate recovery of the oil from the gel; and (f) be capable of being recycled and reused.

Molecular gelators (MGrS) are an alternate class of materials that may be used as solidifiers of oil. These are typically low molecular-weight organic molecules that self-assemble into filaments or fibers in a variety of liquids. At concentrations above the minimum gelator concentration (MGC), the filaments interconnect through noncovalent forces to form volume-filling three-dimensional network. The solvents molecules are entrapped in such network via surface tension, thereby converting the liquid into a coherent gel. Because weak intermolecular interactions (e.g., formed by hydrogen-bonding, van der Waals interactions, or hydrophobic interactions), are involved in self-assembly and hence gelation process, molecular gels tend to be shear-sensitive and thermoreversible. Both these properties are conducive to the oil spill application. For example, oil gelled by MGrS can be easily skimmed off the surface due to the shear-thinning nature of gels. Moreover, the thermoreversibility (gel to sol transition at a temperature above  $T_{gel}$ ) permits the recovery of oil from the gelled mass and also, potentially, the recovery and re-use of the gelator material.

Despite the potential benefits, MGrS are not currently used for oil spill treatment mainly because they fail to satisfy at least one of the criteria laid out above. For example, many MGrS are complex organic moieties that are potentially harmful to the environment.<sup>8c-e</sup> Second, MGrS are often specialized molecules that are synthesized by complex, multi-step procedures – in turn, it is doubtful whether the materials can be delivered at low cost and in large quantities that are required for a major oil spill.<sup>8d-g</sup> Third, the action of MGrS requires their dissolution in the solvent, which is usually

accomplished by *heating* a mixture of the MGr powder and solvent up to a high temperature.<sup>8a-g</sup> This is impractical for oil spill treatment – it is imperative to be able to induce gelation of the oil under *ambient conditions*. Last, and most important, the MGr must be capable of phase-selective gelation, i.e., it must preferentially gel the oil layer even when it is in contact with the water. Stated differently, water should not impair the oil-gelling properties of the MGr. The last requirement can be challenging because many MGr are amphiphilic molecules, i.e., they have water-loving and water-hating parts, and this is a key to their gelling ability. When contacted with water, these molecules partition to the oil-water interface (thereby acting as surfactants or emulsifiers) – as a result, their gelling ability is affected.

Due to the above challenges, only a few phase-selective gelators (PSGr) of the oil phase from an oil-water mixture have been reported (Figure 3.1).<sup>8</sup> However, existing PSGr are complex molecules, they require heat to be dissolved in the solvent, and their environmental suitability is questionable – thus, the practical use of these PSGr for oil spill treatment is limited. There is a need for new and improved PSGr that can avoid the above problems.

In this chapter, a new class of amphiphilic solidifiers has been developed. The amphiphiles are derived from naturally occurring sugar-alcohols, namely mannitol and sorbitol. These amphiphiles have the ability to function as PSGr of the oil phase from a mixture of oil and water. They can potentially satisfy each of the above criteria and therefore are promising model candidates for oil spill remediation. Phase-selective gelation has been achieved for various crude oil fractions (e.g. diesel) under ambient

conditions, i.e., by a process that involves no heat, followed by recovery of the oil from the gel by distillation and re-use of the gelator for further gelling experiments.

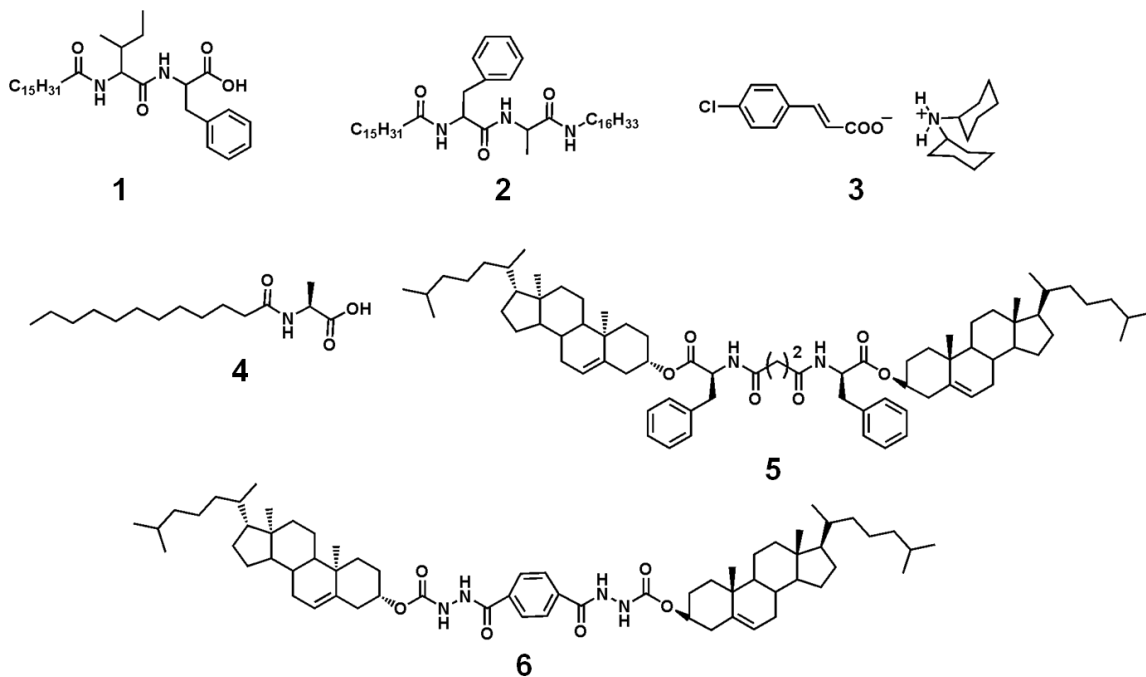


**Figure 3.1.** Molecular structures of representative phase-selective gelators. **1:** Isoleucine phenylalanine palmitoyl conjugate.<sup>8g</sup> **2:** Dipeptide dialkyl conjugate.<sup>8f</sup> **3:** Dicyclohexyl ammonium salt of 4-chloro cinnamic acid.<sup>8c</sup> **4:** N-lauroyl-L-alanine.<sup>8a,b</sup> **5:** Succinic acid amide of dicholesteryl L-phenylalaninate.<sup>8d</sup> **6:** Dicholesteryl hydrazine phthaloyl conjugate.<sup>8e</sup>

### 3.3. Results and Discussion

The PSGr reported here are dioctanoate derivatives of the sugar alcohols, mannitol (M) and sorbitol (S) (Figure 3.2). Conventional routes to such compounds involve multiple steps with protection and deprotection protocols. Here we prepared PSGr in a single step by employing regiospecific enzyme catalysis (as described in

Chapter 2). The ease of synthesis and the abundance of sugar alcohols in nature ensure that the PSGs are low-cost, nontoxic and biodegradable.

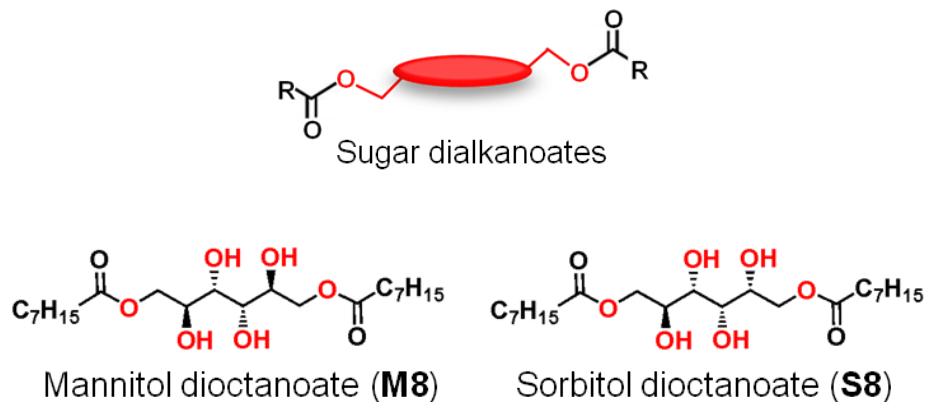


**Figure 3.2.** Generic structure of sugar alcohol dialkanoate and specific molecular structures of mannitol dioctanoate and sorbitol dioctanoate.

### 3.3.1. Evaluation of Gelation Efficiency in Crude Oil Fractions (oils)

The gelling abilities of sugar-gelators are summarized in Table 3.1. In this chapter, the organic solvents and crude oil fractions are commonly referred to as oils. As seen from the table, these gelators precipitated out from smaller chain hydrocarbons (hexane and heptane) but formed gels in longer chain hydrocarbons (alkanes  $C_n \geq 10$ ). The gelators were also able to gel high boiling crude oil fractions such as diesel, mineral and silicone oil, with minimum gelation concentrations (MGCs) ranging from 1.5 to 5% (wt/v). For example, M8 gels diesel at 2.5%, i.e., it immobilizes diesel to ca. 32 times its dry weight.

**Table 3.1.** Gelation abilities of M8 and S8 in various crude oil fractions and oils.<sup>[a]</sup>

Solvent	M8		S8	
	Gelation State	Temperature Range (°C)	Gelation State	Temperature Range (°C)
Heptane	P	-	P	-
Iso-octane	P	-	P	-
Decane	G (2)	118-121	G (2.5)	60-63
Diesel	G (2.5)	102-105	G (3.5)	56-59
Mineral Oil	G (1.2)	120-125	G (1.5)	63-69
Toluene	G (1.5)	80-83	G (2.5)	38-40
Mixture of Hydrocarbons <sup>[b]</sup>	G (2.5)	75-78	G (3.5)	33-35
Pump Oil	G (4.0)	110-120	G (5.0)	60-65
Silicon Oil	PG (5.0)	-	PG (5.0)	-

<sup>[a]</sup> Values in parenthesis are minimum gelation concentration of gelator (% wt/v, mg/100 $\mu$ L). G = opaque gel; PG = partial gel; S = soluble; I = insoluble; P = precipitation.

<sup>[b]</sup> Mixture of aliphatic (pentane, hexane, octane) and aromatic (benzene, toluene and xylene) solvents in 1:1 volume ratio.

To characterize the thermoreversibility of gels, gel-to-sol transition temperatures ( $T_{gel}$ ) were determined and were found to be in the range of 82-125°C for 5 wt% M8 gels and 38-69°C for 5 wt% S8 gels (Table 3.1). They were stable for several months, indicating their temporal stability. As observed and explained in Chapter 2, mannitol-based gelators were more efficient compared to gelators derived from its stereoisomer, sorbitol.

### 3.3.2. Phase-selective Gelation of Oils

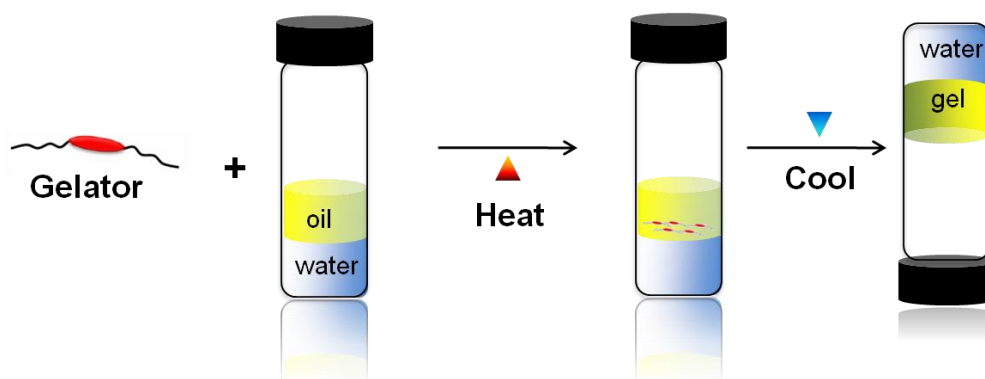


**Figure 3.3.** Schematic representation of phase-selective gelation via conventional heating and cooling method.

The abilities of M8 and S8 to phase-selectively gel oil in the presence of water were investigated by using conventional heating method (Figure 3.3). The amphiphiles were able to selectively gel all the previously tested crude oil fractions, even at MGC values reported in Table 3.1. In a typical selective gelation experiment, a gelator was added to an organic solvent/water mixture (3:7, volume basis) and was heated to dissolve the gelator molecule in the mixture, vortexed at 1000 rpm for around 10 minutes and allowed to settle down. At first, it formed a milky white phase resulting from fine dispersion of oil in water; but eventually, the organic layer was found to be completely gel with clear non-gelled water layer present beneath it. The extent of organic solvent to water ratio had no effect on selective gelling properties of gelators; i.e. similar results were obtained even when the experiment was conducted by reversing the amount of corresponding phases (7:3, volume basis).

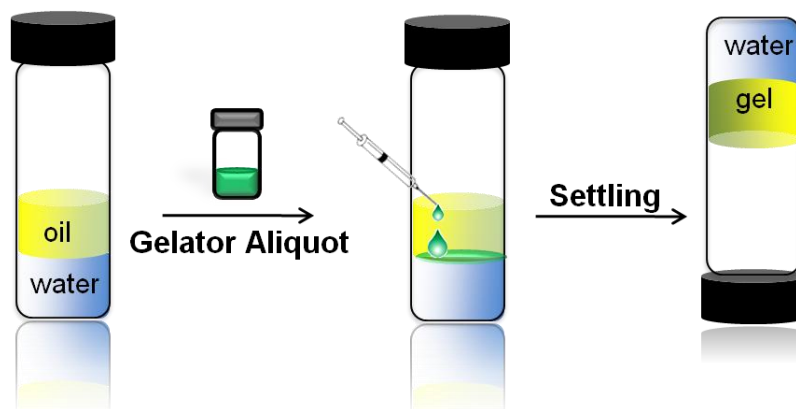


**Figure 3.4.** Schematic representation of room temperature phase-selective gelation method (aliquot method).

Since involvement of a heating step in phase-selective gelation would be impractical for high volume applications like oil-spill recovery, a room-temperature gelation protocol was formulated. The method consisted of making a saturated solution of molecular gelators and gradually injecting the aliquot of the solution at the interface of an organic liquid/water mixture. Hence, the method is referred as *aliquot method*. A schematic representation of phase selective gelation using an aliquot method is depicted in Figure 3.4. The choice of solvent is important and the pre-requisite qualities required for such solvents are: i) it should possess good dissolving power for gelators; and ii) at the same time miscible in water. The mechanism of selective gelation using an aliquot method is hypothesized to occur due to partial solubility of aliquot solvent in water. On injection of aliquot at the oil-water interface, the aliquot solvent partially partitions into the water. As a result, the aliquot in contact with the organic layer becomes supersaturated causing the gelators to spontaneously self-assemble, resulting in gelation of oil phase while the aqueous phase is left intact.

Numerous water miscible solvents were tested for dissolution of gelator. It was found that alcohols (methanol, ethanol and iso-propanol), dioxanes and Tetrahydrofuran (THF) were able to form aliquot with reasonable concentration (~10-15% wt/v for M8 and 40-60% wt/v for S8). Ethanol, the safest among the tested solvent, was chosen as suitable aliquot solvent. The solubility of M8 and S8 in ethanol was found to be 25 and 100 mg in 400  $\mu$ L of ethanol. Compared to M8, S8 exhibited higher solubility (~4-fold high) in all solvents. The solubility differences are related to sterical interactions within the head groups of amphiphiles. The *syn* orientation of three secondary –OH groups present on sorbitol causes it to experience 1,3-*syn*-hydroxyl repulsive interaction. As a result, the linear all-trans conformation of an amphiphile is disturbed, which decreases gelator–gelator interaction or in turn enhances degree of solvation.<sup>9</sup>

Ethanol-based aliquot method was employed to test the room temperature phase-selective gelation efficiency of gelators. By using this method, M8 was able to gel different oils even at MGC values reported in Table 3.1, whereas S8 could only form partial gels, even when thrice its MGC amount was used. The solubility factor can be attributed to this observation; S8 was found to be 4 times more soluble in ethanol than M8. As a result, there is strong possibility that S8 is solubilised in the mixture and is unable to gel oil phase. Hence, efficiency of aliquot method was further investigated only for M8. Gels having variable strength could be obtained by varying the concentration of M8 delivered through aliquot. For instance, soft gels which can hold weight of an organic liquid but not water phase (where it floats on water after tilting the container) to gels strong enough to bear the weight of water too on inversion of the container were developed (Figure 3.5).

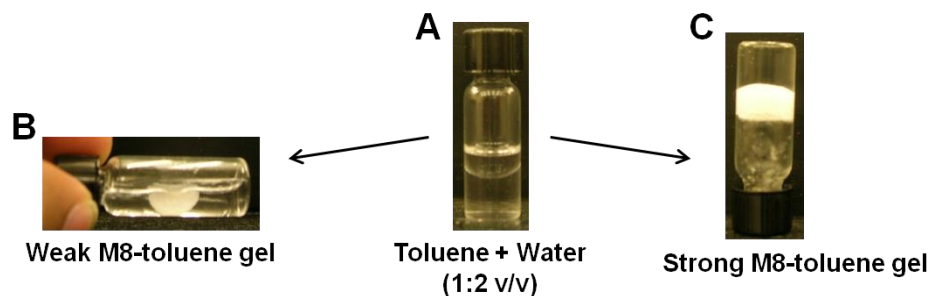


**Figure 3.5.** M8 aided phase-selective gelation of toluene. A) Toluene-water mixture. B) Soft gel of toluene resulting on injection of ethanol aliquot, which delivered M8 equal to MGC amount. C) Strong gel of toluene resulted when M8 (~1.5 times MGC) was delivered through aliquot.

Such efficient phase-selective gelation was observed with various crude oil fractions and mixture of hydrocarbon solvents (aliphatic and aromatic). In addition, the oil to water ratio or the type of water (river water from Hudson River, New York City, USA and sea water from Cooney Island, Brooklyn, USA) did not alter the phase-selective gelation. Even the nature of the aqueous solution, acidic ( $6 \geq \text{pH} \leq 2$ ), basic ( $10 \leq \text{pH} \geq 8$ ), neutral, saturated NaCl (36 g /100 mL) and saturated CaCl<sub>2</sub> solution (74.5 g /100 mL), had no effect on selective gelation efficiency. The results demonstrate the robustness of the phenomenon and the potential applicability of the methodology to real oil spill situations and refinery effluent treatment.

### 3.3.3. Mechanism of Phase-selective Gelation

The properties of oil gels obtained from oil-water mixture (phase-selective gelation, aliquot method) were similar to the gels prepared from pure oils only (heating method). MGC,  $T_{\text{gel}}$  and X-ray diffraction pattern of gels developed from both the methods were comparable (Table 3.2).

**Table 3.2.** Comparison of properties of gels obtained by phase-selective gelation (PSG) by aliquot method or pure solvent gelation by heating method.

Properties	Toluene		Diesel	
	PSG	Pure	PSG	Pure
MGC (% wt/v)	1.5	1.5	2.5	2.5
T <sub>gel</sub> (° C)	81-83	80-83	100-104	102-105
Morphology	Fibrous	Fibrous	Fibrous	Fibrous
Long d-spacing (nm)	2.99	2.98	2.98	3.00

SEM image of pure toluene gel revealed presence of ribbon-like structures (fiber width ~100 nm) (Figure 3.6A). The morphology of phase selective toluene gel exhibited no marked difference in aggregate structures – analogous ribbon like morphology was observed (Figure 3.6B). Similar morphological resemblance was observed for diesel gels too (Figure 3.6C & D). In addition, the XRD diffraction pattern (and long d-spacing) of pure diesel gel and phase-selective diesel gel were in good agreement with each other (Figure 3.6E & F). Based on similarities observed in the properties, it can be concluded that the presence of water or method employed for gelation had no effect on the gelation tendency of M8. In other words, the self-assembly mechanism of M8 was not influenced by gelation protocols. Therefore, as described in Chapter 2, the entangled network of self-assembled M8 fibres present in phase-selective gels are believed to consist of stacks of M8 molecules with the tails tilted relative to the fibre axis (Figure 3.7). The stacking, in turn, is stabilized by extensive intermolecular hydrogen bonding between hydroxyls of adjacent gelator molecules.

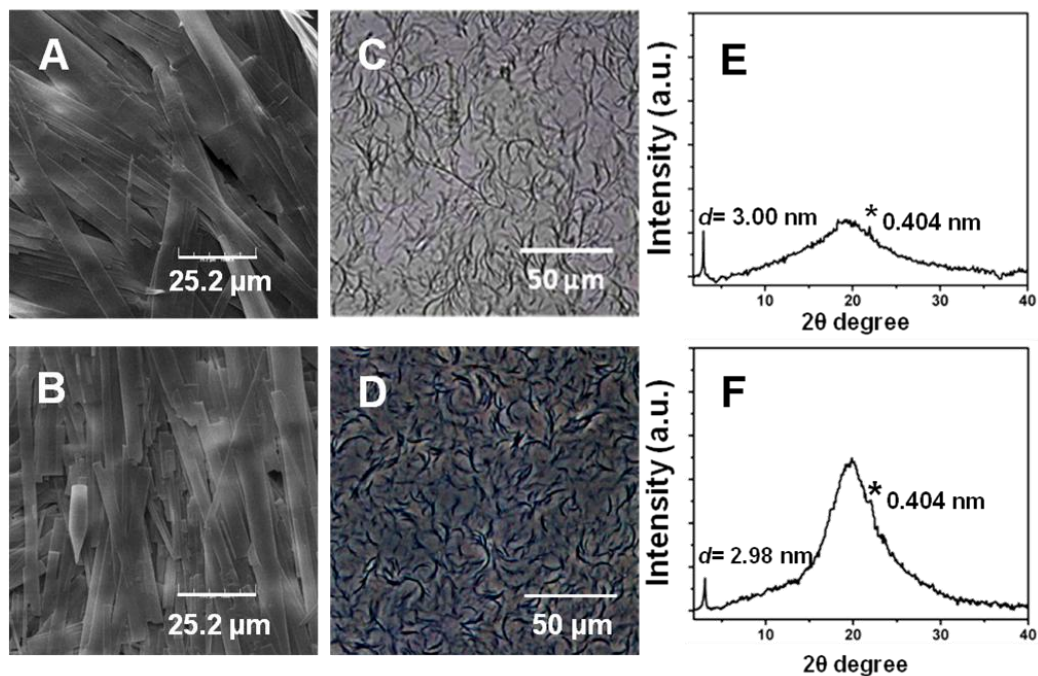


**Figure 3.6.** Characterization of M8 gels obtained from pure or phase-selective gelation of solvents. A, B) SEM images of pure toluene and phase-selective toluene gels. C, D) Optical images of pure diesel and phase-selective diesel gel. E, F) X-ray diffraction pattern of pure diesel and phase-selective diesel gel. ‘\*’ denotes the Bragg’s peak at  $\sim 0.4$  nm, which is a characteristic signal of subcell packing of hydrocarbon chains in the self-assembled lipids.

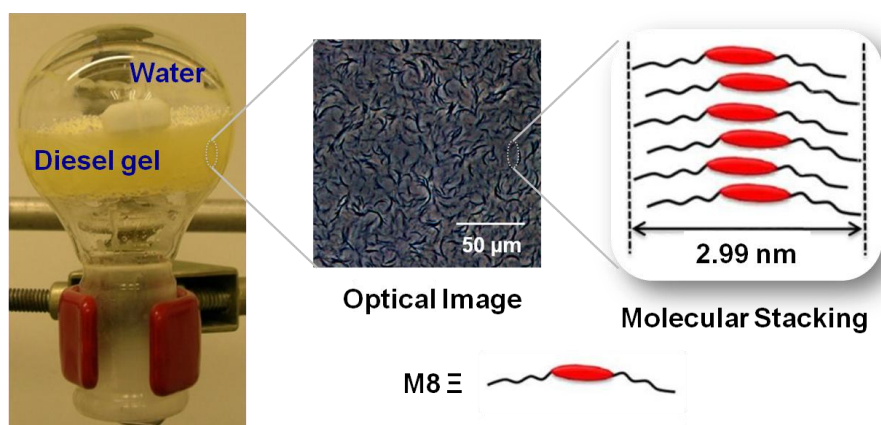


**Figure 3.7.** Schematic representation of self-assembly mechanism of M8 during phase-selective gelation of different oils from oil-water mixture.

The propensity of sugar alcohol amphiphiles to exhibit phase-selective gelation phenomenon is hypothesized to stem from following features: a) exclusive partitioning and high self-assembling tendency in to the oil phase of the mixture and b) inability of water to disrupt intermolecular hydrogen bonding between gelator molecules. The presence of hydrophobic moiety on either side of the sugar head is believed to play a key role in attributing these features. The monoalkanoate derivatives of sugar alcohols, previously described in the literature, are reported to act as surfactant and exhibit emulsification tendency.<sup>10</sup> In contrast, dialkanoate derivatization of sugar alcohols ensures that the amphiphiles are hydrophobic enough to remain in the oil phase of the mixture and do not interact with water or align at the interface to exhibit interfacial activity.

#### **3.3.4. Gelation and Removal of Diesel from Diesel-Water Mixture**

In following section the key subject of this chapter, i.e. demonstrating the potential of developed PSGr and aliquot method in crude oil recovery process is illustrated. In the few existing examples of phase-selective gelators, the recovery of oil from the gels and recycling of the gelator have not been demonstrated. For application in oil remediation, these aspects are vital and hence are addressed in present study. Diesel was chosen as representative fraction and a strong diesel gel was prepared from diesel-water mixture by using M8 and aliquot method. Further, diesel was recovered by vacuum distillation. A schematic representation of phase selective gelation of diesel by M8 and subsequent recovery process is depicted in Figure 3.8.

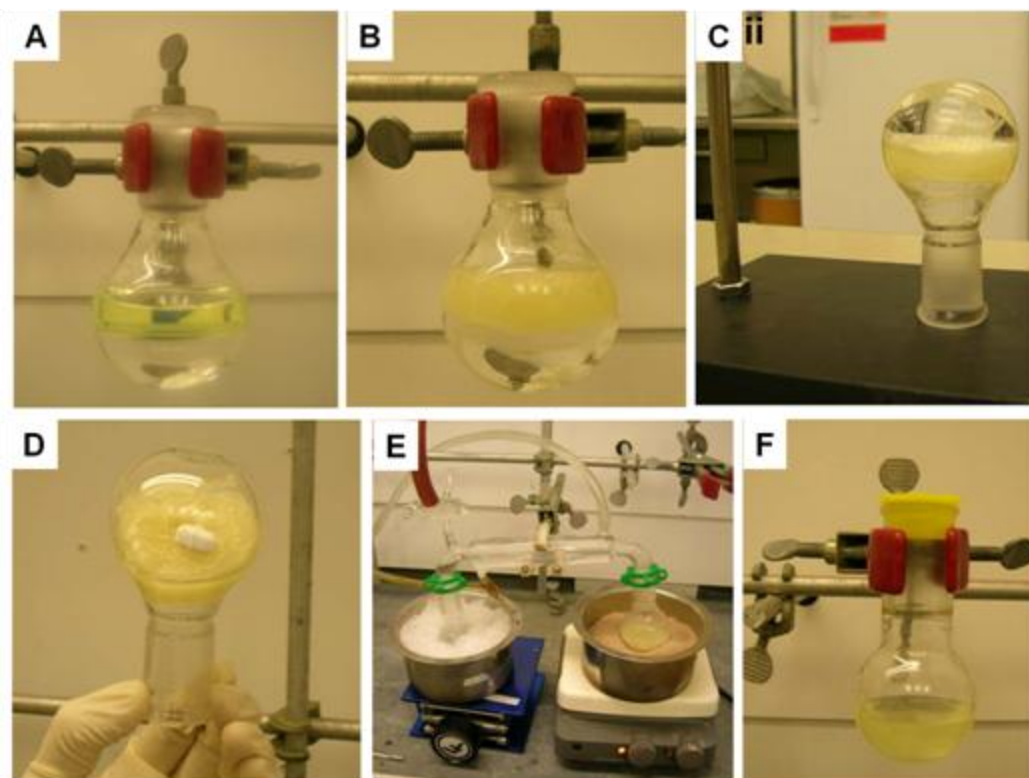


**Figure 3.8.** Phase-selective gelation and diesel recovery from two phase system. Photographs of A) two phase system of diesel-water, B) instantaneously formed gel upon addition of ethanol aliquot of gelator through a syringe, C) Formation of diesel gel strong enough to stop the flow of water upon inversion of flask, D) Remained diesel-gel after removal of bottom water layer, E) Recovery of diesel from the gel through vacuum distillation, and F) recovered diesel.

In a demonstration, to the diesel-water mixture (20:40 mL) a concentrated solution of M8 in ethanol (15 mL) was added through a syringe, such that the concentration of M8 in diesel was 5% (wt/v). The diesel was gelled spontaneously and within 1 hr the gel was strong enough to bear its weight plus that of 40 mL water. The strength of the diesel gels was then studied by rheology.<sup>11</sup> Figure 3.9A shows the frequency response of a gel of 5% M8 in diesel. The elastic modulus  $G'$  is independent of frequency and much higher than the viscous modulus  $G''$  over the frequency range. This

response is typical of gels as it shows that the sample does not relax over long time scales. The value of  $G'$  is a measure of the gel stiffness and its value here ( $\sim 4000$  Pa) indicates a gel of moderate strength. Figure 3.9B is a plot of the moduli  $G'$  and  $G''$  as a function of the stress amplitude  $\sigma_0$  for the same sample. The  $\sigma_0$  at which a sharp decrease in moduli occurs is the yield stress of the gel and its value ( $\sim 30$  Pa) is sufficiently high for the gel to support its weight in an inverted container.

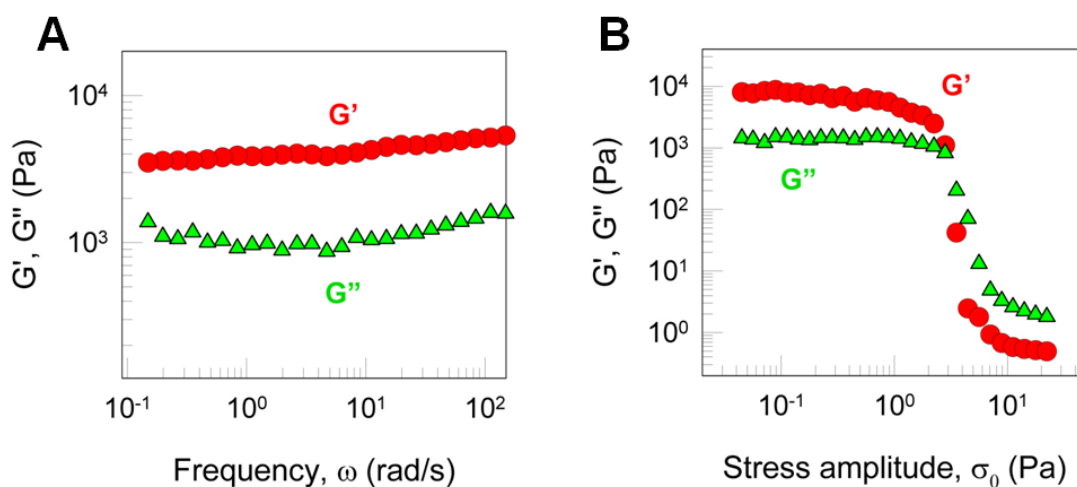


**Figure 3.9.** Dynamic rheology of M8-diesel gel (5 % wt/v). A) Frequency sweep of gel. B) Stress sweep of gel.

Subsequently, water was removed by a syringe and the gel was subjected to distillation at  $125$  °C (above  $T_{\text{gel}}$ ), whereupon the gel liquefied and the diesel was distilled off. Diesel could thus be recovered almost quantitatively. The residue in the flask was characterized by thin layer chromatography and the M8 structure was found to be intact. Recycled M8 could gel a fresh batch of diesel, confirming its reusability. The video of the same process is provided as supplementary information along with this thesis (Supplementary Video1). Phase-selective gelation of oil was also performed on a thin

layer ( $< 1$  mm) of diesel floating on a large pool of water (in a Petri dish). This is also demonstrated in a YouTube video (<http://www.youtube.com/watch?v=IRSZNMplGtc>). The resulting gel could be scooped out with a spatula (Figure 3.10), and the oil in it could again be recovered through distillation (Supplementary Video2). This example mimics the real scenario of an oil spill.



**Figure 3.10.** Scooping out a thin-layer of diesel gel from the top of water

### 3.4. Conclusion

In conclusion, a new class of sugar-gelators has been developed that can selectively gel (solidify) the oil phase from an oil-water mixture at room temperature. Quantitative recovery of oil from the gel has been achieved through simple vacuum distillation. The gelators are easily synthesized, environmentally benign, and can be recovered and reused multiple times. Thus, molecular gelation phenomenon has been conceptually demonstrated as a promising approach for the containment and treatment of oil spills. The only drawback of the present study is requirement of relatively high amount of aliquot solvent (~40 % of total volume of oil required to be immobilized) to induce room temperature gelation of crude oil fractions. Developmental research on this topic should either focus on: i) minimizing the content of aliquot solvent for present

system; or ii) utilize the concept and requirements highlighted in this chapter to develop novel PSGr that gels at room temperature without the aid of the solvent .

### **3.5. Experimental Section**

#### **3.5.1. Materials**

M8 was synthesized by using regiospecific enzyme catalysis, which is described in experimental section of Chapter 2. All the solvents utilized for gelation studies and making aliquots were purchased from Acros, TCI or Spectrum Chemicals. All the solvents were of minimum ACS grade purity.

#### **3.5.2. Experimental Techniques**

##### **Method for Gelation of Pure Solvent**

Typically, gelator (0.1-3 mg) in required solvent (0.1-1mL) was heated until the solid was completely dissolved. The resulting solution was slowly allowed to cool to room temperature, and gelation was visually observed. A gel sample was obtained that exhibited no gravitational flow in inverted tube. All gels obtained are thermally reversible. Above their gelation temperature, the gels dissolved in the solvent, but could be returned to their original gel state upon cooling.

##### **Phase-selective gelation of oil - Conventional Heating Method**

In a selective gelation experiment, a gelator was added to a heterogeneous mixture of organic solvent and water (3:7, volume basis). All the three components were heated to dissolve the gelator molecule in the mixture. The sol was vortexed at 1000 rpm for around 10 minutes and allowed to settle down for about an hour. Successful gelation was said to achieve, when the system exhibited no gravitational flow under the gravity.

### **Degree of Dissolution of Gelator in Aliquot Solvent**

An aliquot of gelator was prepared in a hydrophilic solvent (alcohols, dioxane, and tetrahydrofuran). Initially, 50 mg of gelator was taken in a 4 mL screw cap glass vial, to which 50  $\mu$ L of solvent was added. The mixture was heated for 10 mins on water bath maintained at 50 °C and later allowed to cool down to room temperature. The solvent was added in increments of 50  $\mu$ L, until all of the gelator powder dissolved in it at room temperature. Degree of dissolution was checked by visualization.

### **Phase-selective gelation of oil – Aliquot or Room Temperature Method**

A specific amount of prepared aliquot, capable of delivering at least MGC concentration, was injected at the interface. In a typical phase-selective gelation experiment conducted at 25–30 °C, 25 mg of Man-8 was dissolved in 400  $\mu$ L of ethanol. This aliquot was injected at the interface of the diesel–water mixture (1 mL each). The mixture was allowed to set to obtain gel of only diesel phase.

### **Characterization of Gels**

Evaluation of MGC &  $T_{gel}$  and analysis of gels by XRD/ FT-IR was performed by following the procedures described in Chapter 2.

### **Rheological Studies of Diesel Gel**

Rheological studies were performed on AR 2000 rheometer equipped with a cone and plate arrangement [1° 58' 47'' angle and 40mm diameter with a truncation gap of 47  $\mu$ m]. All the gels were prepared at 5% wt/v and allowed to set for 3 hours. A small portion of set gel was placed on the smooth plate of a rheometer and the cone- plate geometry was lowered to its truncation gap, and the gel was allowed to equilibrate for 10 minutes before starting the experiment. Measurements were performed in frequency

sweep (0.01-10Hz) with either 0.01 or 0.1% strain and strain sweep (0.01% - 100%) modes at a constant frequency of 1Hz. Experiments were repeated twice.

---

## Chapter 4

---

### Molecular Gels-based Controlled Release Devices for Pheromones

---

#### 4.1. Abstract

*Sustained and uniform release of pheromones is essential for superior pest control. Herein, immobilization of liquid pheromones through nanoscale self-assembly of biobased gelators is demonstrated as a potential method to develop efficient controlled released devices (CRDs). Mannitol dioctanoate (M8) immobilized pheromones, 2-heptanone & lauryl acetate, at low concentration (<8% wt/wt) without exhibiting any syneresis; thereby ensuring high loading-capacity and leak-free performance. The gel-based CRD typically consisted of a fruit film, sugar gelator and pheromone. The use of biobased gelators ensures higher biocompatibility and biodegradability of CRDs and eliminates the cost associated with recovering spent devices. The self-assembly mechanism was deciphered by using microscopy, diffraction and rheological measurements, from which nano-width ribbons were observed to be responsible for gelation. The loading capacity of the gel-based device (~92 %wt/wt) was found to be approximately two folds greater than the standard CRD.*

#### 4.2. Introduction

Renewed interest in organic agriculture has revived the reliance on biopesticides to disrupt and control pest attacks, that otherwise adversely affect the agricultural economy.<sup>1</sup> Pheromones are naturally obtained volatile semiochemicals and are considered as effective biopesticides under the integrated pest management concept (Figure 4.1).<sup>1-3</sup>

They induce confusion and impair the sexual communication of pests. The high species-specificity of pheromones further enables pest control without weakening beneficial organisms.

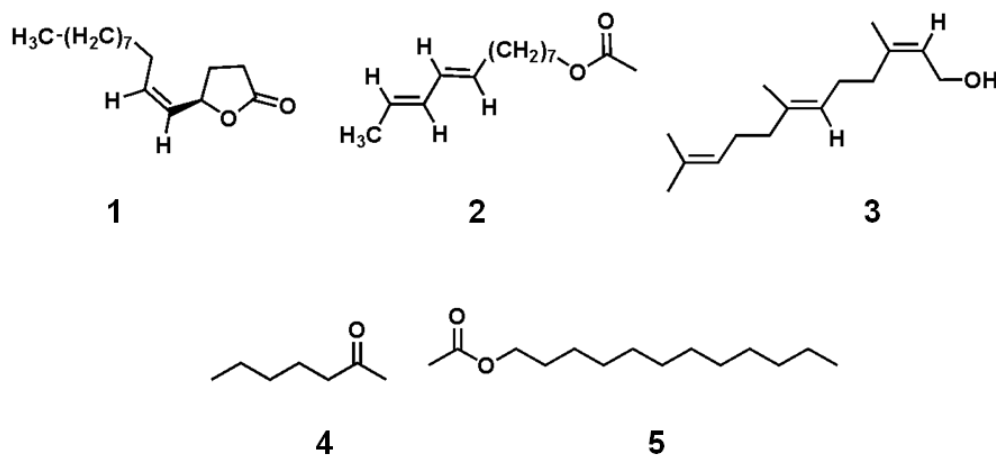


**Figure 4.1.** Molecular structures of representative volatile pheromones. **1:** (R,Z)-5-(1-decenyl)-dihydro-2(3H)-furanone. It is a sex pheromone of Japanese beetle. **2:** (E,E)-8,10-dodecadien-1-ol-acetate, a sex pheromone of the pea moth. **3:** (Z,E)-3,7,11-trimethyl-2,6,10-dodecatrien-1-ol. It is an alarm pheromone of tow-spotted mite *Tetranychus urticae* Koch. **4:** 2-heptanone, a sex pheromone of honey bees. **5:** Lauryl acetate, a sex pheromone of cabbage looper moth.

Numerous reservoir-type controlled release devices (CRDs) have been developed to overcome the high volatility of pheromones and achieve their sustained release over a period of several weeks, essential for effective pest control.<sup>4</sup> However, the current devices are typically polymeric, involve multi-step preparation protocols, exhibit low pheromone-holding capacities and are not readily biodegradable (Figure 4.2). The amount of pheromone encapsulated in these devices range from 36 to 60%. Moreover, most of the devices leak if they are broken or compressed.

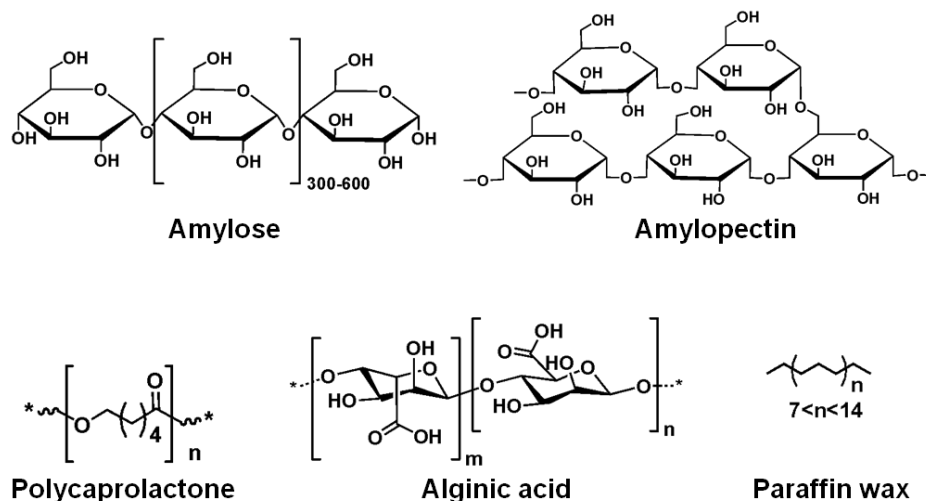


**Figure 4.2.** Chemical structures of polymeric materials used for developing controlled release devices.

Molecular gelators are low molecular weight amphiphilic molecules that self-assemble through non-covalent forces to form a volume-filling 3-D network.<sup>5</sup> Within the network, solvent molecules are immobilized by physical interactions such as surface tension, thereby converting the liquid into a coherent gel. In some cases, extensive solvent-network cohesion causes the gel to be stable even at the boiling point of a solvent.<sup>6</sup> The interactive nature of gels enables them to show a sustained-release property, which has been extensively exploited in drug-delivery applications.<sup>7</sup> The current study aims at utilizing such solvent holding property of molecular gels to control the volatility of pheromones. Such gelators are of particular interest due to their non-polymeric nature, higher biocompatibility and more importantly, they exhibit extremely low minimum gelation concentration (MGC, usually ~5% wt/v). Herein, a biobased molecular gelator as an efficient alternate material for developing reservoir-type release devices has been proposed.

Recently, sugar alcohol-based amphiphiles were developed in our laboratory by employing regiospecific enzyme catalysis. These amphiphiles being conjugates of biobased and highly biocompatible raw materials—sugar alcohols and fatty acids—they are expected to exhibit good biodegradability and minimal carbon footprint. In addition, the amphiphiles showed unprecedented gelation in range of hydrophobic liquids at very low concentration (1.5-5 % wt/v).<sup>8</sup> Owing to such favorable features of sugar alcohol amphiphiles, the versatility of one of the amphiphiles, specifically mannitol dioctanoate (M8) was examined with pheromones, such as 2-heptanone and lauryl acetate. Later, the proficiency of these biobased amphiphiles was demonstrated in developing gel-based controlled release devices.

### 4.3. Results and Discussion

#### 4.3.1. Gelation of pheromones

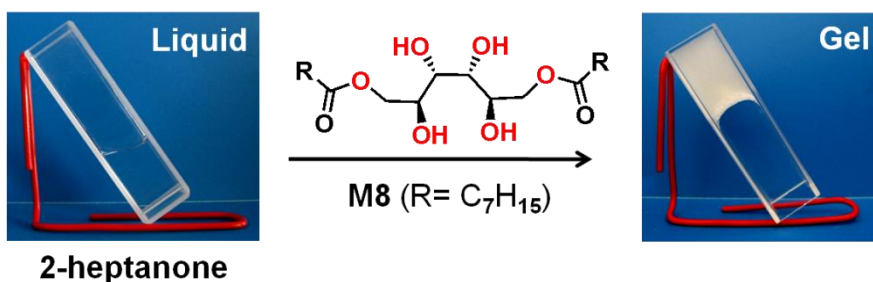


**Figure 4.3.** Photographs of liquid 2-heptanone and its corresponding gel state (the inverted cuvette) obtained after addition of mannitol dioctanoate (M8 at 5% wt/v).

M8 was able to efficiently gel both the pheromones, 2-heptanone and lauryl acetate. The MGC value for M8 was ~3% wt/v, indicating that approximately 96%<sup>9</sup> of the remaining gel is pheromone liquid (Figure 4.3). M8 was further investigated for its

pheromone gelling mechanism and for developing CRD by using 2-heptanone as the model compound. 2-Heptanone is a pheromone, which finds application in the half-billion dollar honey bee (*Apis mellifera* L) industry. 2-Heptanone is a natural compound produced by honey bees that enables them to dissolve plantwaxes as well as beeswax.<sup>10</sup> At elevated levels, it controls parasitic mites, varroa (*Varroa destructor*)<sup>11</sup>, that infest and destroy honey bee colonies in a short period of time.<sup>12</sup> In order to effectively control mites, the miticide (2-heptanone) needs to last at least 2 brood cycles or 42 days. However, due to the high vapor pressure (0.48 kPa at 20 °C) and elevated temperatures existing in bee hives (average 30 °C),<sup>13</sup> the 2-heptanone volatilizes at a faster rate. Therefore, the goal was to develop appropriate CRDs for controlling its evaporation rate.

#### **4.3.2. Thermal and Mechanical Properties of 2-Heptanone Gels**

2-Heptanone gels were made at different concentrations (3, 5 and 7% wt/v) of M8. The gels were characterized for mechanical, syneresis and thermal properties, which are important from an application perspective. Dynamic rheological measurements were performed within a linear viscosity regime to determine the mechanical strength of gels.

From the frequency sweep experiments, the  $G'$  and  $G''$  were found to be independent of oscillatory frequency, except at lower values, where very weak dependency was observed (Figure 4.4). Irrespective of gelator of concentration, the  $G'$  (elastic modulus) values were considerably higher than  $G''$  (viscous modulus) values over the entire experimental frequency range. All the gels exhibited moderate elastic behavior and did not relax over the entire experimental time. For 5 and 7% wt/v gels, average  $G'$  values were found to be greater than that of 3% by an order of magnitude (Table 4.1).

Thus,  $G'$  being a measure of the solid nature of a gel, 3% gel was categorized as soft gel compared to higher concentration gels (5 and 7%), which were well developed and stronger.

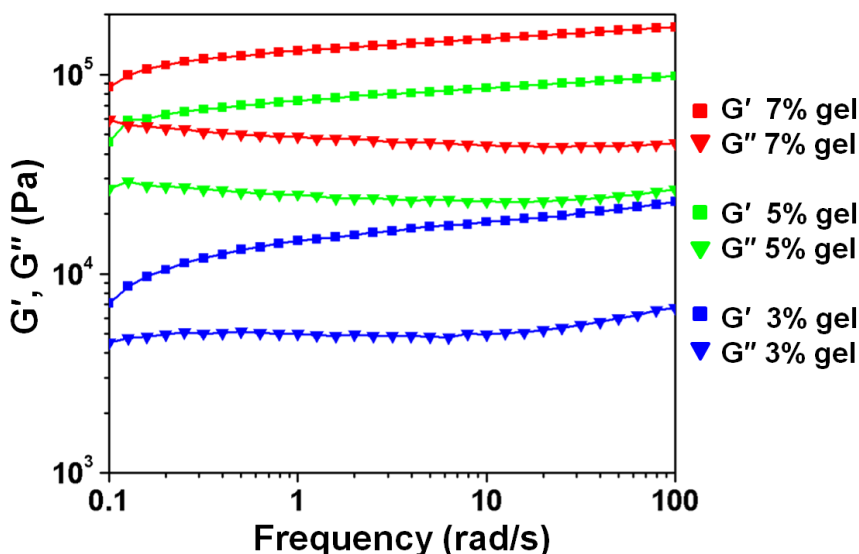


**Figure 4.4.** Oscillatory frequency sweep measurements of 2-heptanone gels containing different concentrations (% wt/v) of M8.

Since a CRD may be compressed during shipment or during placement in honey bee colonies, understanding the behavior of gels under compressive stress is very important. Compression tests indicated that the strength, modulus, and toughness of 2-heptanone gels increased with increasing concentrations of M8 (Table 4.1). Compressive stress-induced syneresis was observed in a 3% gel, whereas a 5 or 7% gel had little or no stress-induced syneresis. Increasing the concentration of gelator, improve: i) the fiber density; ii) compactness of the network; and iii) solvent-network interaction; as a result, the overall mechanical response of the gel is increased. Thermal stability, or the gel-to-sol transition temperature ( $T_{gel}$ ), was determined by the table-top tube inversion method.<sup>14</sup>

Like mechanical properties, the  $T_{\text{gel}}$  was proportional to the concentration of M8 (Table 4.1).  $T_{\text{gel}}$  values were greater than the average bee colony temperature, where the highest  $T_{\text{gel}}$  value was 70 °C for a 7% gel. Initial gel characterization results suggested that gels with M8 concentration of 5% or greater have strong potential as components of CRDs.

**Table 4.1.** Thermal and mechanical properties of 2-heptanone gels of M8.

Properties	M8 gel concentration (% wt/v)		
	3	5	7
$T_{\text{gel}}$ (°C)	62-64	65-68	70-72
$G'$ (kPa)	14.64	73.85	131.7
Modulus (kPa)	6.8 ( $\pm 4.1$ )	13.5 ( $\pm 6.8$ )	23.6 ( $\pm 8.1$ )
Toughness (kPa)	0.77 ( $\pm 0.17$ )	2.4 ( $\pm 0.77$ )	4.7 ( $\pm 1.3$ )
CS <sup>a</sup> (kPa)	1.3 ( $\pm 0.26$ )	4.0 ( $\pm 0.13$ )	7.5 ( $\pm 2.5$ )

<sup>[a]</sup>CS = Compressive Strength.

### 4.3.3. Morphology of 2-Heptanone Gels

Morphology and molecular aggregation were studied using various techniques to elucidate the gelation mechanism. Optical microscopy was effective in documenting the gelling behavior of the M8 in 2-heptanone (Figure 4.5A-H). Samples that were heated to 80°C – to produce sol – and cooled typically demonstrated the appearance of small crystals (Figure 4.5A). The crystals quickly grew and new crystals formed randomly throughout the mixture upon further cooling. Sequential micrographs of the crystals revealed that the crystals typically grew until they reached adjacent crystals. Individual

crystals initially remained distinct as the void spaces were filled. With time, however, it became more difficult to distinguish individual crystal as the gel modified.

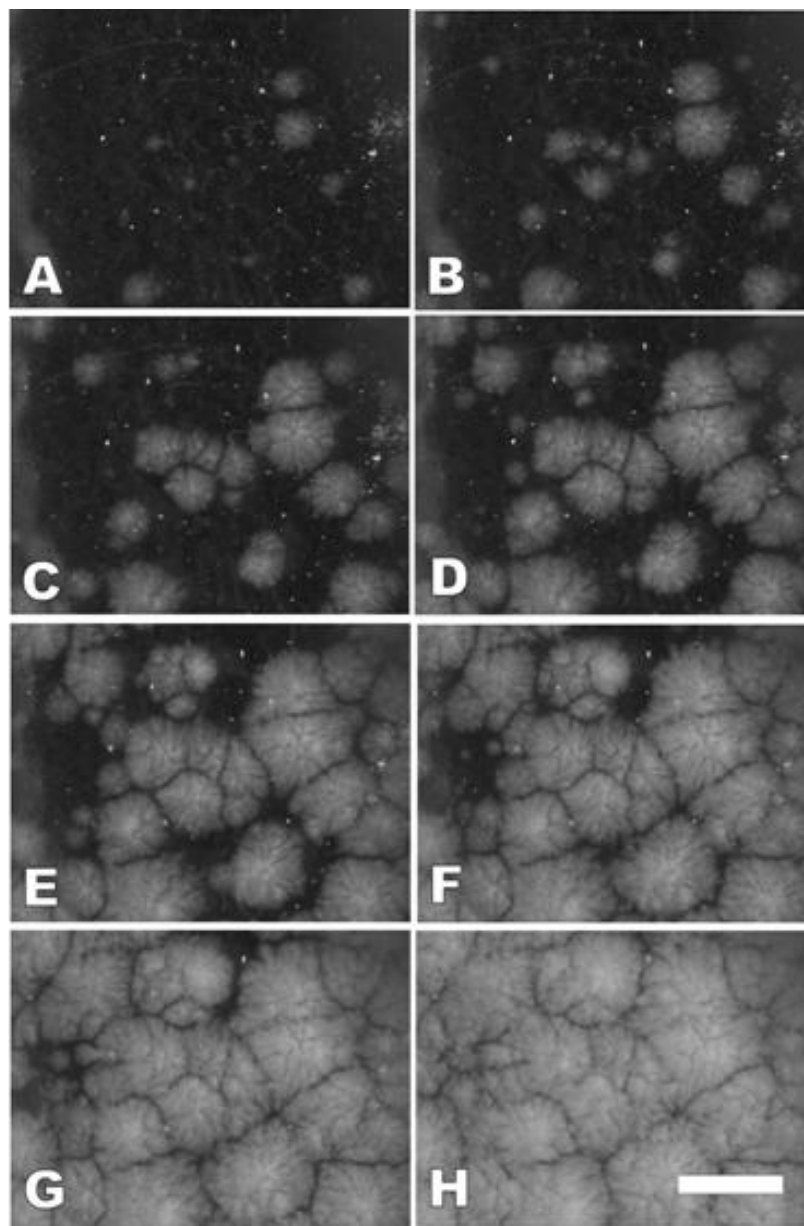


**Figure 4.5.** Optical micrographs of sequential views during the gelling process of M8 in 2-heptanone (3 % wt/v). Scale bar = 1 mm.

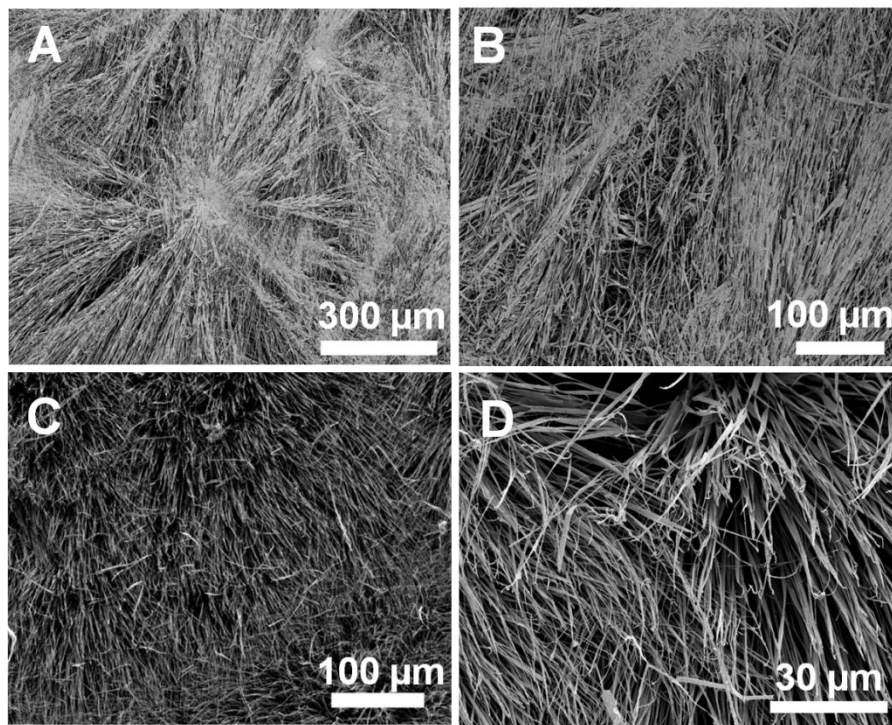


**Figure 4.6.** A–D) Scanning electron micrograph of critical point dried 2-heptanone gel of M8 (5% wt/v) at different magnification level.

Further details on morphology were acquired by using a high resolution field emission scanning electron microscope (SEM). Gels were critical point dried from liquid CO<sub>2</sub> before making samples for SEM.<sup>15</sup> The morphology of the dried sample was in good concordance with that observed in the wet condition under the optical microscopy, indicating that critical point drying preserved the native structure of the gel. Micrographs revealed the star-shaped crystals comprised of ribbons radiating out from the core nucleation site (Figure 4.6A and B). The ribbon density was greatest near the region where nucleation occurred. The terminal points of ribbons were thinner than those near the nucleation site (Figure 4.6C and D). The orientation of ribbon was less apparent in regions where the terminal ends of adjacent crystals intersected. Such intertwining

resulted in the formation of crystal clusters, which most likely contributed to the overall strength and rigidity of the gel structure.

#### 4.3.4. Self-assembly Mechanism of M8 in Pheromones

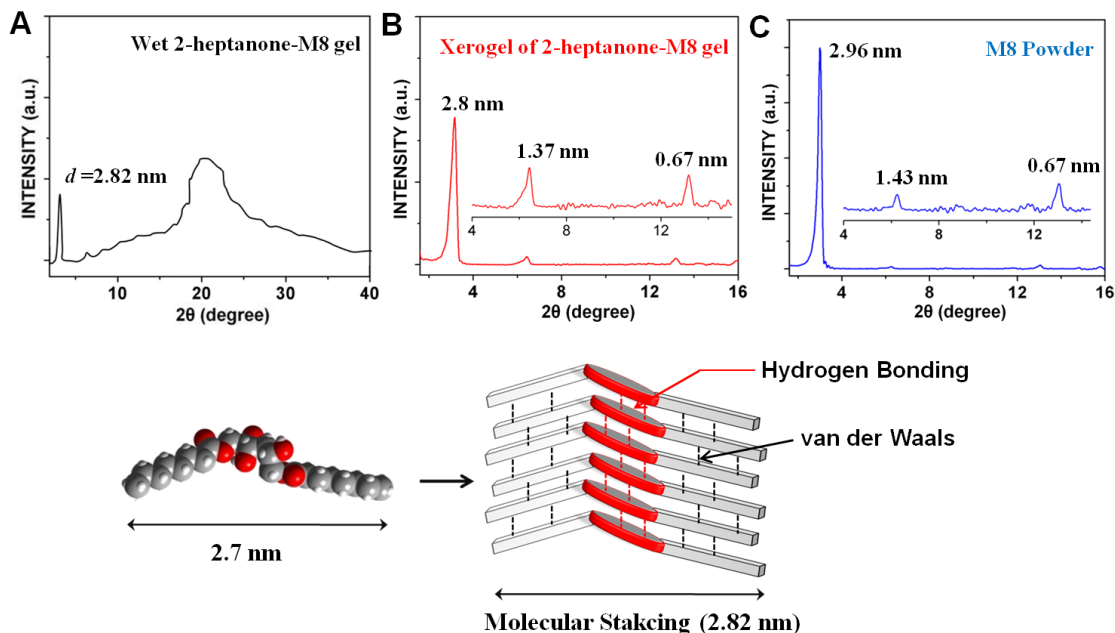


**Figure 4.7.** XRD patterns of different M8 samples. ‘*d*’ indicates the long *d*-spacing values of corresponding samples. A) 2-Heptanone gel of M8 (5% wt/v). ‘\*’ denotes the Bragg peak at  $\sim 0.4$  nm, which is a characteristic signal of subcell packing of hydrocarbon chains in the self-assembled lipids.<sup>16a</sup> B) 2-Heptanone-M8 xerogel with an inset of the magnified region from  $2\theta = 4$ - $15^\circ$ . C) M8 powder with an inset of the magnified region from  $2\theta = 4$ - $14^\circ$ . D) Energy minimized structure of M8 along with deduced molecular stacking and non-covalent interaction between the gelator molecules.

To elucidate possible molecular aggregation, X-ray diffraction (XRD) was performed on xero- and wet gels of M8 in 2-heptanone and compared to that of M8 powder (Figure 4.7A-C). M8 exhibited similar XRD patterns in both xerogel and powder state; i.e. it self-assembles in a similar manner in the gel and the solid state. A strong first

reflection was observed at 2.8 nm, and subsequent peaks were spaced in such that the Bragg spacing ratio was 1 : 1/2 : 1/3 : 1/4, which is a characteristic response of lamellar structures. Based on this analysis, the self-assembly mode for M8 was postulated to follow well-ordered lamellar stacking.<sup>16b</sup> The probable ordered structure was modeled by using an energy-minimized M8 molecule and correlating its size to the d-spacing of the native gel (2.82 nm). The multilayer molecular stacking (Figure 4.7D) is stabilized by extensive hydrogen bonding between the sugar groups and van der Waals interaction between alkyl chains, which was confirmed by FT-IR spectroscopy.

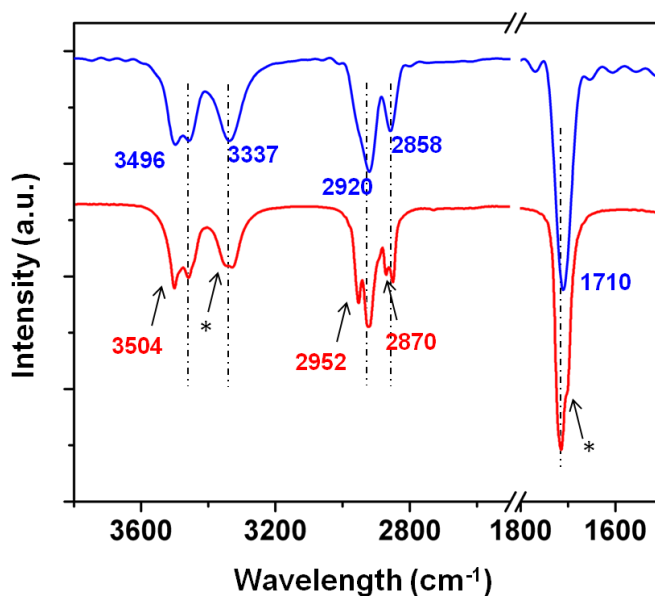


**Figure 4.8.** FT-IR spectra of M8 powder (Blue) and 2-heptanone gel of M8 (Red). The dotted lines indicate the similar transmission frequencies between the two samples. ‘\*’ represent the shoulders to the hydroxyl and carbonyl bands.

FT-IR measurements were done on two M8 samples: crystalline powder and wet gel of 2-heptanone. The IR spectra of wet gel showed transmission bands at: i) 3330-3496  $\text{cm}^{-1}$  corresponding to hydrogen bonded -OH stretching; ii) 2920 and 2850  $\text{cm}^{-1}$  corresponding to methylene stretching with all-trans configuration; and iii) 1712  $\text{cm}^{-1}$

related to hydrogen bonded carbonyl stretching (Figure 4.8). On correlating the two spectra, it was found that the frequencies for characteristic functional groups of M8 (hydroxyl, carbonyl and methylene) are almost similar in both the samples. The resemblance in spectra suggests that the M8 exhibit similar aggregation mode in both the gel and solid crystalline state, which in turn is in good agreement with the conclusion drawn from the XRD data.

Furthermore, the 2-heptanone wet gel sample showed few additional transmission bands corresponding to characteristic functional groups, however at higher frequencies. A peak at  $3504\text{ cm}^{-1}$  (along with a slight shoulder to a band at  $3337\text{ cm}^{-1}$ ) and a shoulder to peak at  $1712\text{ cm}^{-1}$  were observed, which indicate the presence of few gelator molecules of which hydroxyl and carbonyl groups are not involved in hydrogen bonding. Moreover, higher frequency peaks were also observed in the methylene stretching frequency range, specifically at  $2952$  and  $2870\text{ cm}^{-1}$ , suggesting the high gauche conformation of few  $\text{C}_8$  chains of M8.<sup>17</sup> The occurrence of such high frequency values for some of the M8 molecules was attributed to their non-assembled state. Thus, it can be considered that while most of the M8 molecules are engaged in forming solid-like network, few of them do not exhibit any intermolecular interaction and are present as free molecules in the solvent matrix.

#### **4.3.5. Biodegradability of M8**

Before using the M8-based gels for CRDs the 2-heptanone gels of M8 were further analyzed. In general, the materials constituting CRDs must be: (i) biocompatible with the beneficial organism (bees in present case), so that they do not disrupt their normal behavior, and (ii) naturally biodegradable, to preclude the need and associated

cost to recover spent devices.<sup>18</sup> Biodegradability of M8 was computed in terms of mineralization rate and was compared to that of a starch control. Starch is a common food commodity and is one of the most readily degradable polymers in nature. As depicted in Figure 4.9, M8 is a readily biodegradable material, since it mineralized at nearly the same rate as the starch control. In 43 days, nearly 60% of M8 was mineralized as compared to 70% mineralization of starch. Thus, the use of biobased precursors – mannitol and caprylic acid – ensures that the gelators are safe and biodegradable. The use of sugar-gelators, such as M8, in agricultural controlled release devices could provide important functionality and environmental compatibility.

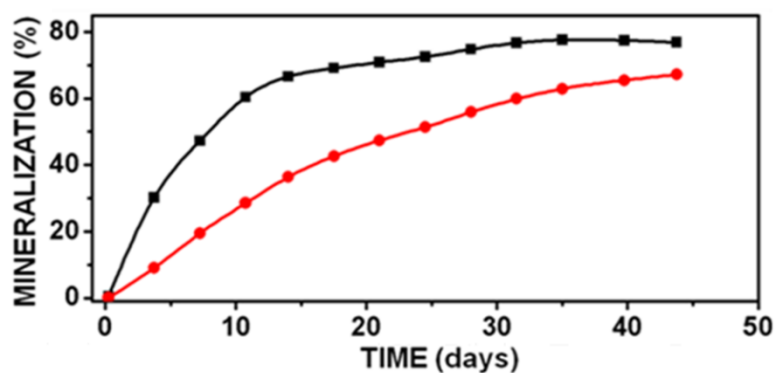


**Figure 4.9.** Biodegradability of M8 (red) and starch control (black) in terms of percent mineralization over time (days).

#### 4.3.6. Evaporation Rate of 2-Heptanone from M8-gel

To determine the efficacy of the gel matrix per se in controlling the release of pheromone, the relative rate of evaporation between liquid 2-heptanone and a 2-heptanone gel (7% wt/v) was investigated by monitoring weight loss of both materials under the same conditions. The data demonstrates that the 2-heptanone volatilized as quickly from the gel as it did from liquid 2-heptanone (Figure 4.10), indicating that the

degree of interaction of 2-heptanone with the self-assembled structure is very low. Therefore, the inefficiency in controlling the release was hypothetically attributed to the clustered aggregation of the self-assembled structure. Clusters aggregations of fibers are known to be less effective in entrapping organic liquids than the entanglement fibers through physical cross-linking.<sup>19</sup> However, the ability of M8 to immobilize pheromones at low concentration (~7% wt/v) without exhibiting any syneresis on application of high compressive stress ensures a high loading-capacity and leak-free performance which, in turn, enhance its utilization in developing a reservoir type CRD.

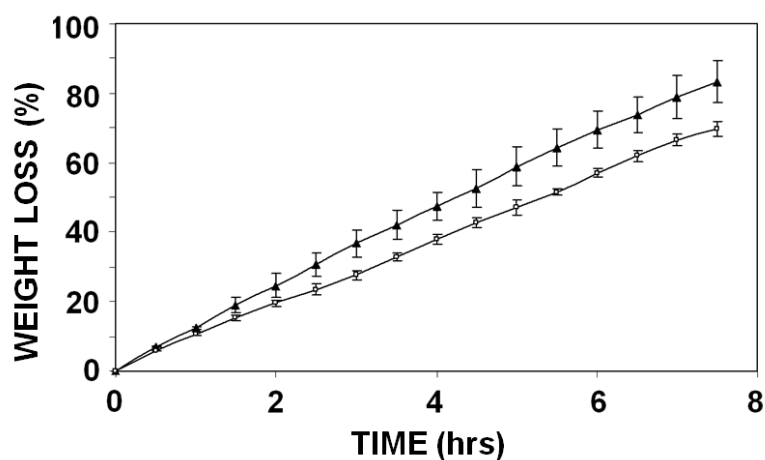


**Figure 4.10.** Weight loss from evaporation of 2-heptanone from a liquid (O) or 2-heptanone gel (▲).

## 4.3.7. M8-gel Based CRD

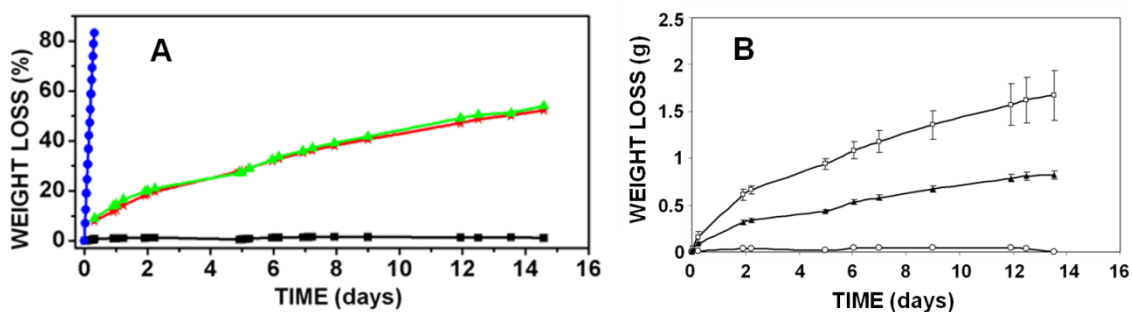


**Figure 4.11.** A) Percent weight loss over time of two controls and two activated control-release devices. Controls consisted of a gel without a vapor barrier (**blue**) and a gel completely sealed in a vapor barrier film (**black**). Activated control-release devices were sealed in a vapor barrier film that contained a small opening. The devices contained either a 2-heptanone gel (**green**) or a blend of beeswax and 2-heptanone (**red**). B) Weight loss over time of control-release devices. The control (O), which was sealed in vapor barrier film, had very little weight loss during the time period tested. The device containing 2-heptanone gel (□) had double the weight loss compared to the devices containing beeswax (▲).

Finally, a reservoir-type CRD was developed by using M8. Like previously developed CRDs, the current device consisted of a reservoir of a 2-heptanone gel (7% wt/v) sealed in a pouch made from a semi-permeable membrane (vapor barrier film). The membrane is a fruit film made entirely of agricultural materials and is easily heat sealable, which facilitates encasing the reservoir.<sup>20</sup> The rate of 2-heptanone loss was markedly reduced by sealing the 2-heptanone gel in a vapor barrier film (Figure 4.11A). Very little change in weight was observed in a completely sealed CRD. However, samples activated by boring a small hole in the vapor barrier slowly released 2-heptanone over time (Figure 4.11A). The gel-based CRD was compared to a standard controlled

release device made with beeswax as the reservoir material. The percent weight loss of the gel-based CRDs was similar to the CRD consisting of 1 : 1 blends of beeswax and 2-heptanone.

Advantageously, the loading capacity of the gel-based device (~92% wt/wt) was approximately two-fold greater than that of the beeswax containing device (50% wt/wt). As a result, for controlled release devices of a given weight, the gel-containing device delivers approximately twice the amount of active ingredient as the control device (Figure 4.11B). The results suggest that the M8 immobilizes the 2-heptanone in the reservoir and provides a means of loading a very high concentration of 2-heptanone into the reservoir. The high concentration loading capacity will allow for smaller devices with equal or higher delivering capacity than other devices. In addition, the high solid content in CRDs made with other reservoir materials will reduce the degradation rate of devices. The degrading material may attract unwanted pests and cause problems. On the contrary, owing to minimal solid content and high biodegradability of gelators, gel-based CRDs, once spent, will degrade rapidly, thereby minimizing the unwanted pest attraction problem.

#### **4.4. Conclusion**

In conclusion, the application of molecular gels in the agricultural industry was demonstrated by utilizing efficient pheromone-gelling sugar gelators, such as M8, to develop reservoir-type CRDs. The use of a biobased gelator ensures higher biocompatibility and biodegradability of devices. Thus, CRDs with high loading capacity and the delivery of pheromone at high concentration were developed. The efficiency of gels pertaining to targeted application depends on various factors, for example gel–

solvent interactions, gel morphology, etc., which can be explored for future development of effective molecular gel-based CRDs.

## **4.5. Experimental Section**

### **4.5.1. Materials**

2-Heptanone (CAS registry No. 110-43-0) was purchased from the Sigma-Aldrich Co. (St. Louis, MO). Peach fruit film (100  $\mu\text{m}$  thickness) processed from a 3:1 blend of peach puree:pectin (Origami Foods, Stockton, CA) was used as a vapor barrier film for making controlled release devices. Beeswax was purchased locally (Protex, Berkeley, CA). M8 was synthesized by using regiospecific enzyme catalysis, which is described in experimental section of Chapter 2.

### **4.5.2. Experimental Techniques**

The experimental measurements discussed in this paper were conducted in two research facilities, namely: The City College of New York (CCNY) and Agricultural Research Service (USDA-ARS, California) Experiments like synthesis of M8, preliminary gelation of pheromones, evaluation of MGC &  $T_{\text{gel}}$  and analysis of gels by XRD/ FT-IR was performed in CCNY. The procedures for these experiments are described in Chapter 2. The rest of the experiments were performed in USDA-ARS and the details are given below.

### **2-Heptanone Gels**

Gels were made by pipetting out 5 mL of 2-heptanone in an empty glass vial (1.5 cm dia., 2.5 cm length) and adding the prescribed amount of 3, 5, or 7% wt/v of M8 in 2-

heptanone. The vial was capped and then partially submerged in a water bath (80 °C) using a clamp. The vial contents were swirled intermittently to facilitate dissolution. Once the M8 had completely dissolved in the 2-heptanone, the temperature of the water bath was slowly lowered. Formation of gel was confirmed when no gravitational flow of 2-heptanone was observed on inversion of a vial.

### **Optical Microscopy**

Gel formation was monitored through a flat-bottomed 25 ml glass vial containing a 2 mL sol of 2-heptanone and M8 (at 3% w/v concentration). The sol temperature was maintained at 80 °C by immersing it in water bath. The sol was placed on the microscope stage and was to allowed to cool at atmospheric rate. Crystallization and gel formation during cooling were documented using a digital camera (Retiga 2000R, Q-Imaging, Surrey, BC, Canada) mounted on a stereo light microscope (Leica Model MZ 16F, Leica GmbH, Wetzlar, Germany). Photographs were taken every 3 seconds starting at the moment the first crystal was observed.

### **Scanning Electron Microscopy (SEM)**

SEM was done by first preparing a 5 %wt/v M8 gel in 2-heptanone as previously described. The gel was removed from the glass vial and sliced into pieces (ca. 5 mm). The samples were immediately placed in the chamber of a critical point dryer (Tousimis Autosamdri 815, Tousimis, Rockville, MD) and equilibrated in liquid CO<sub>2</sub> for several hours to displace the 2-heptanone. After several exchanges over a period of several hours the samples were critical point dried before sputter coating with gold-palladium in a Denton Desk II Sputter Coating Unit (Denton Vacuum, Inc., Moorestown, NJ). The

samples were viewed and photographed with a Hitachi S4700 field emission scanning electron microscope (Hitachi, Japan).

### **Mechanical Properties**

The mechanical properties of the gels were determined using both a penetrometer test as well as rheometry.

*Penetrometer Test:* 3, 5, and 7% wt/v M8 gels in 2-heptanone was prepared in glass vials as previously described. Gel thickness was approximately 30 mm. Penetrometer tests were performed without removing the gels from the vials so that measurements could be recorded on undisturbed sample. Penetrometer tests were performed by pressing a flat-faced cylindrical probe (8 mm dia.) into the gel sample to a depth of 3 mm at a rate of 5 mm/min using a universal testing machine (model 4500, Instron Corp., Canton, MA). A load cell (100 N) was used to detect compressive force. Peak force, modulus, and toughness were determined from force/deformation data. Five samples were tested for each of the gel concentrations.

*Dynamic Rheological Tests:* Gel samples were performed using a Peltier plate rheometer

(TA Instruments, model AR2000, New Castle, DE). The gel was scooped from the vials with a spatula and placed on a Peltier plate. A stainless steel parallel plate (60 mm) was lowered onto the sample. The sample thickness was held constant at 1 mm. Dynamic rheological tests were used to characterize the elastic modulus ( $G'$ ) and viscous modulus ( $G''$ ). The elastic modulus is a measure of the solid-like response of the material, whereas the viscous modulus is a measure of the liquid-like response of the material. All dynamic

measurements were obtained at a frequency of 1 rad/s and a strain of 2%. In addition, all experiments were performed within the linear viscoelastic region.

### **Biodegradation of M8**

The relative degradation rate of samples was determined using a respirometer (Micro-Oxymax System, Columbus Instruments, Columbus, OH). The respirometer CO<sub>2</sub> sensor was calibrated with a CO<sub>2</sub> standard gas (8,000 ppm). The carbon content of the samples (60.8%) was determined according to ASTM methods using a CHN elemental analyzer (Perkin Elmer 2400, Boston, MA). The analyzer was equipped with a thermoconductivity detector and was operated using helium gas. The combustion temperature was 975 °C and the reduction temperature was 680 °C.

Commercial compost was purchased locally and adjusted to 58 % moisture (dry weight basis). The glass sample bottles (250 ml) were filled with 20.0 g compost and 0.30 g test sample that was gently mixed with the compost. The sample bottles were initially flushed with CO<sub>2</sub>-free air and sealed. Respirometry experiments were conducted at room temperature (22 °C) and CO<sub>2</sub> concentration was read every 12 hr. Three replications were tested for each treatment and data were expressed in terms of percentage mineralization.

### **Evaporation Rate of 2-Heptanone from M8 gel**

The relative rate of evaporation between liquid 2-heptanone and a 2-heptanone gel (M8 concentration 7% wt/v) was determined by monitoring weight loss of both materials under the same conditions. The tests were performed using aluminum sample dishes (50 mm dia., 20 mm depth). The dishes were filled (5 g) with 2-heptanone liquid (control) or gel (treatment). For making a dish containing gel, the mixture of 2-heptanone and M8 (7% wt/v) was heated to sol state and the solution (~ 5 g) was poured into an

aluminum sample dish and immediately covered to minimize evaporation. The samples were allowed to equilibrate 1 hr at room temperature. All samples were uncovered and placed in a poly(methyl methacrylate) cabinet equipped with a ventilation fan. The airflow velocity was 9.8 m/s, and the airflow volume was 4.7 volume changes per second (9.9 m<sup>3</sup>/min). All tests were performed at room temperature. The samples were weighed regularly to monitor weight loss.

### **Controlled-Release Devices**

Controlled-release devices made with M8 gel in 2-heptanone (7 %wt/v) were compared with a standard controlled-release device made with beeswax as a reservoir material. The beeswax devices were made by first preparing the reservoir material. This was accomplished by dissolving beeswax in 2-heptanone (1:1) in a sealed glass jar at elevated temperatures (80 °C). The molten mixture was poured into a disk mold (3 mm thick, 10 cm diameter) and allowed to cool and solidify. Specimens weighing 3.2 g were cut from the beeswax/2-heptanone disc and sealed within a vapor barrier film envelope using a heat sealer (Model 2526, Clamco, Cleveland, OH) operated at 405 °C. The M8 gel in 2-heptanone (7% wt/v) was heated to sol state in a water bath and sample weighing 3.2-3.5 g was poured into a film envelope and sealed closed as previously described and in the literature.<sup>20</sup> All control-release experiments were performed in duplicate. Loss of 2-heptanone from the devices was measured as weight loss. To activate release of 2-heptanone, an 8 mm hole was made in the film envelope of each sample. Experiments were run until 50% or more of the 2-heptanone had been lost.

---

## Chapter 5

### Medium Chain Sugar Amphiphiles: Healthy & Alternative Vegetable Oil Structuring Agents

---

#### 5.1. Abstract

*Vegetable oils are frequently structured or solidified, to enhance their organoleptic and mechanical properties. This is usually achieved by increasing the net amount of long chain saturated and/or trans fatty acids in the oil. With the risk of coronary heart disease associated with these fatty acids, the food industry is urgently looking for better alternatives. In this context, as a healthy alternative, the medium chain dialkanoates of low calorie sugars (sugar alcohol dioctanoates) are investigated for their ability to structure vegetable oils. Specifically, the non-toxic mannitol and sorbitol dioctanoate (M8 and S8) were explored for their structuring efficiency in wide range of oils (canola, olive, soybean and grapeseed oil). The efficiency was computed in terms of mechanical, thermal and structural properties of the structured oils. Based on systematic investigation, it was observed that M8 was a better structuring agent than S8.*

#### 5.2. Introduction

Vegetable oils are an important and widely used source of lipids in human diet.<sup>1</sup> They constitute an integral part of everyday foodstuffs including chocolate, spreadings, shortenings, ice-creams, and bakery products. However, due to their fluid-like behavior, oils are frequently incorporated as structured oil, i.e., oils with improved mechanical properties.<sup>2</sup> Structuring of vegetable oil is a process, which converts fluidic oil to semi-

solid plastic material. It also enhances the organoleptic properties (consistency, texture, flavor and stability) of oils.<sup>2,3</sup> More importantly, it prevents the migration or exudation of oil from the food products.<sup>4</sup>

The structuring process typically involves increasing the melting point of oils by altering their fatty acid profiles.<sup>2,3</sup> Commercially employed structuring strategies are hydrogenation, inter-esterification, and addition of saturated fat. Hydrogenation converts naturally occurring *cis* unsaturated fatty acids to *trans*/saturated counterparts. Inter-esterification substitutes the unsaturated fatty acids present in the triacylglycerides with the saturated ones. Addition of saturated fat involves physical mixing of saturated animal/vegetable fat with the oil. All these methods essentially focus on raising the saturated fatty acids (SFA) or *trans* fatty acid (TFA) content of oils.

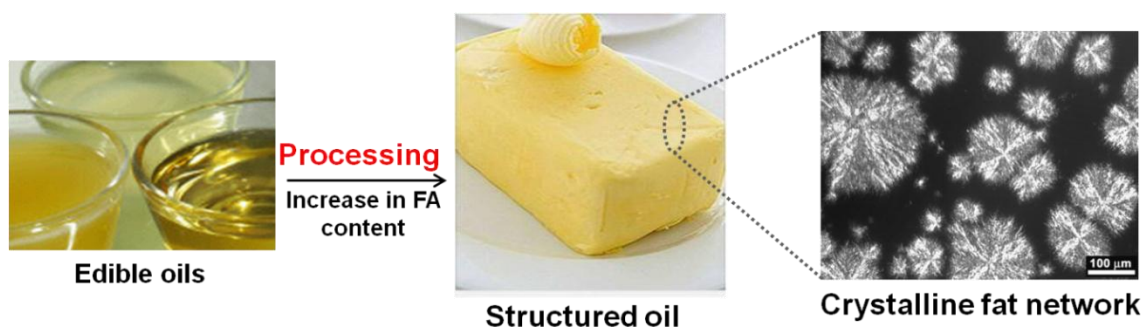


**Figure 5.1.** Pictorial depiction of liquid and structured oil. An optical micrograph of structured oil showing the crystalline fat network present in it.

Increase in the amount of these fatty acids leads to development of colloidal network of polycrystalline fat crystals, which in turn entraps the oil molecules (Figure 5.1).<sup>5</sup> The crystalline network is responsible for structuring and enhancing the organoleptic properties of oil. However, consumption of SFA and TFA is known to elevate the risk of cardio-vascular diseases and metabolic syndromes.<sup>6</sup> ‘American Heart

Institutes' and 'Food policies of USA' demand complete elimination of TFA and limit the energy intake from SFA to 10% of daily need.<sup>7</sup> Conscious effort has been taken to reduce fat content and improve nutritional profile of food products. As a result, food technologists have focused on developing alternative strategies for structuring that will conform to above dietary requirements, and yet provide the same level of structuring performance.

Recently, the molecular gelation phenomenon has received increased attention in structuring applications.<sup>5,8</sup> Molecular gelators when dispersed in the solvent matrix self-assemble with the aid of weak intermolecular interactions to form 3-D network. The resulting network entraps the solvent molecules, leading to formation of a gel. Thus, the gelation process enables conversion of the liquid state of a solvent to a solid state. Due to mechanistic resemblance of molecular gelators to fats crystals in entrapping liquid molecules, molecular gelation has emerged as a potential alternative structuring method. Moreover, the vast diversity in the structure of molecular gelators can be explored to make the network, and hence structured oil, with desired range of mechanical and melting properties.

To date, several molecular gelators systems have been proposed for structuring oils. Fatty alcohols<sup>9</sup>, fatty acids<sup>10</sup>, wax esters<sup>11</sup>, monoglycerides<sup>12</sup>, sorbitan alkylates<sup>13</sup>, and phytochemicals<sup>14</sup> are representative classes of gelators explored for structuring applications (Figure 5.2). However, problems exist with most of these current classes. Addition of fatty acids, fatty alcohols and wax esters is not currently permitted in the food products. Sorbitan alkylates, e.g. sorbitan monostearate, gels oils at relatively high concentration (~15% wt/v). Phytochemicals like lecithin are able to gel oil only in the

presence of water and additional gelling component like sorbitan tristearate. Presence of water makes the gel susceptible to microbial spoilage and autoxidation resulting in development of rancidity and foul flavors. Furthermore, the metabolism of all these existing gelators will produce long chain fatty acids, thereby lowering the nutritional profile of gelators.

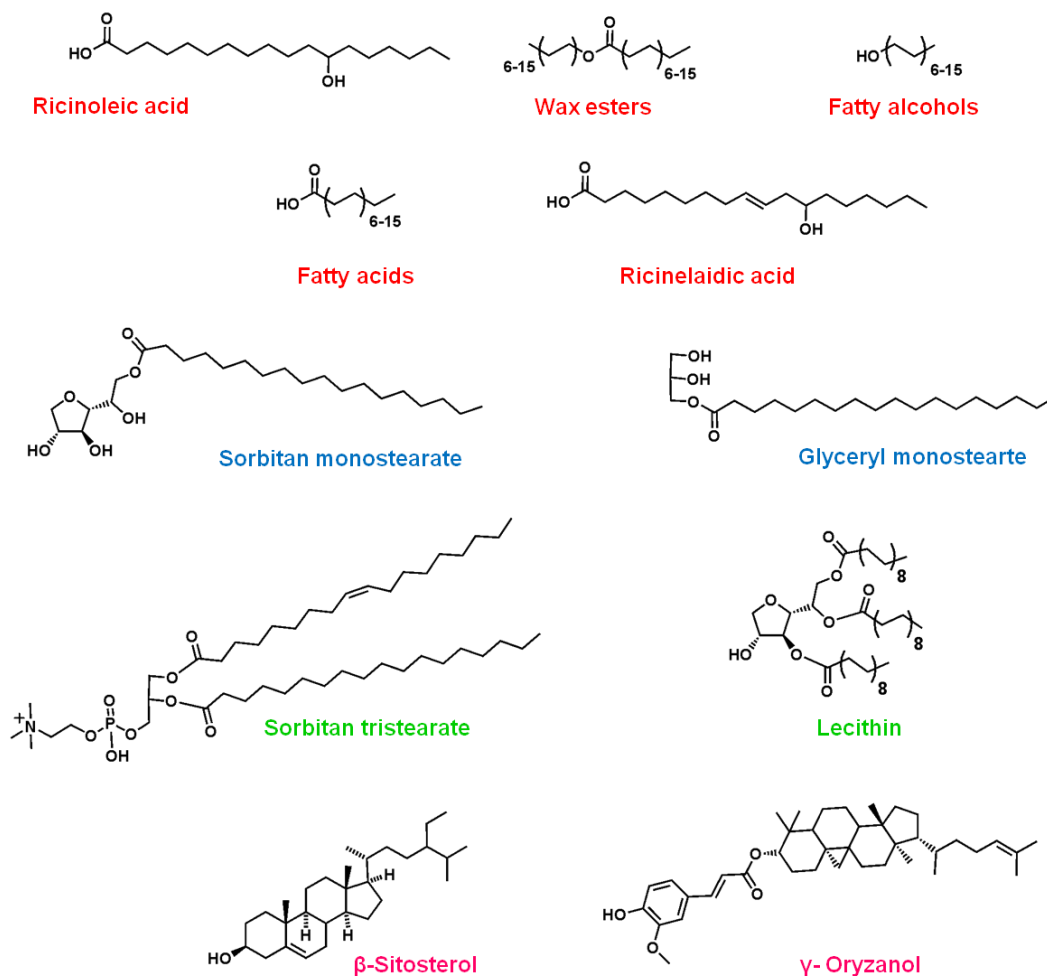


**Figure 5.2.** Molecular structures of different classes of gelators that have been investigated for structuring applications. Gelators in red font are not permitted by FDA to be added in food products. Gelators in blue font do gel oils but at high concentration (10-15 %wt/v). Gelators in green font are used in combination, but require addition of water for gelation. Finally, gelators in pink font are used in combination, but they are not abundantly available and are expensive.

Consequently, there is a strong urge to develop novel gelators, which truly behave as an alternative and have been proven to exhibit no effects on human health. In this context, sugar alcohol-based gelators consisting of medium chain fatty acids, namely mannitol dioctanoate and sorbitol dioctanoate, have been proposed as food-grade and healthy structuring agent. The sugar dioctanoate essentially consist of two octanoic acid (C<sub>8</sub>) appended to two ends of sugar alcohol molecule via enzyme-labile ester bond. Therefore, these molecules are expected to be highly biocompatible. Moreover, the building blocks (mannitol, sorbitol and octanoic acid) exhibit favorable physiological advantages. Compared to typical sugars, sugar alcohols have low calorific values and are highly noncariogenic.<sup>15</sup> Medium chain fatty acids, especially octanoic acid, are effective antimicrobial entities.<sup>16a</sup> Because of their relatively smaller chain length, they show enhanced membrane crossing ability, a vital behavior responsible for lysing a bacterial cell. In addition, medium chain fatty acids do not easily re-esterify to form triglycerides, accounting for high plasma clearance in the body.<sup>16b,c</sup> They are non-hypercholesterolemic and get readily metabolized to provide energy. Therefore, in addition to gelation these sugar gelators are expected to impart additional functionalities to structured oil.

## **5.3. Results and Discussion**

### **5.3.1. Cytotoxicity of M8 and S8**

The determination of toxicity of sugar alcohol-derived gelators is imperative as they are being investigated for edible applications such as structuring of vegetable oils. Hence, the cytotoxicity of M8 and S8 was initially tested against human hepatocellular

carcinoma cells (HepG2) by using a MTT {3-(4,5-dimethyl-2-thiazolyl)-2,5-diphenyl-2H-tetrazolium bromide} based cell viability assay.<sup>17</sup>

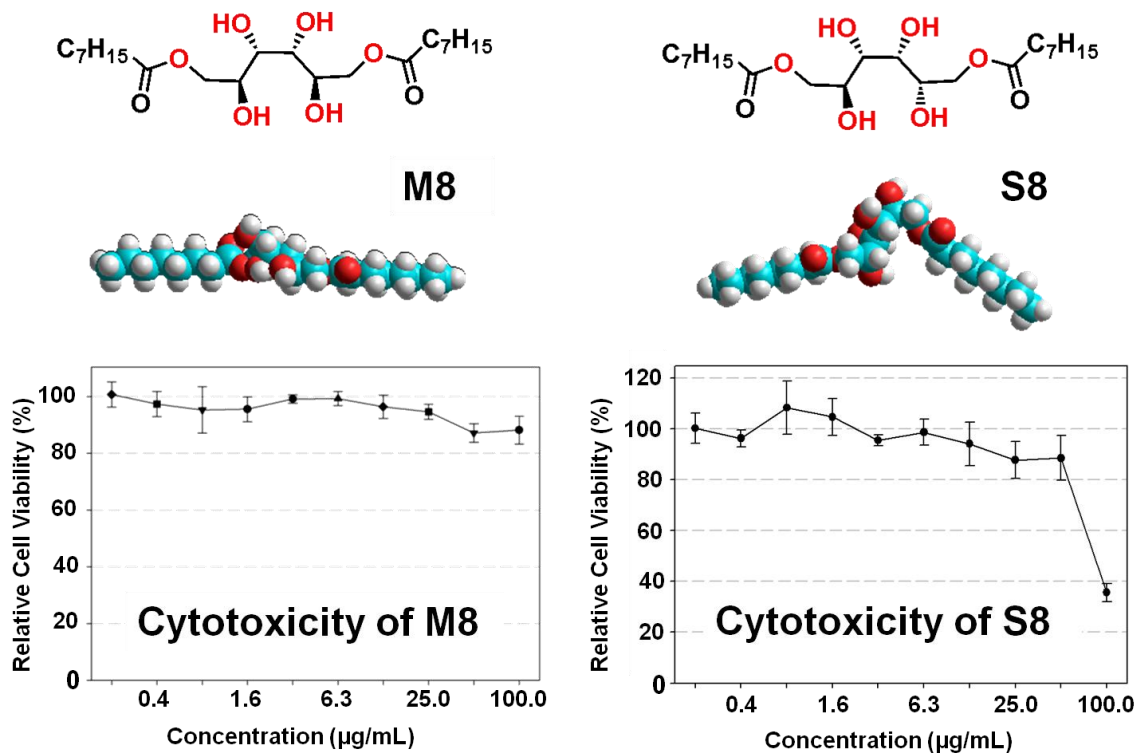


**Figure 5.3.** Molecular and 3-D space filling model of M8 and S8 along with their cytotoxicity data. Cytotoxicity was deduced in terms of cell viability that is plotted against gelator concentration (dissolved in DMSO).

Figure 5.3 illustrates the concentration dependence cell viability of the gelators (greater the cell viability, higher the biocompatibility). The gelators exhibited ~83% viability up to a concentration of 50 µg/mL. On increasing their concentration to 100 µg/mL, the gelators behaved differently. The cytotoxicity of M8 was not affected even at 100 µg/mL. In contrast, a steep increase in cytotoxicity was observed for S8, and the cell viability decreased to 35% at 100 µg/mL. The dissimilarity in degree of biocompatibility can be attributed to the type of sugar present in the head group, since it is the only

difference between the gelators. However, FDA has categorized mannitol and sorbitol as generally recognized as safe (GRAS) chemicals and their LC<sub>50</sub> (oral LC<sub>50</sub> rat) values are almost comparable at 15000 mg/Kg.<sup>18</sup> Thus, the exact reason for acute behavior of S8 is unclear. Nonetheless, it can be believed that the sugar alcohol gelators are biocompatible at moderate dose concentration.

### 5.3.2. Vegetable Oil Gelation: Efficiency and Self-assembly Mechanism

The efficiency and versatility of mannitol and sorbitol dioctanoates were examined by using a wide range of vegetable oils such as olive oil (OO), canola oil (CO), soybean oil (SO) and grapeseed oil (GO). The results are summarized in Table 5.1. Both, M8 and S8, displayed excellent gelation tendency in all the tested oils. Furthermore, all the gels were stable for months. The gelation efficiency of M8 and S8, in terms of MGC, was found to be independent of type of oil used to make gels.

**Table 5.1.** Vegetable oil gelation efficiency and long range d-spacings of M8 and S8.<sup>a</sup>

Oils <sup>b</sup>	M8		S8	
	MGC	<i>d</i> -spacing	MGC	<i>d</i> -spacing
Olive oil	G (1.0)	2.94 nm	TG (3.0)	2.45 nm
Canola oil	G (1.0)	2.95 nm	TG (3.0)	2.41 nm
Soybean oil	G (1.3)	2.95 nm	TG (3.0)	2.42 nm
Grapeseed oil	G (1.3)	2.92 nm	TG (3.0)	2.42 nm

<sup>[a]</sup> Values in parenthesis are MGC of corresponding gelator (% wt/v). G= opaque gel; TG= Translucent gel. <sup>[b]</sup> Oils are arranged in increasing order of unsaturations in their triglycerides profile.

MGC values of mannitol-derived amphiphile were 2-fold lower than those of sorbitol analogue, i.e., MGCs of M8 and S8 were  $\sim 1.3$  and  $3.0$  %wt/v respectively. The M8 gels were opaque in appearance, whereas S8 gels were translucent. Thus, the stereochemical difference between mannitol and sorbitol was found to markedly affect the vegetable oil gelation capabilities of these gelators. The relative orientations of  $-\text{OH}$  groups in sugar alcohols are known to influence their structural conformation (Chapter 2). M8 attains a linear conformation, whereas its isomer, S8, exist as bent structure (Figure 5.3). Because of the bent structure, S8 exhibit not only lower degree of inter-gelator interactions, but also higher solubility in solvents.<sup>19</sup> The inefficient self-assembling ability compounded by high solubility in oils results in lower gelation efficiency of S8. Investigation of optical microscope images revealed the morphological difference between the self-assembled aggregates of the two gelators. The M8 gels consisted of micron-size, high-aspect-ratio fibers, which were densely packed to form a 3-D network thereby explaining the opaqueness of oil gels (Figure 5.4A). The network of S8 gels consisted of thin needle-like microcrystalline aggregates with few clusters of microcrystallites randomly dispersed in an oil matrix (Figure 5.4B).

To elucidate the gelation mechanism, X-ray diffraction (XRD) was performed on oil gels. The long  $d$ -spacing values, or the length of the unit cell for M8 ( $d = \sim 2.95\text{nm}$ ) and S8 ( $d = \sim 2.42\text{nm}$ ) were found to be independent of the type of oils (Table 5.1). Moreover, on comparison of X-ray diffractograms of oil gels with those of organic solvents (organic solvents discussed in Chapter 2), it can be inferred that the long  $d$ -spacing values and the profile of diffractograms are similar in both liquid systems. Thus, it is hypothesized that the mode of molecular stacking for M8 and S8 in oils is on par

with that in organic solvents; i.e. gelator molecules stack together in layered arrangement with the tails tilted relative to the fiber axis. Self-assembly is driven by intermolecular hydrogen bonding between the hydroxyl groups and van der Waals forces between the alkyl chains. These fibers undergo lateral aggregation with each other, thereby forming a volume-filling 3-D network. Owing to the non-covalent nature of interactions involved in self-assembly process, the network is transient and is responsive towards external stimuli like temperature, shear etc.

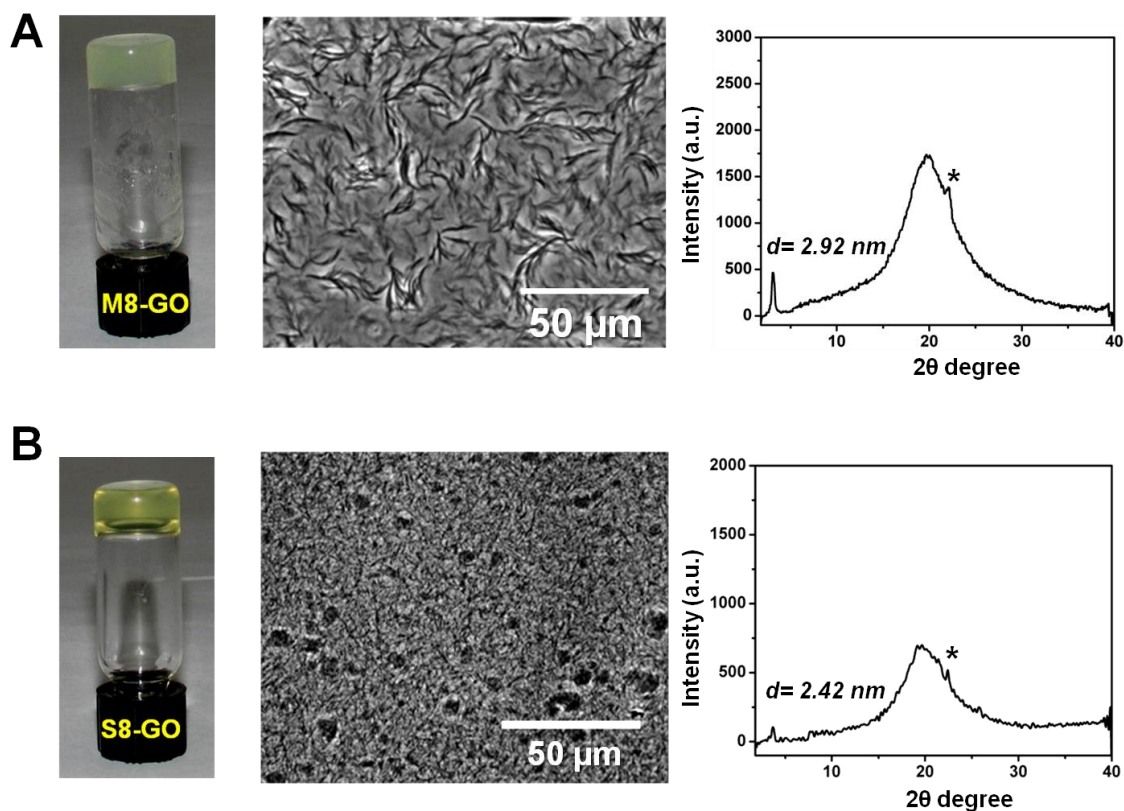


**Figure 5.4.** Photograph, optical microscope image and XRD pattern of grapeseed oil gels (5% wt/v). A) M8 gel and B) S8 gel. ‘ $d$ ’ denotes the long  $d$ -spacing values of respective gels. ‘\*’ denotes the Bragg’s peak at  $\sim 0.4$  nm, which is a characteristic signal of subcell packing of hydrocarbon chains in the self-assembled lipids.

### 5.3.3. Structuring Efficiency of Gelators

After conducting the typical gelation characterizations, the sugar gelators and gelation phenomenon were investigated for their potential application as structuring systems for vegetable oils. Hence forth, the terms ‘structured oils’ and ‘oil gels’ will be used interchangeably. Canola oil (CO) was used as model vegetable oil for studying the structuring efficiency of sugar gelators. CO is widely recognized for its nutritional attributes. It contains lowest level of SFA (~ 7% of total FA amount), whereas the unsaturated FA content is very high. It is an excellent source of  $\omega$ -6 and  $\omega$ -3 FA. Hence, it is one of the major oil consumed in the U.S.A. for household and industrial applications. The CO structured using M8 and S8 was analyzed for its morphology and thermal and mechanical properties. The morphology of the network and the thermal behavior (melting profile) of the structured oil dictate its organoleptic properties. For example, the presence of crystalline fiber network imparts palatable texture, whereas large melting range (10-15 °C) results in dislikeable greasy mouth sensation of structured oil. Mechanical strength governs the firmness, consistency and processing ability of structured oil.

The morphology was studied by using optical microscope, and thermal property was computed in terms of gel-to-sol transition temperature ( $T_{\text{gel}}$ ). Dynamic oscillatory rheology was performed to determine the various mechanical factors such as: i)  $G'$  (elastic modulus, measure of firmness), ii)  $G''$  (viscous modulus, measure of liquidity), and iii)  $\sigma_y$  (yield strain, measure of stiffness).<sup>20</sup> Effect of different parameters such as concentration of gelators, ageing of oil gels and continuous application of small deformation on the properties of structured oil were examined.

## 5.3.4. Effect of Concentration of Gelators

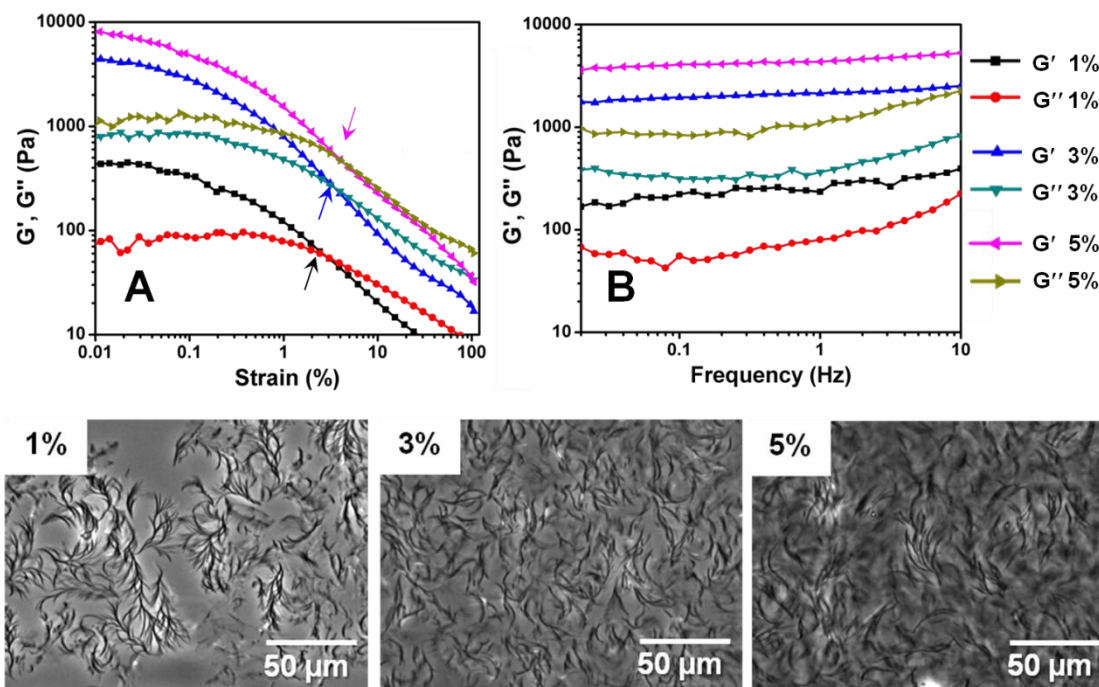


**Figure 5.5.** Rheological and optical analyses of M8-CO gels at various concentrations of M8 (1, 3 and 5% wt/v). A) Oscillatory strain sweep measurements. The arrows indicate the yield strain points for M8-CO gels. B) Oscillatory frequency sweep measurements.

At first the effect of concentration of gelators on the properties of CO gels was examined. An oscillatory strain sweep measurement shows that for all the M8-CO gels within its linear viscoelastic region (i.e. where  $G'$  and  $G''$  values does not change appreciably),  $G'$  greatly predominates  $G''$ . For example, M8-CO gel (5% wt/v) exhibit linear region until 0.1% strain. Over this region, the value of  $G'$  of ~7500 Pa exceeds that of  $G''$  by ~8 times (Figure 5.5A). More importantly, the yield strain ( $\sigma_y$ ) values of gels exponentially increased with the concentration of M8;  $\sigma_y$  for 1% gel is 2.39 whereas  $\sigma_y$  for 5% gel is 4.09 (Table 5.2). ' $\sigma_y$ ' signifies a point beyond which the 3-D gel network is

completely destroyed and gel behaves more like viscous liquid. Thus, it can be inferred that with increase in concentration of M8, the gel strength is increased exponentially.

The increment in the firmness of CO gels was also observed in the frequency sweep measurements (Figure 5.5B). Irrespective of the M8 concentration, the  $G'$  exceeds  $G''$  over the entire experimental frequency range, which is a typical response of gels. At low concentration of M8 (1% wt/v),  $G'$  exhibited slight dependency on higher frequency, indicating that the 1% gels may lose its elastic nature on application of shear at high frequencies for extended period of time. However, with increase in gelator concentration the  $G'$  progressively became more independent, and for 5% gels it was constant over the entire range. As in case of  $\sigma_y$ ,  $G'$  was also observed to exponentially increase with the concentration of gelator.  $G'$  value of 5% gel was 4300 Pa which is 2-fold higher than 3% gel (2052 Pa) and 17-fold higher than 1% gel (247 Pa). The level of  $G'$  characterizes the strength and firmness of the gel.

The improvement in the gel strength with gelator concentration was attributed to the enhancement of density of 3-D network (solid content). Higher content of gelator in the oil causes higher degree of supersaturation and hence nucleation sites, which in turn boost the number and length of self-assembled fibers. As a result, more fibers and entanglement exist in a unit area of the network. Such enrichment of network makes the gel stronger and inflects the rheological parameters ( $G'$  and  $\sigma_y$ ). Analysis of optical microscope images of the gels corroborates above hypothesis. 1% gel exhibited few fibrous structures, which were loosely connected to form a network. As the M8 content was raised to 3 and 5%, the fiber density and network compactness both progressively increased, thereby improving the gel strength. Like mechanical properties, the thermal

property ( $T_{\text{gel}}$ ) of gels was also found to be greatly influenced by the gelator concentration. More importantly, the M8-based CO gels exhibited melting profile over relatively narrow temperature range. The complete list of rheological and  $T_{\text{gel}}$  data is presented in Table 5.2

**Table 5.2.** Mechanical, thermal and structural data obtained for CO gels with varying concentration of M8 and S8.

	Amount (% wt/v)	$\sigma_y^a$ (%)	$G'^b$ (Pa)	$G''^c$ (Pa)	$\delta^d$ (°)	$T_{\text{gel}}^e$ (°C)	Morphology
<b>M8</b>	1	2.39	247	83	20.21	79-82	
	3	3.13	2052	426	11.60	99-103	Fibrous
	5	4.09	4300	1176	14.80	109-111	
<b>S8</b>	3	0.49	449	132	16.36	45-49	
	5	1.26	2093	485	13.21	59-61	Micro-crystallites

<sup>[a]</sup> Yield strain, defined as the applied strain value at  $G'/G''$  crossover. <sup>[b]</sup> Average value of elastic modulus in the linear viscoelastic region. <sup>[c]</sup> Average value of viscous modulus in the linear viscoelastic region. <sup>[d]</sup> Phase angle in the linear viscoelastic region.

Similarly, in case of S8-CO gels, the mechanical and thermal properties of CO gels were found to be proportional to the S8 concentration. The values of elastic modulus ( $G'$ ), yield strain ( $\sigma_y$ ),  $T_{\text{gel}}$  were enhanced by several factors by increasing the amount of gelator in the oil (Table 5.2). The S8 gels, too, exhibited narrow gel-to-sol transition range. The strain sweep measurements show the usual dominance of  $G'$  over  $G''$  in the linear viscoelastic region (Figure 5.6A). For S8-CO gels, as in case of M8-CO gels, the linear region was found to be till 0.1% strain. The frequency sweep measurements

exhibits negligible dependency of  $G'$  over the entire frequency range, confirming their gel-like state (Figure 5.6B). Increment in the concentration of S8 in gels from 3% to 5%, improved the density of microcrystallites and increased the number of clusters of microcrystallites, thereby leading to strengthening of gels ( $G'$  and  $\sigma_y$  were increased by factor of 5 and  $\sim 3$  respectively).

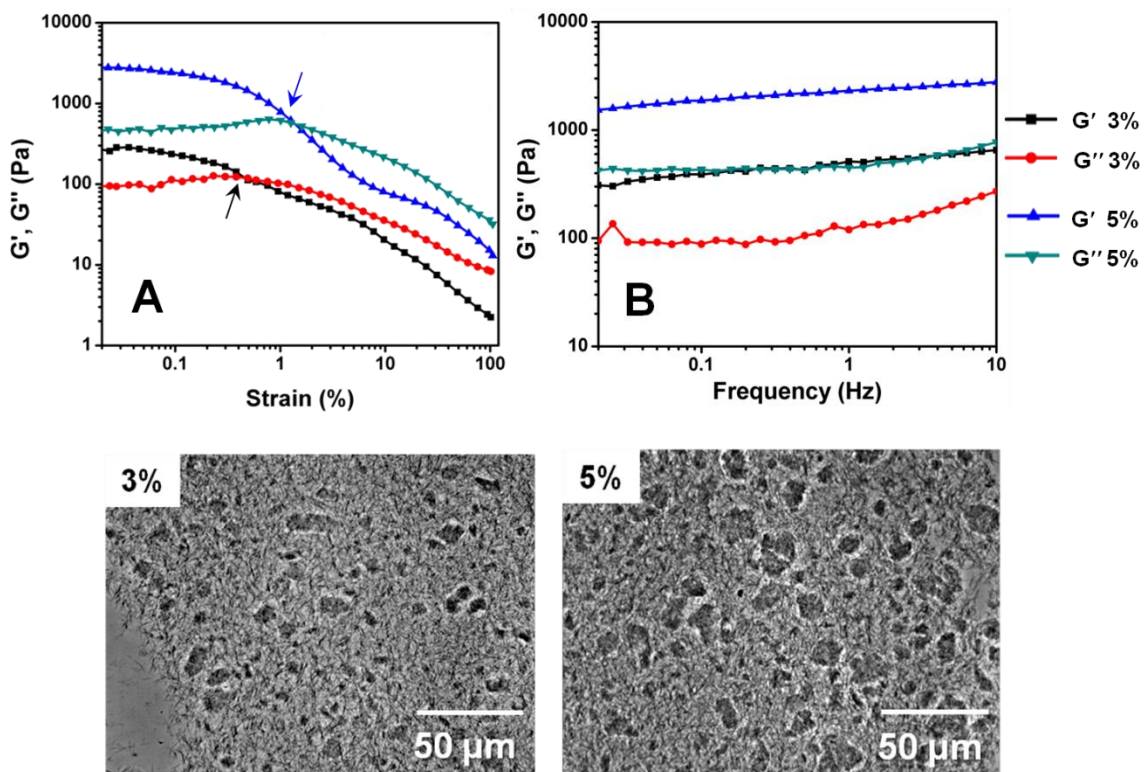


**Figure 5.6.** Rheological and optical analyses of CO gels developed by using various concentrations of S8 (3 and 5% wt/v). A) Oscillatory strain sweep measurements. The arrows indicate the yield strain points for S8-CO gels. B) Oscillatory frequency sweep measurements.

In addition to analogous concentration dependent behavior of M8 and S8 gels, a more striking observation was the difference in the properties of gels with same concentration of M8 and S8. At a given gelator concentration, the M8 gels were found to

be much stiffer and yield at higher yield strain values as compared to S8 gels. For instance,  $G'$  and  $\sigma_y$  values for 5% M8 gels were greater than those of 5% S8 gels by at least a factor of 3. The gel-to-sol transition temperatures too were relatively higher for M8 gels, 109-111 °C for 5% M8 gels compared to 58-61 °C for 5% S8 gels. Thus, it can be inferred that the subtle difference in the stereochemistry of the sugar group markedly affects the self-assembly mechanism, gelation efficiency and gel properties of sugar alcohol gelators. Such influence of differing molecular structures will allow for modulation of gel properties and develop structured vegetable oil as per the requirement of an application.

### **5.3.5. Effect of Ageing on Properties of Structured Oil**

The structured vegetable oils are widely used in food products that may or may not have long shelf lives. It is always desired that the properties of the structured oil remain the same or do not change considerably, when stored for a long period of time. In other words, the network of structuring agents should not change temporally. However, many gel systems, especially polymer gels, are known to undergo morphological transformations over a period of time. Either the self-assembled structures of gel-network are entirely changed, or the network is spatially rearranged to a thermodynamically stable state. As a result, the aged gels exhibit different properties compared to fresh ones. In order to check the morphological transformations in case of M8 and S8, their CO gels (5% wt/v concentration) were aged for different time lengths and analyzed for their mechanical, structural and thermal properties. Figure 5.7 (A and B) represents the rheological response of M8 and S8 gels on ageing for 1, 7 and 30 days.

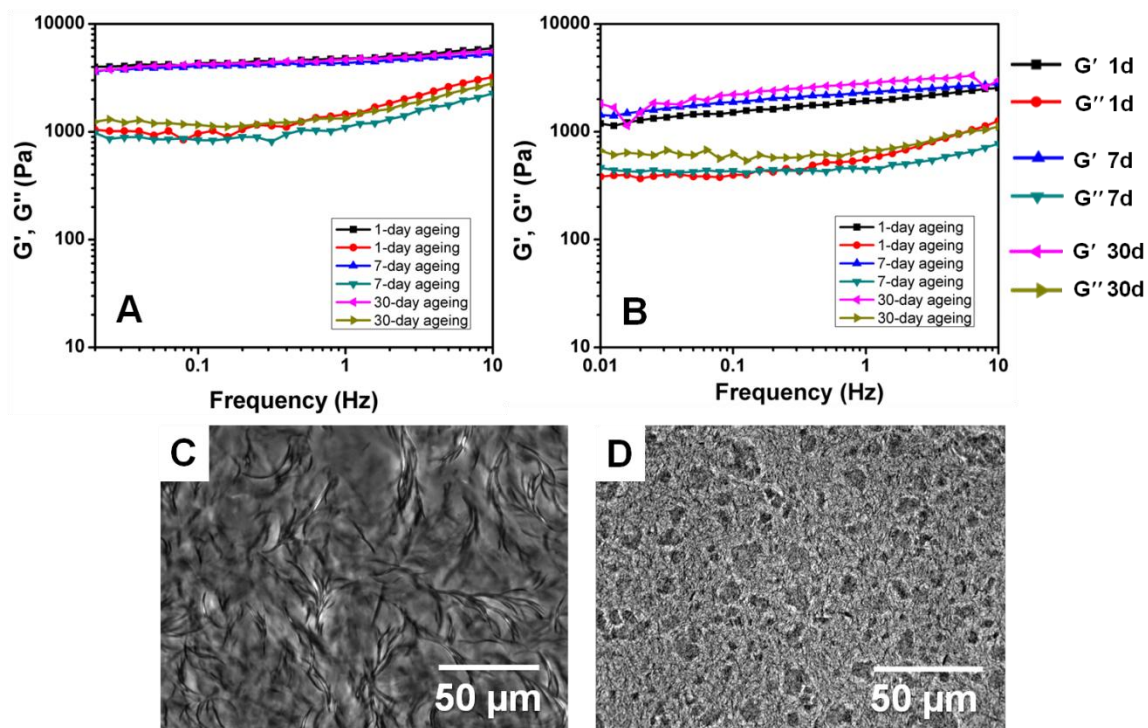


**Figure 5.7.** Effect of ageing on the mechanical and structural properties of CO gels (5 wt/v). Oscillatory frequency sweep measurements A) M8 and B) S8. Optical microscope images of CO gels of C) M8 and D) S8.

Frequency sweep measurements of M8 gels (Figure 5.7A) indicate that their rheological responses are alike. For all three samples, the  $G'$  ( $\sim 4400$  Pa) and  $\sigma_y$  ( $\sim 3.17\%$ ) were found to be similar (Table 5.3), which can be interpreted as the overall gel strength remained the same. Similarly, the thermal properties of gels ( $T_{\text{gel}}$ ) did not show any variations with ageing duration. Such identical responses of M8 gels stem from the ability of M8 to form thermodynamically stable self-assembled structure as soon as the M8-CO sol is cooled. The thermodynamic stability of the aggregates inhibits further transformation or even rearrangement of the network. Figure 5.7C supports the above arguments, as it shows that the morphology of the gel aged for 30 days is identical to that of gel aged for 7 days, which is shown in Figure 5.5.

In contrast to M8-CO gels, S8-CO gels exhibited slight dependency on ageing period. The gel strength was found to increase, although marginally, with ageing duration (Figure 5.7 B and Table 5.3).  $G'$  and  $\sigma_y$  progressively increased by factor of 1.26 and 2 respectively. Morphological analyses of these gels did not exhibit noticeable transformations in the microcrystalline self-assembled structures of S8 (Figure 5.7D). Thus the enhancement in the mechanical properties of S8 gels could only be attributed to the spatial rearrangement of aggregates to increase the lateral interactions, thereby improving the compactness of the network.

**Table 5.3.** Mechanical, thermal and structural data obtained for CO gels (5% wt/v) aged for different time scale.

	Ageing	$G'$ (Pa)	$G''$ (Pa)	$\sigma_y$ (%)	$T_{gel}$ (°C)	Morphology
<b>M8</b>	1 day	4579	1534	3.17	108-111	
	7 days	4300	1176	4.09	109-111	Fibrous
	30 days	4460	1514	3.17	110-112	
<b>S8</b>	1 day	1761	572	0.46	58-61	
	7 days	2093	485	1.26	59-61	Micro- Crystallites
	30 days	2444	699	2.5%	59-61	

### 5.3.6. Effect of Small Deformation for Long Time

Oscillatory time sweeps experiments facilitate inspection of any macro- or micro-structural changes to a gel may undergo when subject to constant shear for a long time. The structured oils are frequently processed in other food products, where they are continuously deformed to achieve uniform dispersion in the food matrix. In addition, these experiments substantiate the effect of ageing on rheological behavior of gels. Thus, the CO gels of M8 and S8 were analyzed for time dependent rheological properties. A constant strain (0.1%) was applied on gels at a frequency of 1 Hz over a period of 50 min. As depicted in Figure 5.8, both M8 and S8 gels exhibit excellent uniformity in the rheological response, which indicates the gels do not undergo any structural changes on application of continuous deformation. Elastic and viscosity moduli remained constant for both the gel samples.

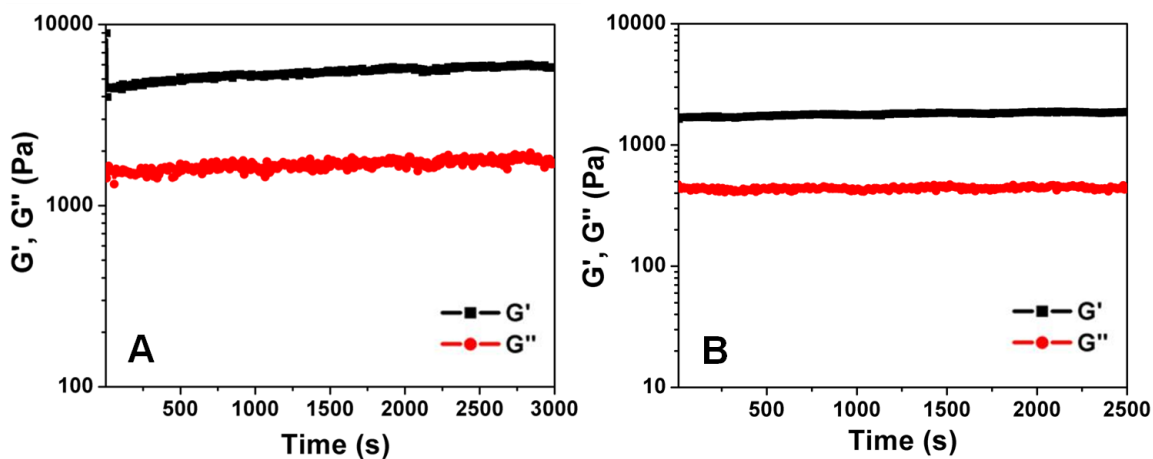


**Figure 5.8.** Oscillatory time sweep measurements of CO gel (5% wt/v). A) M8 and B) S8.

### 5.3.7. Effect of the Type of Oil

Finally, the effect of different oils on the gelation efficiency of M8 and S8 was studied by investigating their mechanical and thermal properties. Oils selected for the study exhibit varying amount of unsaturations in their triglyceride profile. OO and CO are high in monounsaturated FA (oleic acid) content. SO contains high amount of mono- and diunsaturated FA (linoleic acid), whereas GO predominantly contains di- and triunsaturated FA (linolenic acid). Because of these variations, these oils differ in their physical properties like melting point, polarity and dissolving power. As a result, the type of oils may affect the structuring ability of the agent. However, in present case, it was found that the self-assembly mechanism and morphology of M8 and S8 is independent of oil type (Table 5.1). Hence, the bulk properties of gels are also expected to follow similar trend.

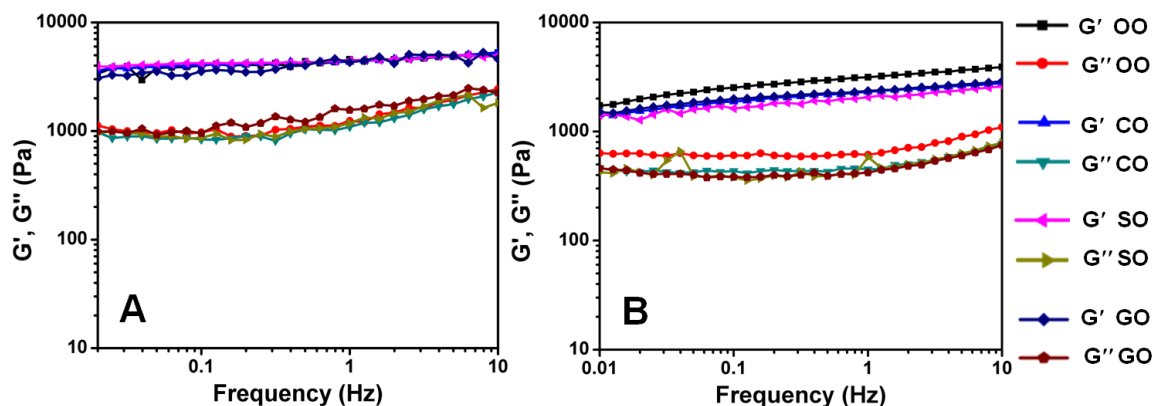


**Figure 5.9.** Frequency sweep measurements of different oil gels (5% wt/v). A) M8 and B) S8. Oils listed in legend are arranged in increasing order of unsaturations in their triglycerides profile.

Figure 5.9 illustrate the rheological behavior of different oil gels of M8 and S8. The gel firmness ( $G'$ ) was found to be of similar magnitude for M8 (~4000 Pa) and S8 (~2000 Pa) oil gels (Table 5.4). Moreover, the profiles of  $G'$  and  $G''$  were akin over the entire experimental frequency range (0.01-10Hz), indicating that in addition to gel firmness the viscoelastic behavior of different oil gels are equivalent. Similar to rheological responses, the thermal properties exhibited similar trend. The  $T_{gel}$  range of OO, SO and GO gels was narrow and on par with that of C) gels,  $T_{gel}$  of M8 gels was ~108-111 °C and  $T_{gel}$  of S8 gels was 59-61 °C. Thus, it can be inferred that in the case of sugar alcohol gelators, the properties of oil gels are an exclusive function of the type and concentration of gelators used for gelation of oils.

**Table 5.4.** Structuring data obtained for M8 and S8 gels (5% wt/v) in different vegetable oils.

Oils	M8 <sup>a</sup>			S8 <sup>b</sup>		
	$G'$ (Pa) <sup>c</sup>	$G''$ (Pa) <sup>d</sup>	$T_{gel}$ (°C)	$G'$ (Pa)	$G''$ (Pa)	$T_{gel}$ (°C)
<b>OO</b>	4296	1289	108-111	2832	681	59-61
<b>CO</b>	4300	1176	109-111	2093	485	58-61
<b>SO</b>	4379	1219	109-112	1900	480	59-60
<b>GO</b>	3905	1293	109-111	2167	458	60-62

#### 5.4. Conclusion

In conclusion, it can be stated that the developed sugar alcohol dioctanoates M8 and S8 are efficient vegetable oil structuring agents. The biocompatibility of the gelators was confirmed by conducting cytotoxicity studies, which indicated negligible toxicity of

M8 and S8 and high cell viability at concentration as high as 50  $\mu\text{g/mL}$ . The M8 and S8 effectively structured range of vegetable oil at very low concentrations (1-3% wt/v). The mechanical, structural and thermal properties of structured oil were found to be a function of type and concentration of sugar alcohol gelator employed for structuring. Compared to S8, M8 produced structured oil with better properties. The gel strength ( $G'$  and  $\sigma_y$ ) of M8 oil gels was always found to be greater than that of S8 oil gels by several times. M8 self-assembled in oils to form dense fibrous structures and consequently produced opaque gels. On the other hand, S8 self-assembled in oils to form loosely connected microcrystallites and produced translucent gels. Such significant variations in oil gels resulting from the subtle changes in the chemical structure of gelator will enable modulation of gel properties and develop structured vegetable oil as per the requirement of an application.

## **5.5. Experimental Section**

### **5.5.1. Materials**

Refined vegetable oils were purchased from local supermarket: Canola oil (ConAgra Foods, Inc.), Olive oil (Wakefern Food Corp.), Soybean oil (USDA, Ca) and Grapeseed oil (Wakefern Food Corp.). M8 and S8 were synthesized by using regiospecific enzyme catalysis, which is described in experimental section of Chapter 2.

HepG2 cells were generously provided by Dr. Mou-Tuan Huang, Department of Chemical Biology, Rutgers, The State University of New Jersey. Minimum Essential Medium (MEM), fetal bovine serum (FBS), Phosphate buffered saline (PBS), 100X penicillin and Streptomycin, and 0.25% trypsin with ethylenediaminetetraacetic acid

(EDTA) and RPMI-1640 media, were all purchased from Fisher Scientific. 3-(4,5-Dimethylthiazol-2-yl)-2,5-Diphenyltetrazolium Bromide (MTT) was obtained from Sigma Aldrich.

## **5.5.2. Experimental Techniques**

### **Cytotoxicity Assay**

The cytotoxicity of amphiphiles were assessed by the microculture MTT reduction assay as used in the literature. This assay is based on the reduction of a soluble tetrazolium salt by the mitochondrial dehydrogenase of the viable cells to form an insoluble colored product, formazan. The amount of formazan formed can be measured spectrophotometrically after dissolution of the dye in DMSO. The activity of the enzyme and the amount of the formazan produced is proportional to the number of cells alive. Reduction of the absorbance value is attributed to the killing of cells or inhibition of cell proliferation by amphiphiles.

HepG2 cells were seeded in 96-well plates at a density of 10,000 cells per well in a final volume of 100  $\mu$ l cell culture media. A stock solution of M8 and S8 was prepared in DMSO. On the second day, the stock solutions were diluted to different concentrations (0.1-100 ppm) and incubated with HepG2 cells for 24 hours. Untreated cells were used as a control. Subsequently, cell culture media were removed and cells were incubated with 100  $\mu$ l RPMI 1640 media containing 0.5mg/mL MTT for 2 h at 37 °C. MTT solution was then carefully aspirated and the formazan crystals formed were dissolved in 100  $\mu$ l DMSO in each well. Light absorbance at 560 and 670nm was recorded with plate reader (Synergy HT, Biotek). Relative cell viability was expressed as A560-A670 normalized to

that of the untreated wells. Data were presented as mean  $\pm$  standard deviation with 4 well repeats.

### **Gel Preparation**

Gel samples were prepared by adding desired weight percentage of M8 or S8 (1-5 % wt/v based on oil) in the oil. The heterogeneous mixture of gelator and oil was heated to 130 °C for M8 (or to 90 °C for S8) to produce sol. The sol was held at this temperature with continuous agitation for 10 min, in order to remove any self-assembly history of gelator molecules. Furthermore, the sol was cooled to room temperature and aged to specified number of days.

### **Characterization of Gels**

Evaluation of MGC &  $T_{gel}$  and analysis of gels by XRD was performed by following the procedures described in Chapter 2.

### **Optical Microscopy**

The microstructures were analyzed by using Leica DM LB2 microscope stage and the phase changes were observed with 20x PH1 phase contrast objective. A very small portion of gel was placed on slide and gently covered with cover slip to minimize development of artifacts.

### **Rheological Measurements**

Dynamic rheological measurements were performed on a stress-controlled rheometer (AR 2000 ex) with a cone and plate geometry [1° 58' 47'' angle and 40mm diameter with a truncation gap of 45  $\mu$ m]. The rheometer was equipped with a peltier plate. About 1 mL of gel was loaded on the plate and the cone was lowered to specified truncation gap. Excess gel was trimmed from the periphery of cone to ensure optimal

filling within the geometry. Precautions such as careful loading of sample and gradual lowering of geometry were taken to minimize shear induced disruption of gel network. Before the measurements, the loaded sample was allowed to equilibrate within the cone and plate geometry for 10 minutes. Oscillatory strain sweep measurements were performed from 0.02-100% deformation at a fix frequency of 1Hz. Oscillatory stress sweep measurements were performed in the frequency domain of 0.01-10 Hz with a constant strain of 0.1%, which is within the linear viscoelastic regime of the sample. All the experiments were conducted at a temperature of 25 °C. For each experiment, at least two tests were carried out.

**Note**

1. Prior to characterization of gel samples for structural, thermal or mechanical properties, the gels were aged for 7 days at room temperature (25-30 °C) unless a given set of experiments necessitated different ageing durations.

## Appendices

**Appendix 1.** Gel-to-sol transition temperature of the organogels developed using sugar alcohol-based amphiphile ( $T_{gel}$  °C). Gelator concentration = 5% wt/v.

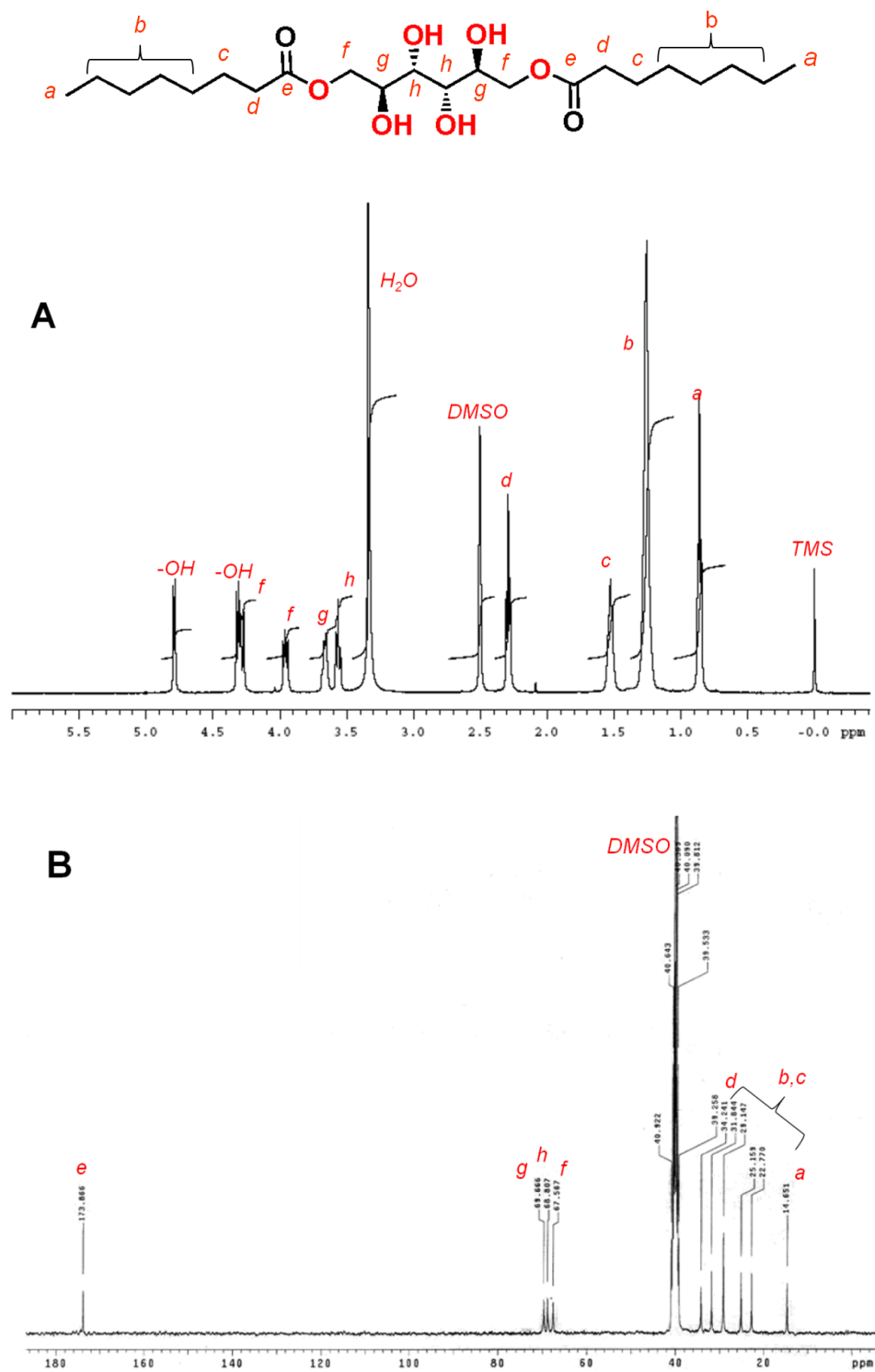
<b>Solvents</b>	<b>M4</b>	<b>M8</b>	<b>M14</b>	<b>S4</b>	<b>S8</b>	<b>S14</b>
HCs ( $n < 10$ ) <sup>c</sup>	<b>P</b>	<b>P</b>	<b>P</b>	<b>P</b>	<b>P</b>	<b>P</b>
Dodecane	<b>P</b>	123-130	110-113	<b>P</b>	67-70	76-78
1-bromododecane	104-108	112-115	97-100	<b>P</b>	65-67	80-83
Methylaurate	78-81	90-94	89-92	<b>P</b>	<b>C</b>	62-65
1-bromooctane	105-108	104-108	85-87	<b>P</b>	59-61	69-72
Methyloctanoate	78-80	86-90	80-83	<b>P</b>	<b>PG</b>	<b>PG</b>
2-octanone	70-72	78-80	75-77	<b>P</b>	<b>C</b>	<b>C</b>
Octanamine	<b>S</b>	<b>S</b>	<b>S</b>	<b>S</b>	<b>S</b>	<b>S</b>
Octanol	61-64	62-64	58-60	<b>P</b>	<b>S</b>	<b>PG</b>
Octanoic acid	60-63	76-78	76-80	<b>P</b>	<b>C</b>	63-66
1,8-dibromooctane	100-103	100-102	93-96	45-50	62-64	74-76
Cyclohexane	96-99	97-99	89-90	50-52	49-52	63-65
Benzene	84-86	82-84	75-77	40-42	42-43	<b>P</b>
Toluene	83-85	80-83	73-75	41-42	56-59	<b>P</b>
Squalene	<b>P</b>	133-135	121-124	<b>P</b>	75-78	79-81
Mineral Oil	<b>PG</b>	120-125	122-124	<b>PG</b>	63-69	85-87
Canola Oil	103-106	109-111	103-105	45-48	59-61	79-83

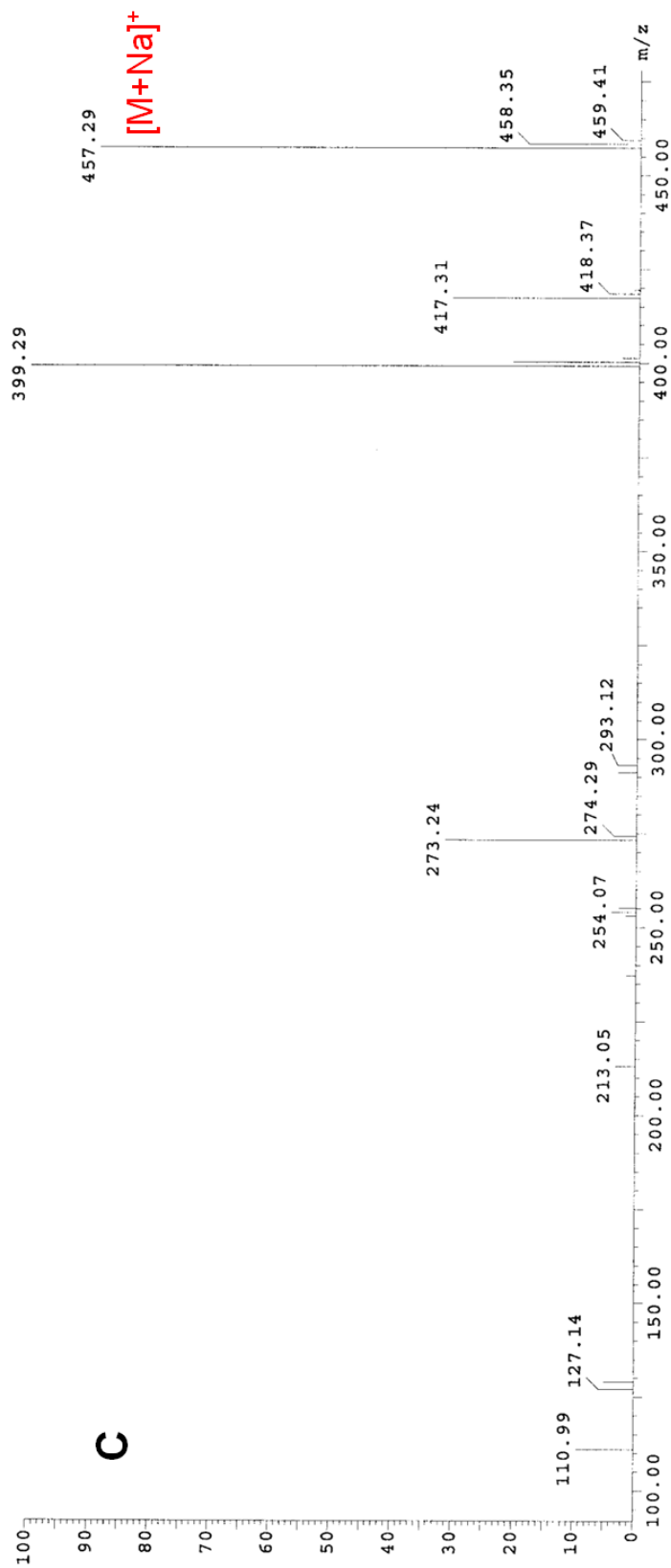
**Appendix 2.** Effect of different classes of solvents (bromo, esters and alcohols) and the length of their hydrophobic chain on the gelation efficiency of M8 and S8.<sup>a,b</sup>

Solvents	M8		S8	
	MGC	T <sub>gel</sub>	MGC	T <sub>gel</sub>
Dodecane	<b>G</b> 2.5%	123-130	<b>G</b> 2.5%	67-70
1-bromobutane	<b>G</b> 3.33%	91-93	<b>PG</b>	-
1-bromohexane	<b>G</b> 3.33%	100-104	<b>PG</b>	-
1-bromooctane	<b>G</b> 3.00%	104-108	<b>G</b> 3.33%	59-61
1-bromododecane	<b>G</b> 3.00%	112-115	<b>G</b> 3.33%	65-67
Butanol	<b>G</b> 5.0%	43-44	<b>S</b>	-
Hexanol	<b>G</b> 3.33%	47-50	<b>S</b>	-
Octanol	<b>G</b> 1.67%	62-64	<b>S</b>	-
Decanol	<b>G</b> 1.67%	68-70	<b>S</b>	-
Methylbutyrate	<b>G</b> 3.33%	80-82	<b>S</b>	-
Methyloctanoate	<b>G</b> 1.67%	86-90	<b>PG</b>	-
Methylaurate	<b>G</b> 1.00%	90-94	<b>C</b>	-

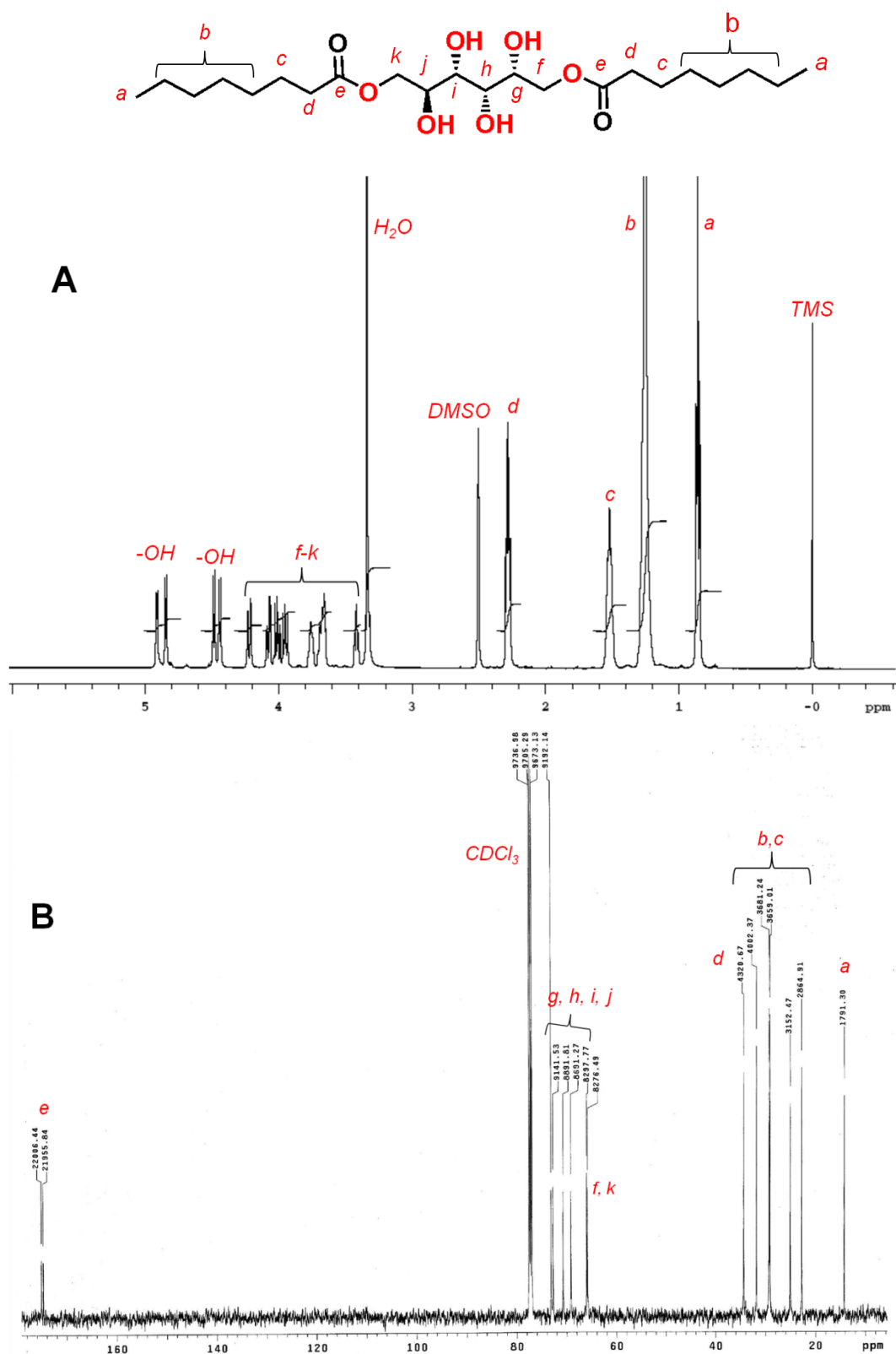
<sup>[a]</sup> MGC: Minimum gelation concentration (% wt/v). <sup>[b]</sup> T<sub>gel</sub>: Gel-to-sol transition temperature of gels (° C) (gelator concentration = 5% wt/v)

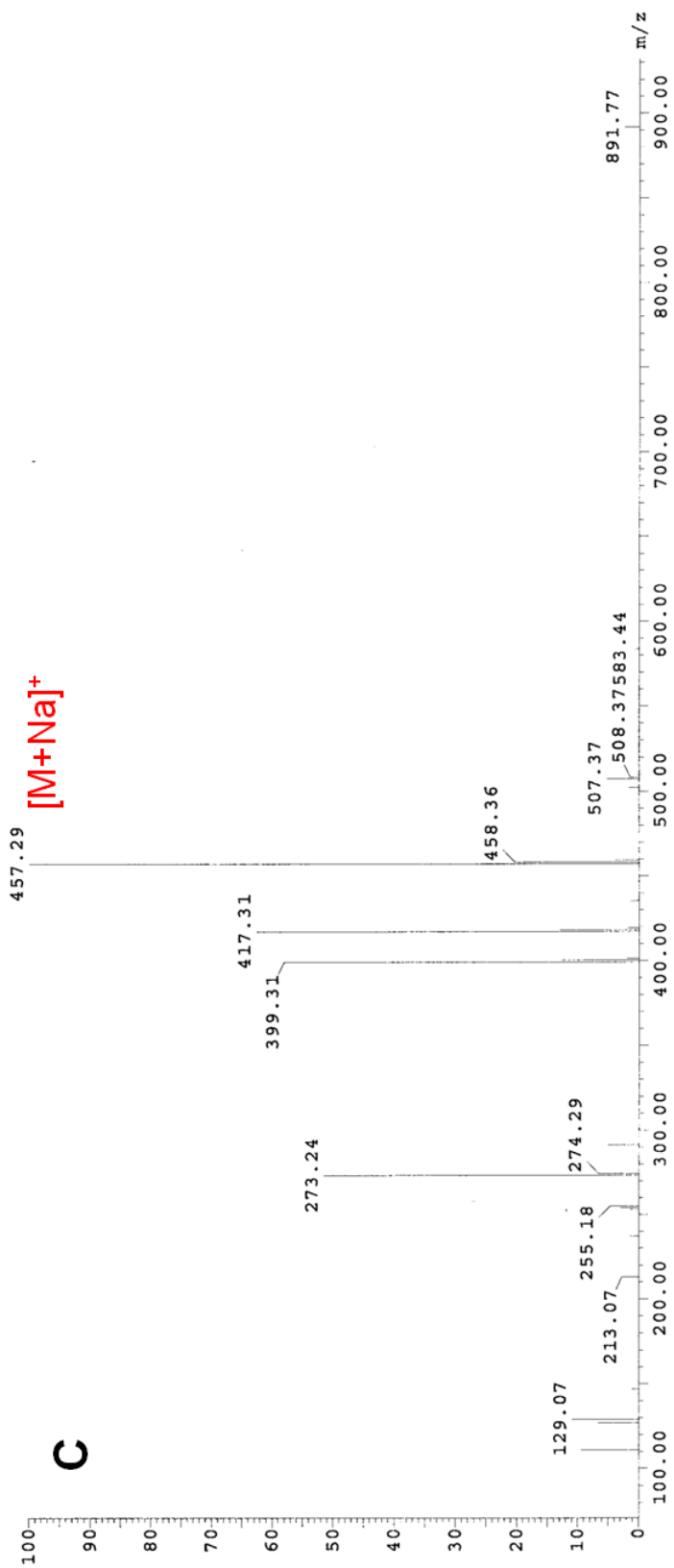
**Appendix 3.** Spectroscopic Characterization of Mannitol dioctanoate (M8). A)  $^1\text{H}$  NMR, B)  $^{13}\text{C}$  NMR and C) EI-MS spectrum.



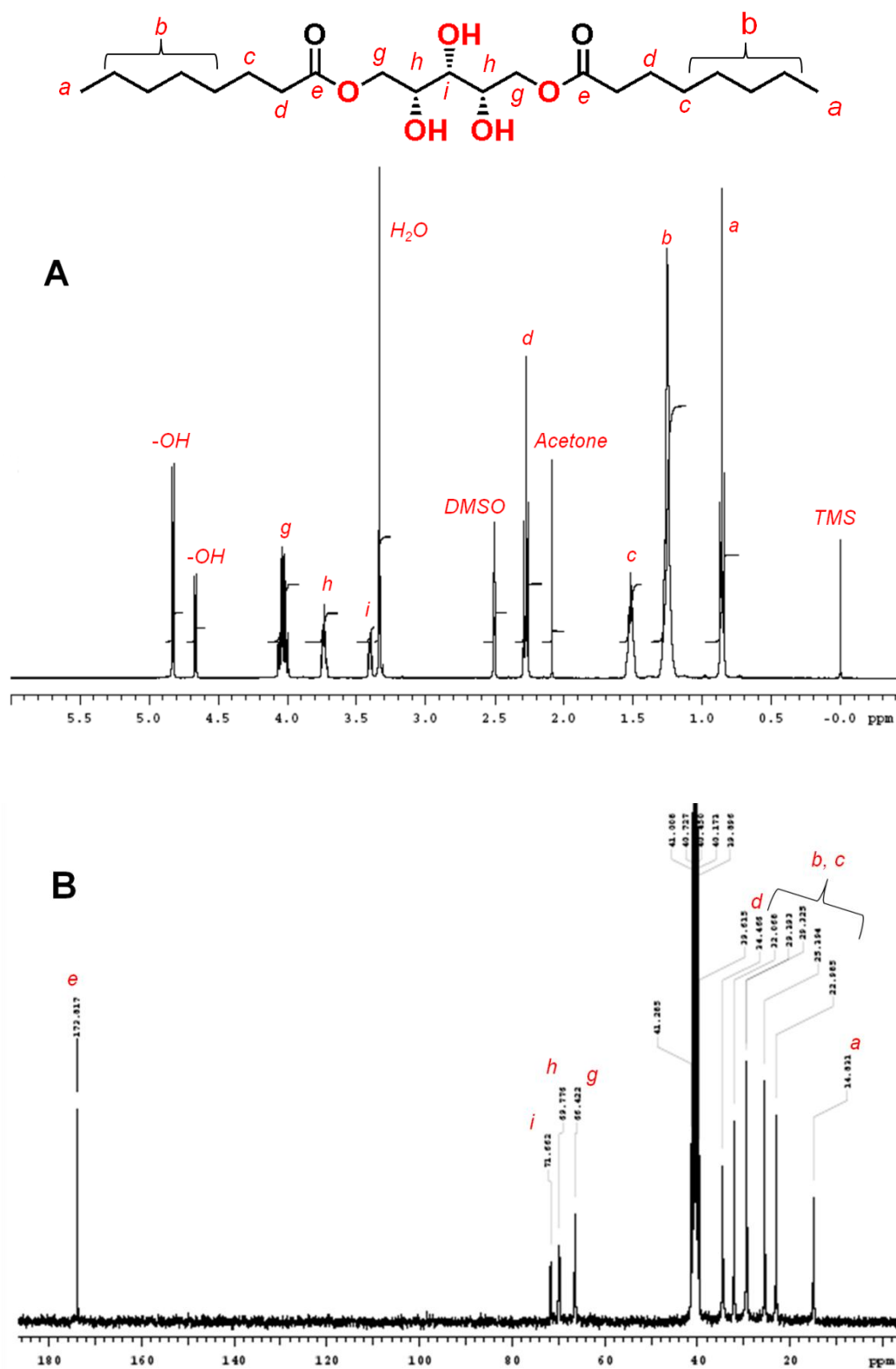


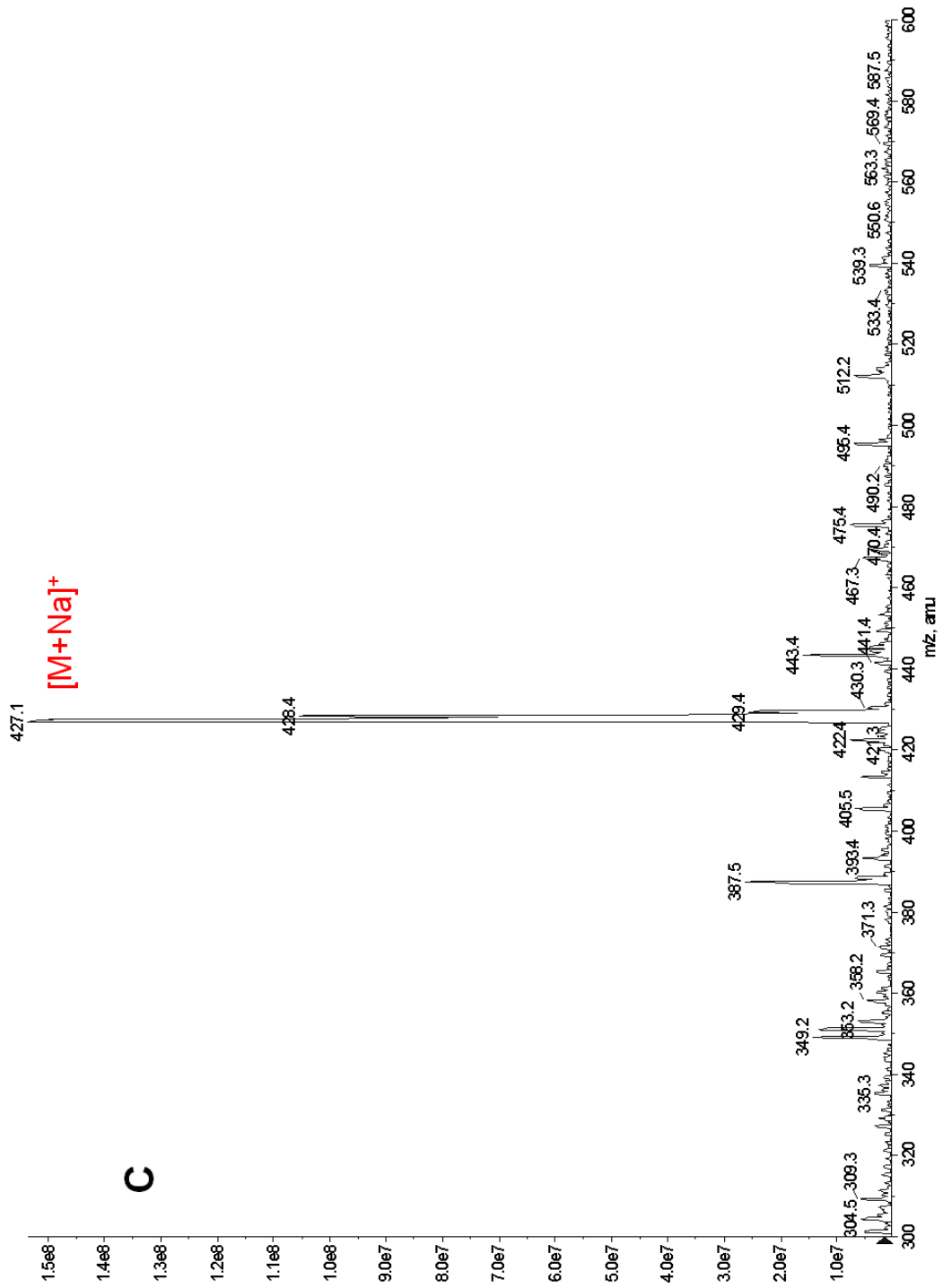
**Appendix 4.** Spectroscopic characterization of sorbitol dioctanoate (S8). A)  $^1\text{H}$  NMR, B)  $^{13}\text{C}$  NMR and C) EI-MS spectrum.





**Appendix 5.** Spectroscopic characterization of xylitol dioctanoate (X8). A)  $^1\text{H}$  NMR, B)  $^{13}\text{C}$  NMR and C) EI-MS spectrum.



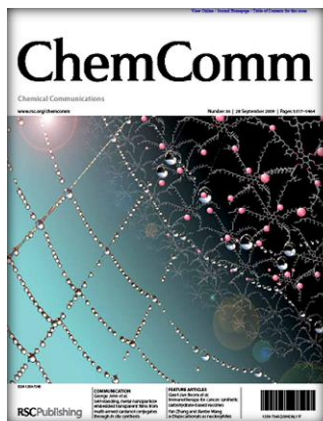


---

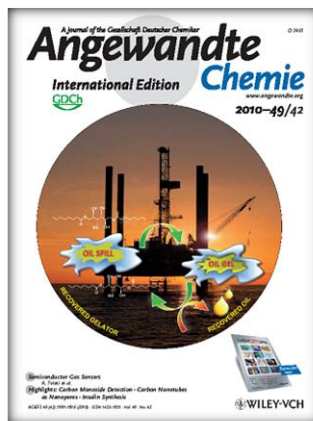
## List of Publications

1. K. Jyothish, P. K. Vemula, **S. R. Jadhav**, L. C. Francesconi and G. John, "Self-standing, metal nanoparticle embedded transparent films from multi-armed cardanol conjugates through in situ synthesis" *Chem. Commun.* **2009**, 5368-5370 (*cover feature*).
2. **S. R. Jadhav**, P. K. Vemula, R. Kumar, S. Raghavan and G. John, "Sugar-derived phase-selective molecular gelators as model solidifiers for oil spills" *Angew. Chem. Int. Ed.*, **2010**, *49*, 7695-7698 (*cover feature*, highlighted in C&EN, Discovery News, Nature Materials, Nature Chemistry).
3. **S. R. Jadhav\***, K. Jyothish\* and G. John, "A vegetable oil derived chemodosimeter for the selective detection of Hg<sup>2+</sup> in aqueous media: a potential green laboratory method" *Chem. Commun.*, **2010**, *12*, 1345-1348 (\* denotes equal contribution, *cover feature*).
4. G. John, B. V. Shankar, **S. R. Jadhav** and P. K. Vemula, "Biorefinery: a design tool for molecular gelators" *Langmuir* **2010**, *26*, 17843-17851 (invited review and *cover feature*).
5. B. V. Shankar, **S. R. Jadhav**, P. Pradhan, S. De Carlo and G. John, "Adhesive vesicles through adaptive response of a biobased surfactant" *Angew. Chem. Int. Ed.*, **2010**, *49*, 9509-9512 (*cover feature*).
6. **S. R. Jadhav**, B. -S. Chiou, D. F. Wood, G. Degrande-Hoffman, G. M. Glenn and G. John, "Molecule gels-based controlled release devices for pheromones" *Soft Matter* **2011**, *7*, 864-867 (*cover feature*).
7. **S. R. Jadhav**, Q. Huang and G. John, "Medium chain sugar amphiphiles: alternative vegetable oil structuring agents" (Manuscript under preparation).

## Cover Pages



Paper 1



Paper 2



Paper 3



Paper 4



Paper 5



Paper 6

---

## Bibliography

### Chapter 1

1. B. P. Toole, *Nat. Rev. Cancer* **2004**, *4*, 528–539.
2. C. Storm, J. J. Pastore, F. C. MacKintosh, T. C. Lubensky and P. A. Janmey, *Nature* **2005**, *435*, 191–194.
3. S. Frey, R. P. Richter and D. Goerlich, *Science* **2006**, *314*, 815–817.
4. R. Yoshida, *Curr. Org. Chem.*, **2005**, *9*, 1617-1641.
5. A. R. Hirst, B. Escuder, J. F. Miravet and D. K. Smith, *Angew. Chem. Int. Ed.*, **2008**, *47*, 8002 – 8018.
6. P. Flory, *J. Discuss. Faraday Soc.*, **1974**, *57*, 5.
7. J. Van Esch, F. Schoonbeek, M. De Loos, E. M. Veen, R. M. Kellogg and B. L. Feringa, ‘Supramolecular Science: where it is and where it is going’ *in: Nato ASI Series C: Mathematical and Physical Sciences*, R. Ungaro, Ed. (Kluwer Academic Publishers, **1999**, Vol. 527, pp. 233-259).
8. Y. Osada and A. R. Khokhlov, Eds. *Polymer Gels and Networks* (Marcel Dekker, Inc., New York, USA, **2002**).
9. S. Chatterjia, I. K. Kwonb and K. Park, *Prog. Polym. Sci.*, **2007**, *32*, 1083–1122.
10. A. Fernandez-Barbero, I. J. Suarez, B. Sierra-Martin, A. Fernandez-Nieves, F. J. de Las Nieves, M. Marquez, J. Rubio-Retama and E. Lopez-Cabarcos, *Adv. Colloid Interfac.*, **2009**, *147-148*, 88-108.
11. F. Fages, ‘Low Molecular Mass Gelators: Design, Self-assembly Function’ *in: Topics in Current Chemistry* (Springer, New York, **2005**, Vol. 256).

12. R. G. Weiss and P. Terech, *Molecular Gels: Materials with Self-assembled Fibrillar Networks* (Springer, Dordrecht, The Netherlands, **2006**).
13. J. N. Israelachvili, *Intermolecular and Surface Forces*, 2<sup>nd</sup> ed. (Academic Press: New York, **1991**).
14. J. -L. Li and X. -Y. Liu, *Adv. Funct. Mater.*, **2010**, *20*, 3196–3216.
15. S. R. Raghavan, *Langmuir* **2009**, *25*, 8382-8385.
16. M. J. Meunier, *Ann. Chim. Phys.*, **1891**, *22*, 412.
17. Y. -C. Lin, B. Kachar and R. G. Weiss, *J. Am. Chem. Soc.*, **1989**, *111*, 5542-5551.
18. K. Murata, M. Aoki, T. Nishi, A. Ikeda and S. Shinkai, *J. Chem. Soc., Chem. Commun.*, 1991, 1715-1718.
19. N. M. Sangeetha and U. Maitra, *Chem. Soc. Rev.*, **2005**, *34*, 821-836.
20. Y. -C. Lin and R. G. Weiss, *Macromolecules* **1987**, *20*, 414-417.
21. K. Hanabusa, M. Yamada, M. Kimura and H. Shirai, *Angew. Chem. Int. Ed.*, **1996**, *35*, 1949-1951.
22. J. H. van Esch, *Langmuir* **2009**, *25*, 8392-8394.
23. W. Weng, J. B. Beck, A. M. Jamieson and S. J. Rowan, *J. Am. Chem. Soc.*, **2006**, *128*, 11663-11672.
24. J. J. van Gorp, J. A. J. M. Vekemans and E. W. Meijer, *J. Am. Chem. Soc.*, **2002**, *124*, 14759-14769.
25. G. Wang, S. Cheuk, H. Yang, N. Goyal, P. V. N. Reddy and B. Hopkinson, *Langmuir* **2009**, *25*, 8696–8705.
26. G. Wang and A. D. Hamilton, *Chem. Commun.*, **2003**, 310-311.

- 
27. K. Rajangam, H. A. Behanna, M. J. Hui, X. Han, J. F. Hulvat, J. W. Lomasney and S. I. Stupp, *Nano Lett.*, **2006**, *6*, 2086-2090.
28. D. K. Smith, *Chem. Commun.*, **2006**, 34-44.
29. A. Ajayaghosh and V. K. Praveen, *Acc. Chem. Res.* **2007**, *40*, 644–656.
30. (a) P. Terech and R. G. Weiss, *Chem. Rev.* **1997**, *97*, 3133-3159; (b) O. Gronwald, E. Snip and S. Shinkai, *Curr. Opin. Colloid Interface Sci.*, **2002**, *7*, 148-156; (c) L. A. Estroff and A. D. Hamilton, *Chem. Rev.*, **2004**, *104*, 1201-1218; (d) M. de Loos, B. L. Feringa and J. H. van Esch, *Eur. J. Org. Chem.*, **2005**, 3615-3631; (e) P. Dastidar, *Chem. Soc. Rev.*, **2008**, *37*, 2699-2715; (f) S. Banerjee, R. K. Das and U. Maitra, *J. Mater. Chem.*, **2009**, *19*, 6649-6687; (g) D. K. Smith, *Chem. Soc. Rev.*, **2009**, *38*, 684-694; (h) J. W. Steed, *Chem. Commun.*, **2011**, *47*, 1379-1383; (i) A. Dawn, T. Shiraki, S. Haraguchi, S. –C. Tamaru and S. Shinkai, *Chem. Asian J.*, **2011**, *6*, 266 – 282.
31. (a) D. K. Smith, *Tetrahedron* **2007**, *63*, 7283–7284; (b) G. M. Whitesides and B. Grzybowski, *Science* **2002**, *295*, 2418-2421; (c) J. –M. Lehn, *Proc. Natl. Acad. Sci. USA* **2002**, *99*, 4763-4768.
32. (a) D. Philp and J. F. Stoddart, *Angew. Chem. Int. Ed. Engl.*, **1996**, *35*, 1154 – 1196; (b) D. J. Kushner, *Microbiol. Mol. Biol. Rev.*, **1969**, *33*, 302-345; (c) E. L. Shakhnovich, V. Abkevich and O. Ptitsyn, *Nature* **1996**, *379*, 96-98; (d) A. Klug, *Angew. Chem. Int. Ed. Engl.* **1983**, *22*, 565-582.
33. E. Carretti, L. Deia and R. G. Weiss, *Soft Matter* **2005**, *1*, 17-22.
34. J. A. Foster, M. -O. M. Piepenbrock, G. O. Lloyd, N. Clarke, J. A. K. Howard and J. W. Steed, *Nat. Chem.*, **2010**, *2*, 1037-1043.

- 
35. S. Yamamichi, Y. Jinno, N. Haraya, T. Oyoshi, H. Tomitori, K. Kashiwagi and M. Yamanaka, *Chem. Commun.*, **2011**, 47, 10344–10346.
36. B. Escuder, F. Rodríguez-Llansola and J. F. Miravet, *New J. Chem.*, **2010**, 34, 1044–1054.
37. (a) X. Yang, G. Zhanga and D. Zhang, *J. Mater. Chem.*, **2012**, DOI: 10.1039/C1JM13205A; (b) R. J. Mart, R. D. Osborne, M. M. Stevens and R. V. Ulijn, *Soft Matter*, **2006**, 2, 822–835; (c) J. J. D. de Jong, B. L. Feringa and J. van Esch, 'Responsive Molecular Gels' in: *Molecular Gels: Materials with Self-assembled Fibrillar Networks*, R. G. Weiss and P. Terech, Eds. (Springer, Dordrecht, The Netherlands, **2006**, pp 895-927).
38. Z. Yang, G. Liang and B. Xu, *Acc. Chem. Res.*, **2008**, 41, 315-326.
39. Q. Liu, Y. Wang, W. Li and L. Wu, *Langmuir* **2007**, 23, 8217-8223.
40. (a) W. T. Truong, Y. Su, J. T. Meijer, P. Thordarson and F. Braet, *Chem. Asian J.*, **2011**, 6, 30–42; (b) F. Zhao, M. L. Ma and B. Xu, *Chem. Soc. Rev.*, **2009**, 38, 883–891.
41. A. Vintiloiu and J. –C. Leroux, *J. Control. Release* **2008**, 125, 179–192.
42. J. D. Hartgerink, E. Beniash and S. I. Stupp, *Science* **2001**, 294, 1684-1688.
43. (a) J. D. Hartgerink, E. Beniash and S. I. Stupp, *Proc. Natl. Acad. Sci. USA* **2002**, 99, 5133-5138; (b) V. M. T. Mattiace, V. Sahni, K. L. Niece, D. Birch, C. Czeisler, M. G. Fehlings, S. I. Stupp and J. A. Kessler, *J. Neurosci.*, **2008**, 28, 3814-3823.
44. P. K. Vemula, G. A. Cruikshank, J. M. Karp, G. John, *Biomaterials* **2009**, 30, 383-393.
45. L. Zang, Y. Che and J. S. Moore, *Acc. Chem. Res.*, **2008**, 41, 1596–1608.

- 
46. A. Friggeri, O. Gronwald, K. J. C. van Bommel, S. Shinkai and D. N. Reinhoudt, *J. Am. Chem. Soc.*, **2002**, *124*, 10754-10758.
47. B. Xing, M. -F. Choi and B. Xu, *Chem. Eur. J.*, **2002**, *8*, 5028-5032.
48. K. J. C. van Bommel, A. Friggeri and S. Shinkai, *Angew. Chem. Int. Ed.*, **2003**, *42*, 980-999.
49. K. Sugiyasu, S. -I. Tamaru, M. Takeuchi, D. Berthier, I. Huc, R. Oda and S. Shinkai, *Chem. Commun.*, **2002**, 1212-1213.
50. (a) G. Gundiah, S. Mukhopadhyay, U. G. Tumkurkar, A. Govindaraj, U. Maitra and C. N. R. Rao, *J. Mater. Chem.*, **2003**, *13*, 2118-2122; (b) S. Kobayashi, K. Hanabusa, N. Hamasaki, M. Kimura, H. Shirai and S. Shinkai, *Chem. Mater.*, **2000**, *12*, 1523-1525.
51. G. Kickelbick, *Hybrid Materials* (Wiley-VCH Verlag GmbH & Co. KGaA, Weinheim, **2007**).
52. (a) M. Moriyama, N. Mizoshita, T. Yokota, K. Kishimoto and T. Kato, *Adv. Mater.*, **2003**, *15*, 1335-1338; (b) E. R. Zubarev, M. U. Pralle, E. D. Sone and S. I. Stupp, *Adv. Mater.*, **2002**, *14*, 198 – 203; (c) J. L. Bideau, L. Viau and A. Vioux, *Chem. Soc. Rev.*, **2011**, *40*, 907-925; (d) P. K. Vemula and G. John, *Chem. Commun.*, **2006**, 2218-2220.
53. S. K. Samanta, A. Pal, S. Bhattacharya and C. N. R. Rao, *J. Mater. Chem.*, **2010**, *20*, 6881-6890.
54. (a) J. P. H. van Wyk, *Trends Biotechnol.*, **2001**, *19*, 172-177; (b) A. J. Ragauskas, C. K. Williams, B. H. Davison, G. Britovsek, J. Cairney, C. A. Eckert, W. J. Frederick, J. P. Hallett, D. J. Leak, C. L. Liotta, L. R. Mielenz, R. Murphy, R. Templer and T.

- Tschaplinski, *Science* **2006**, *311*, 484-489; (c) J. O. Metzger and U. Bornscheuer, *Appl. Microbiol. Biotechnol.*, **2006**, *71*, 13-22.
55. (a) P. Lorenz and H. Zinke, *Trends Biotechnol.*, **2005**, *23*, 570-574; (b) A. Corma, S. Iborra and A. Velty, *Chem. Rev.*, **2007**, *107*, 2411-2502; (c) M. E. Himmel, S. -Y. Ding, D. K. Johnson, W. S. Adney, M. R. Nimlos, J. W. Brady and T. D. Foust, *Science* **2007**, *315*, 804-807.
56. S. Herrera, *Nat. Biotechnol.*, **2004**, *22*, 671-675.
57. (a) B. Kamm, P. R. Gruber and M. Kamm, *Biorefineries - Industrial Processes and Products: Status Quo and Future Directions* (Wiley-VCH, Weinheim, Germany, **2005**); (b) U. Bierman, W. Friedt, S. Lang, W. Luhs, G. Machmuller, J. O. Metzger, M. K. Ruschgen, H. J. Schafer and M. P. Schneider, *Angew. Chem. Int. Ed.*, **2000**, *39*, 2206-2224; (c) R. J. Koopmans, *Soft Matter* **2006**, *2*, 537-543.
58. (a) P. K. Vemula and G. John, *Acc. Chem. Res.*, **2008**, *41*, 769-782; (b) G. John and P. K. Vemula, *Soft Matter* **2006**, *2*, 909-914.
59. G. John, V. S. Balachandran, S. R. Jadhav and P. K. Vemula, *Langmuir* **2010**, *26*, 17843-17851.
60. K. N. Syrigos, G. Rowlinson-Busza and A. A. Epenetos, *Int. J. Cancer* **1998**, *78*, 712-719.
61. P. K. Vemula, J. Li and G. John, *J. Am. Chem. Soc.*, **2006**, *128*, 8932-8938.
62. J. H. Crowe and L. M. Crowe, *Nat. Biotechnol.*, **2000**, *18*, 145-146.
63. T. Higashiyama, *Pure Appl. Chem.*, **2002**, *74*, 1263-1269.
64. G. John, G. Zhu, J. Li and J. S. Dordick, *Angew. Chem. Int. Ed.*, **2006**, *45*, 4772-4776.
65. P. K. Vemula, U. Aslam, V. A. Mallia and G. John, *Chem. Mater.*, **2007**, *19*, 138-140.

66. H. Kobayashi, Y. Ito, T. Komanoya, Y. Hosaka, P. L. Dhepe, K. Kasai, K. Hara, and A. A. Fukuoka, *Green Chem.*, **2011**, *13*, 326-333.
67. O. Akinterinwa, R. Khankal and P. C. Cirino, *Curr. Opin. Biotech.*, **2008**, *19*, 461-467.
68. G. Vrancken, T. Rimaux, L. De Vuyst and F. Mozzi, 'Low-Calorie Sugars Produced by Lactic Acid Bacteria' in: *Biotechnology of Lactic Acid Bacteria: Novel Applications*, F. Mozzi, R. R. Raya and G. M. Vignolo, Eds. (Wiley-Blackwell, Ames, Iowa, USA, **2010**, pp 193-209).
69. (a) M. F. Salama and S. E. Mohamed, *Egypt J. Food Sci.*, **2000**, *28*, 81-96; (b) G. S. Radhika and S. N. Moorthy, *Trends in Carbohydrate Research* **2009**, *1*, 71-79; (c) C. Zacharis, *NutraCos* **2007**, *6*, 18-19; (d) R. B. Friedman, 'Monosaccharides and Polyols in Foods' in: *Glycoscience: Chemistry and Chemical Biology*, 2<sup>nd</sup> ed., B. O. Fraser-Reid, K. Tatsuta and J. Thiem, Eds. (Springer, Berlin, Heidelberg, **2008**, pp. 841-856).
70. (a) H. Schiweck, A. Bar, R. Vogel, E. Schwarz and M. Kunz, 'Sugar Alcohols' in: *Ullmann's Encyclopedia of Industrial Chemistry*, 6<sup>th</sup> ed. (Wiley-VCH; **2003**, pp 487-513); (b) G. Livesey, *Nutr. Res. Rev.*, **2003**, *16*, 163-191.

## Chapter 2

1. (a) M. Boncheva and G. M. Whitesides, *MRS Bull.*, **2005**, *30*, 736-742; (b) B. Grzybowski and G. M. Whitesides, *Science* **2002**, *295*, 2418-2421.
2. R. G. Weiss and P. Terech, *Molecular Gels: Materials with Self-assembled Fibrillar Networks* (Springer, Dordrecht, The Netherlands, **2006**).
3. O. Gronwald and S. Shinkai, *Chem. Eur. J.*, **2001**, *7*, 4329-4334.

4. Z. Yang, G. Liang, M. Ma, A. S. Abbah, W. W. Lu and B. Xu, *Chem. Commun.*, **2007**, 843–845.
5. S. Bhattacharya and S. N. G. Acharya, *Chem. Mater.*, **1999**, *11*, 3504-3511.
6. S. –I. Tamaru, M. Nakamura, M. Takeuchi and S. Shinkai, *Org. Lett.*, **2001**, *3*, 3631-3634.
7. L. S. Birchall, S. Roy, V. Jayawarna, M. Hughes, E. Irvine, G. T. Okorogheye, N. Saudi, E. De Santis, T. Tuttle, A. A. Edwards and R. V. Ulijn, *Chem. Sci.*, **2011**, *2*, 1349-1355.
8. K. Araki and I. Yoshikawa, *Top. Curr. Chem.*, **2005**, *256*, 133-165.
9. M. J. Meunier, *Ann. Chim. Phys.*, **1891**, *22*, 412.
10. (a) J. –H. Fuhrhop and C. Boettcher, *J. Am. Chem. Soc.*, **1990**, *112*, 1768-1776; (b) J. –H. Fuhrhop, S. Svenson, C. Boettcher, E. Rossler and H. –M. Vieth, *J. Am. Chem. Soc.*, **1990**, *112*, 4307-4312; (c) J. –H. Fuhrhop, P. Blumtritt, C. Lehmann and P. Lugert *J. Am. Chem. Soc.*, **1991**, *113*, 7437-7439; (d) J. –H. Fuhrhop, P. Schnieder, E. Boekema and W. Helfricho, *J. Am. Chem. Soc.*, **1988**, *110*, 2861-2867.
11. S. Mizrahi, D. Rizkov, N. Hayat and O. Le, *Chem. Commun.*, **2008**, 2914–2916.
12. (a) R. J. H. Hafkamp, M. C. Feiters and R. J. M. Nolte, *J. Org. Chem.*, **1999**, *64*, 412-426; (b) R. J. H. Hafkamp, B. P. A. Kokke, I. M. Danke, H. P. M. Geurts, A. E. Rowan, M. C. Feiters and R. J. M. Nolte, *Chem. Commun.*, **1997**, 545-546.
13. K. Yabuuchi, A. E. Rowan, R. J. M. Nolte and T. Kato, *Chem. Mater.*, **2000**, *12*, 440-443.
14. G. Buhler, M. C. Feiters, R. J. M. Nolte and K. H. Dotz, *Angew. Chem. Int. Ed.*, **2003**, *42*, 2494 – 2497.

- 
15. U. Beginn, S. Keinath and M. Moller, *Macromol. Chem. Phys.*, **1998**, *199*, 2379-2384.
16. (a) S. Yamamoto, *Kougyou Kagaku Zasshi* **1942**, *45*, 695; (b) S. Yamasaki, Y. Ohashi, H. Tsutsumi and K. Tsujii, *Bull. Chem. Soc. Jpn.*, **1995**, *68*, 146-151; (c) M. Watase, Y. Nakatani and H. Itagaki, *J. Phys. Chem. B* **1999**, *103*, 2366-2373; (d) E. A. Wilder, C. K. Hall, S. A. Khan and R. J. Spontak, *Langmuir* **2003**, *19*, 6004-6013.
17. (a) N. Mohmeyer, P. Wang, H. -W. Schmidt, S. Z. Zakeeruddin and M. Gratzel, *J. Mater. Chem.*, **2004**, *14*, 1905-1909; (b) T. Schamper, M. Jablon, M. H. Randhawa, A. Senatore and J. D. Warren, *J. Soc. Cosmet. Chem.*, **1986**, *37*, 225-231; (c) C. M. Pereira, J. M. Oliverira, R. M. Silva and F. Silva, *Anal. Chem.*, **2004**, *76*, 5547-5551.
18. E. A. Wilder, K. S. Wilson, J. B. Quinn, D. Skrtic and J. M. Antonucci, *Chem. Mater.*, **2005**, *17*, 2946-2952.
19. W. -C. Lai, *Soft Matter*, **2011**, *7*, 3844-3851.
20. A. Vidyasagar, K. Handore and K. M. Sureshan, *Angew. Chem. Int. Ed.*, **2011**, *50*, 8021-8024.
21. P. K. Vemula and G. John, *Acc. Chem. Res.*, **2008**, *41*, 769-782.
22. (a) A. Coniglio, H. E. Stanley and W. Klein, *Phys. Rev. B* **1982**, *25*, 6805-6821; (b) P. Jonkheijm, P. van der Schoot, A. P. H. J. Schenning, E. W. Meijer, *Science* **2006**, *313*, 80-83; (c) G. Zhu and J. S. Dordick, *Chem. Mater.*, **2006**, *18*, 5988-5995; (d) A. R. Hirst, I. A. Coates, T. R. Boucheteau, J. F. Miravet, B. Escuder, V. Castelletto, I. W. Hamley and D. K. Smith, *J. Am. Chem. Soc.*, **2008**, *130*, 9113-9121; (e) W. Edwards, C. A. Lagadec and D. K. Smith, *Soft Matter* **2011**, *7*, 110-117.

- 
23. M. C. R. Symons, N. G. M. Pay and G. Eaton, *J. Chem. Soc., Faraday Trans. 1* **1982**, 78, 1841-1846.
24. C. Reichardt, *Solvents and solvent effects in organic chemistry*, 3<sup>rd</sup> ed. (Wiley-VCH, Verlag GmbH & Co. KGaA, Weinheim, Germany, **2003**).
25. (a) M. O. Roy, J. Uppenberg, S. Robert, M. Boyer, J. Chopineau, and M. Jullien, *Eur. Biophys. J.*, **1997**, 26, 155-162; (b) L. Perez, J. L. Torres, A. Manresa, C. Solans and M. Rosa Infante, *Langmuir* **1996**, 12, 5296-5301.
26. V. P. Vassilev, E. E. Simanek, M. R. Wood and C. Wong, *Chem. Commun.*, **1998**, 1865-1866.
27. (a) J. Peng, K. Liu, J. Liu, Q. Zhang, X. Feng and Y. Fang, *Langmuir* **2008**, 24, 299-3000; (b) J. Makarevic, M. Jokic, B. Peric, V. Tomisic, B. Kojic-Prodic and M. Zinic, *Chem. Eur. J.*, **2001**, 7, 3328-3341.
28. (a) R. G. Snyder, *J. Mol. Spectrosc.*, **1960**, 4, 411-434; (b) R. G. Snyder, *J. Mol. Spectrosc.*, **1961**, 7, 116-144; (c) P. Wolfangel, R. Lehnert, H. H. Meyerb and K. Mueller, *Phys. Chem. Chem. Phys.*, **1999**, 1, 4833-4841; (d) N. V. Venkataraman, S. Bhagyalakshmi, S. Vasudevan, and R. Seshadri, *Phys. Chem. Chem. Phys.*, **2002**, 4, 4533-4538.
29. (a) M. Anne, 'X-Ray diffraction of Poorly Organized Systems and Molecular Gels' in: *Molecular Gels: Materials with Self-assembled Fibrillar Networks*, R. G. Weiss and P. Terech, Eds. (Springer, Dordrecht, The Netherlands, **2006**); (b) W. I. F. David, K. Shankland, L. B. McCusker, and C. Baerlocher, *Structure Determination from Powder Diffraction Data* (Oxford University Press: New York, Vol. 13, **2002**).

30. (a) M. A. Rogers, A. J. Wright and A. G. Marangoni, *Soft Matter* **2009**, *5*, 1594-1596; (b) S. Zhou, C. Xu, J. Wang, W. Gao, R. Akhverdiyeva, V. Shah and R. Gross, *Langmuir* **2004**, *20*, 7926-7932.
31. J. –H. Fuhrhop and C. Endisch, *Molecular and Supramolecular Chemistry of Natural Products and Their Model Compounds* (Marcel Dekker, Inc., New York, USA, **2000**, pp 167-242).
32. (a) F. M. Menger, *Acc. Chem. Res.*, **1979**, *12*, 111-117; (b) D. F. Evans, *Langmuir* **1988**, *4*, 3-12.

### Chapter 3

1. <http://www.nytimes.com/2010/05/03/us/03spill.html>.
2. National Research Council, *The Oil Spill Recovery Institute: Past, Present, and Future Directions* (National Academies Press: Washington D.C., **2003**).
3. (a) L. Guterman, *Science*, 2009, *20*, 1558-1559; (b) J. F. Piatt and C. J. Lensink, *Nature* **1989**, *342*, 865-866.
4. (a) M. Roulia, K. Chassapis, Ch. Fotinopoulos, Th. Savvidis and D. Katakis, *Spill Science & Technology Bulletin* **2003**, *8*, 425-431; (b) M. O. Adebajo, R. L. Frost, J. T. Kloprogge, O. Carmody and S. Kokot, *J. Porous Mater.*, **2003**, *10*, 159-170.
5. R. R. Lessard and G. Demarco, *Spill Science and Technology Bulletin* **2000**, *6*, 59-68.
6. (a) Ch. Teas, S. Kalligeros, F. Zanikos, S. Stoumas, E. Lois and G. Anastopoulos, *Desalination* **2001**, *140*, 259-264; (b) J. Yuan, X. Liu, O. Akbulut, J. Hu, S. L. Suib, J. Kong, and F. Stellacci, *Nature Nanotech.*, **2008**, *3*, 332-336.

7. (a) W. L. Stanley and A. G. Pittman, *Process for containing oil spills* US patent 3,869,385 (**1975**); (b) F. E. Lowther, *Treatment of spills with gelatin* US patent 5,259,973 (**1993**).
8. (a) S. Bhattacharya and Y. Krishnan-Ghosh, *Chem. Commun.*, **2001**, 185-186; (b) S. Bhattacharya and A. Pal, *J. Phys. Chem. B* **2008**, *112*, 4918-4927; (c) D. R. Trivedi, A. Ballabh, P. Dastidar and B. Ganguly, *Chem. Eur. J.*, **2004**, *10*, 5311– 5322; (d) J. Peng, K. Liu, X. Liu, H. Xia, J. Liu and Y. Fang, *New J. Chem.*, **2008**, *32*, 2218–2224; (e) M. Xue, D. Gao, K. Liu, J. Peng and Y. Fang, *Tetrahedron* **2009**, *65*, 3369-3377; (f) S. Debnath, A. Shome, S. Dutta and P. K. Das, *Chem. Eur. J.*, **2008**, *14*, 6870-6881; (g) T. Kar, S. Debnath, D. Das, A. Shome and P. K. Das, *Langmuir* **2009**, *25*, 8639–8648.
9. (a) J. –H. Fuhrhop, S. Svenson, C. Boettcher, E. Rossler and H. –M. Vieth, *J. Am. Chem. Soc.*, **1990**, *112*, 4307-4312; (B) J. –H. Fuhrhop and J. Koning, *Membranes and Molecular Assemblies: The Synkinetic Approach* (The Royal Society of Chemistry, Cambridge, UK, **1994**, pp 120-123).
10. (a) J. Piao and S. Adachi, *Innovat. Food Sci. Emerg. Tech.*, **2006**, *7*, 211-216; (b) J. Piao, Y. Kawahara-Aoyama, T. Inoue and S. Adachi, *Biosci. Biotechnol. Biochem.*, **2006**, *70*, 263-265.
11. F. M. Menger and K. L. Caran, *J. Am. Chem. Soc.*, **2000**, *122*, 11679-11691.

## Chapter 4

1. L. G. Copping and J. J. Menn, *Pest Manage. Sci.*, **2000**, *56*, 651-656.
2. (a) P. Witzgall, *IOBC wprs Bull.*, **2001**, *24*, 114-122; (b) L. Stowers and T. F. Marton, *Neuron.*, **2005**, *46*, 699–702.

3. D. R. Thomson, L. J. Gut and J. W. Jenkins, 'Pheromones for Insect Control' in: *Biopesticides: Use and Delivery*, F. R. Hall and J. J. Menn, Eds.(Humana Press Inc., New Jersey, **1999**, pp. 385–412).
4. (a) H. H. Shorey, C. B. Sisk and R. G. Gerber, *Environ. Entomol.*, **1996**, *25*, 446-451; (b) G. M. Glenn, A. P. Klamczynski, C. Ludvik, J. Shey, S. H. Imam, B. –S. Chiou, T. Mchugh, G. Degrandi-Hoffman, W. Orts, D. Wood and R. Offeman, *J. Agric. Food Chem.*, **2006**, *54*, 3297-3304; (c) I. Yosha, A. Shani and S. Magdassi, *J. Agric. Food Chem.*, **2006**, *56*, 8045-8049; (d) G. M. Glenn, A. P. Klamczynski, J. Shey, B.-S. Chiou, K. M. Holtman, D. F. Wood, C. Ludvik, G. DeGrandi-Hoffman, W. Orts and S. Imam, *Polym. Adv. Technol.*, **2007**, *18*, 636-642; (d) S. Heuskin, F. J. Verheggen, E. Haubruge, J. –P. Wathelet and G. Lognay, *Biotechnol. Agron. Soc. Environ.*, **2011**, *15*, 459-470.
5. (a) A. R. Hirst, B. Escuder, J. F. Miravet and D. K. Smith, *Angew. Chem., Int. Ed.*, **2008**, *47*, 8002-8018; (b) F. Zhao, M.-L. Mab and B. Xu, *Chem. Soc. Rev.*, **2009**, *38*, 883-891.
6. R. J. H. Hafkamp, M. C. Feiters and R. J. Nolte, *J. Org. Chem.*, **1999**, *64*, 412-416.
7. (a) A. -C. Couffin-Hoarau, A. Motulsky, P. Delmas and J. -C. Leroux, *Pharm. Res.*, **2004**, *21*, 454-457; (b) K. J. C. van Bommel, C. van der Pol, I. Muizebelt, A. Friggeri, A. Heeres, A. Metsma, B. L. Feringa and J. van Esch, *Angew. Chem., Int. Ed.*, **2004**, *43*, 1663-1667; (c) P. K. Vemula, J. Li and G. John, *J. Am. Chem. Soc.*, **2006**, *128*, 8932-8938.
8. S. R. Jadhav, P. K. Vemula, R. Kumar, S. R. Raghavan and G. John, *Angew. Chem., Int. Ed.*, **2010**, *49*, 7695-7698.

9. The 96% content of pheromone liquid is based on percent weight ratio of M8 and 2-heptanone.  $MGC_{(2\text{-heptanone})} = 3\%$  wt/v; i.e. 3 g of M8 is required to gel 100 mL of 2-heptanone ( $\rho = 0.8 \text{ g mL}^{-1}$ ). On converting the units of MGC values to % wt/wt, the  $MGC_{(2\text{-heptanone})} = 3.75\%$  or  $\sim 4\%$ .
10. (a) A. Vallet, P. Cassier and Y. Lensky, *J. Insect Physiol.*, **1991**, 37, 789-804; (b) C. H. Sakamoto, A. E. Soares and J. N. Lopes, *J. Apic. Res.*, **1990**, 29, 194-198.
11. E. H. Erickson, G. DeGrandi-Hoffman, C. G. Becker, R. S. Whitson and T. A. Deeby, *Control of Parasitic Mites of Honey Bees* US Patent 6,843,985 B2 (**2005**).
12. D. De Jong, H. P. De Jong and L. S. Goncales, *J. Apic. Res.*, **1982**, 21, 165-167.
13. B. Bujok, M. Kleinhenz, S. Fuchs and J. Tautz, *Naturwissenschaften* **2002**, 89, 299-301.
14. S. R. Raghavan and B. H. Cipriano, 'Gel Formation: Phase Diagrams Using Tabletop Rheology and Calorimetry' in: *Molecular Gels: Materials with Self-assembled Fibrillar Networks*, R. G. Weiss and P. Terech, Eds. (Springer, Dordrecht, The Netherlands, **2006**, pp 241-252).
15. C. Folgar, D. Folz, C. Suchicital and D. Clark, *J. Non-Cryst. Solids* **2007**, 353, 1483-1490.
16. (a) S. Zhou, C. Xu, J. Wang, W. Gao, R. Akhverdiyeva, V. Shah and R. Gross, *Langmuir* **2004**, 20, 7926-7932; (b) W. I. F. David, K. Shankland, L. B. McCusker, and C. Baerlocher, *Structure Determination from Powder Diffraction Data* (Oxford University Press: New York, Vol. 13, **2002**).
17. R. G. Snyder, *J. Mol. Spectrosc.*, **1961**, 7, 116-144.

18. X. P. Hu, B. S. Shasha, M. R. McGuire and R. J. Prokopy, *J. Controlled Release* **1998**, *50*, 257-265.
19. F. M. Menger and K. L. Caran, *J. Am. Chem. Soc.*, **2000**, *122*, 11679-11691.
20. G. M. Glenn, A. P. Klamczynski, C. Ludvik, J. Shey, S. Imam, B.-S. Chiou, T. McHugh, G. DeGrandi-Hoffman, W. Orts, D. F. Wood and R. Offeman, *J. Agric. Food Chem.*, **2006**, *54*, 3297-3304.

## Chapter 5

1. F. D. Gunstone, *Vegetable Oils in Food Technology* (Blackwell Publishing Ltd., Oxford, UK, **2002**).
2. (a) F. D. Gunstone *Modifying lipids for use in food* (Woodhead Publishing Limited, Cambridge, UK and CRC Press LLC, USA, **2006**); (b) E. Floter and A. Bot, 'Developing Products with Modified Fats' in: *Improving the Fat Content of Foods*, C. M. Williams and J. Buttriss, Eds. (Woodhead Publishing Limited, Cambridge, UK, **2006**, pp. 411–427).
3. A. G. Marangoni, S. H. J. Idziak, C. Vega, H. Batte, M. Ollivon, P. S. Jantzi and J. W. E. Rush, *Soft Matter* **2007**, *3*, 183–187.
4. N. E. Hughes, A. G. Marangoni, A. J. Wright, M. A. Rogers and J. W. E. Rush, *Trends. Food Sci. Tech.*, **2009**, *20*, 470-480.
5. M. Perneti, K. F. van Malssen, E. Floter and A. Bot, *Curr. Opin. Colloid In.*, **2007**, *12*, 221–231.
6. (a) J. T. Judd, B. A. Clevidence, R. A. Muesing, J. Wittes, M. E. Sunkin and J. J. Podczasy, *Am. J. Clin. Nutr.*, **1994**, *59*, 861–868; (b) M. B. Katan, P. L. Zock and R. P. Mensink, *Annu. Rev. Nutr.*, **1995**, *15*, 473–493.

- 
7. American Heart Association (Know your facts):  
[http://www.heart.org/HEARTORG/Conditions/Cholesterol/PreventionTreatmentofHighCholesterol/Know-Your-Fats\\_UCM\\_305628\\_Article.jsp#.TszLarJFuso](http://www.heart.org/HEARTORG/Conditions/Cholesterol/PreventionTreatmentofHighCholesterol/Know-Your-Fats_UCM_305628_Article.jsp#.TszLarJFuso).
  8. M. A. Rogers, *Food Res. Int.*, **2009**, *42*, 747-753.
  9. (a) F. G. Gandolfo, A. Bot and E. Floter, *J. Am. Oil Chem. Soc.*, **2004**, *81*, 1–6; (b) J. Daniel and R. Rajasekharan, *J. Am. Oil Chem. Soc.*, **2003**, *80*, 417–421.
  10. (a) T. Tamura, T. Suetake, T. Ohkubo and K. Ohbu, *J. Am. Oil Chem. Soc.*, **1994**, *71*, 857–861; (b) C. A. Elliger, D. G. Guadagni and C. E. Dunlap, *J. Am. Oil Chem. Soc.*, **1972**, *49*, 536–537; (c) A. J. Wright and A. G. Marangoni, *J. Am. Oil Chem. Soc.*, **2007**, *84*, 3–9; (d) S. S. Narine and A. G. Marangoni, *Phys. Rev. E* **1999**, *60*, 6991–7000.
  11. J. F. Toro-Vazquez, J. A. Morales-Rueda, E. Dibildox-Alvarado, M. Charó-Alonso, M. Alonzo-Maciasa and M. M. González-Chávez, *J. Am. Oil Chem. Soc.*, **2007**, *84*, 989-1000.
  12. N. K. O. Ojijo, E. Kesselman, V. Shuster, S. Eichler, S. Eger and I. Neeman, *Food Res. Int.*, **2004**, *37*, 385–393.
  13. S. Murdan, G. Gregoriadis and A. T. Florence, *J. Pharm. Sci.*, **1999**, *88*, 608–614.
  14. (a) M. Perneti, K. van Malssen, D. Kalnin and E. Floter, *Food Hydrocolloid* **2007**, *21*, 855–861; (b) A. Bot and W. G. M. Agterof, *J. Am. Oil Chem. Soc.*, **2006**, *83*, 513–521; (c) A. Bot, R. den Adel and E. C. Roijers, *J. Am. Oil Chem. Soc.*, **2008**, *85*, 1127-1134; (d) M. A. Rogers, A. J. Wright and A. G. Marangoni, *Soft Matter* **2009**, *5*, 1594–1596.

- 
15. (a) H. Schiweck, A. Bar, R. Vogel, E. Schwarz and M. Kunz, 'Sugar Alcohols' in: *Ullmann's Encyclopedia of Industrial Chemistry*, 6<sup>th</sup> ed. (Wiley-VCH; **2003**, pp 487–513); (b) R. B. Friedman, 'Monosaccharides and Polyols in Foods' in: *Glycoscience: Chemistry and Chemical Biology*, 2<sup>nd</sup> ed., B. O. Fraser-Reid, K. Tatsuta and J. Thiem, Eds. (Springer, Berlin, Heidelberg, **2008**, pp. 841-856).
16. (a) J. J. Kabara, 'Medium-chain Fatty Acids and Esters' in: *Antimicrobials in Foods*. 2<sup>nd</sup> ed., P. M. Davidson and A. L. Branen, Eds. (Marcel Dekker, New York, **1993**, pp. 307-342); (b) V. K. Babayan, 'Medium Chain Triglycerides' in: *Dietary Fat Requirements in Health and Development*, J. Beare-Rogers, Ed. (American Oil Chemists' Society, Champaign, IL, **1988**, pp 73-86); (c) C. C. Akoh, 'Structured lipids' in: *Food Lipids—Chemistry, Nutrition, and Biotechnology*, 2<sup>nd</sup> ed., C. C. Akoh and D. B. Min, Eds. (Marcel Dekker, New York, **2002**, pp. 877–908).
17. R. N. Mitra, A. Shome, P. Paul and P. K. Das, *Org. Biomol. Chem.*, **2009**, 7, 94-102.
18. MSDS of mannitol and sorbitol (Sigma Aldrich).
19. (a) J. –H. Fuhrhop and J. Koning, *Membranes and Molecular Assemblies: The Synkinetic Approach* (The Royal Society of Chemistry, Cambridge, UK, **1994**, pp 120-123); (b) J. –H. Fuhrhop and C. Endisch, *Molecular and Supramolecular Chemistry of Natural Products and Their Model Compounds* (Marcel Dekker, Inc., New York, USA, **2000**, pp 167-242).
20. K. L. Liu, J. –L. Zhu and J. Li, *Soft Matter* **2010**, 6, 2300-2311.